Analyzing the Impacts of Policy Supports and Incentive Programs on Resource Management

A Dissertation Presented for the

Doctor of Philosophy

Degree

The University of Tennessee, Knoxville

Bijay Prasad Sharma

August 2018

Copyright © 2018 by Bijay P. Sharma.

All rights reserved.

Dedication

In the loving memory of Late Krishna Maya Sharma.

Acknowledgements

I would like to express sincere appreciation to my major advisor Dr. T. Edward Yu, who provided uninterrupted guidance, showed immense patience and constantly encouraged me throughout my doctoral education. I would like to gratefully acknowledge the research support from my doctoral committee members Dr. Burton C. English, Dr. Seong-Hoon Cho, Dr. Christopher N. Boyer and Dr. Donald G. Hodges. I appreciate Dr. Paul R. Armsworth and Dr. James A. Larson for their constructive comments and suggestions.

My gratitude goes to all faculty and staff of the Department of Agricultural and Resource Economics who provided valuable assistance and a friendly environment during my PhD program. I would also like to acknowledge my past and present fellow graduate students including Ayuska Ojha, Jia Zhong, Evan Markel, Santosh Neupane, Duc Cao and Katryn Pasaribu who provided academic as well as emotional support in many ways.

The first two papers of the dissertation were partially funded by the Federal Aviation Administration through the Aviation Sustainability Center (ASCENT), also known as the Center of Excellence for Alternative Jet Fuels and Environment. Any opinions, findings, and conclusions or recommendations expressed are solely mine and do not necessarily reflect the views of the FAA, NASA or Transport Canada.

Abstract

Feedstock-based renewable fuels, and ecosystem restoration practices such as afforestation are long-term solutions to mitigating greenhouse gas (GHG) emissions. This dissertation aligns with assessing the effects of policy supports and voluntary incentive programs on renewable fuel production and forest-based carbon sequestration.

Higher investment risks and novelty of the feedstock-based conversion technologies hinder large-scale deployment of renewable fuels at present. In the first essay, a two-stage stochastic model is employed to evaluate the impact of federal subsidies in designing a switchgrass-based bioethanol supply chain in west Tennessee wherein decisions driven by minimized expected and Conditional Value-at-Risk of system cost reflected the risk-neutral and risk-averse perspective of the biofuel sector, respectively. Major contribution of this study is the impact assessment of Biomass Crop Assistance Program (BCAP) on investment decisions (including land allocation) of a risk-sensitive biofuel industry under feedstock supply uncertainty.

In the second essay, impacts of renewable jet fuel (RJF) production from switchgrass on farmland allocation, processing facility configuration, and GHG emissions are estimated in response to fulfilling the RJF demand at the Memphis International Airport in Tennessee. Importantly, a potential carbon market is used to explore the impact of hypothetical carbon credits on the GHG emissions reduction and net supply-chain welfare while addressing the economic motives of the supply-chain participants. Considering the attention paid by the Unites States aviation sector with respect to GHG emissions, this study highlights the importance of Renewable Identification Number (RIN) credits and tradable carbon credits in achieving the

desired economic viability and emission abatement goals through a Stackelberg interaction between the feedstock suppliers and the feedstock processor.

In the third essay, discriminatory-price auction and agent-based model are used to examine the cost-efficiency of cost-ranked and cost-benefit-ranked auction-based payment designs for forest-based carbon sequestration with varying degree of correlation between opportunity costs of afforestation and carbon sequestration capacities, when bidders learn in multi-round procurement auctions. Simulation outcomes are expected to guide decision makers in choosing an optimal payment design that ensures efficiency gains for auction-based payments compared to fixed-rate payments, and more importantly ensures minimal loss in cost-efficiency in a dynamic setting.

Table of Contents

Chapter I. Introduction 1
References 10
Chapter II. Economic Impact of Government Subsidies on a Cellulosic Biofuel Sector Assimilating Its Risk Preferences toward Feedstock Yields Uncertainty 16
Abstract 17
2.1. Introduction 18
2.2. Literature Review 21
2.3. Conceptual Framework 23
2.4. Analytical Methods 27
2.4.1. Expected Cost Minimization Model (Model 1) 27
2.4.2. CVaR Minimization Model (Model 2) 30
2.4.3. Estimating Impact of BCAP Subsidies 32
2.5. Data 33
2.6. Results and Discussions 34
2.6.1. Influence of Risk Preference over Supply Chain Decisions 34
2.6.2. Influence of BCAP Subsidies over Supply Chain Decisions 37
2.6.3. Comparison of Models with and without BCAP Subsidies 39
2.7. Conclusions 40
References 43
Appendices 51
Chapter III. Welfare Analysis of Carbon Credits to the Renewable Jet Fuel Sector: A Game-theoretic Perspective 62
Abstract 63
3.1. Introduction 64
3.2. Literature Review 67
3.3. Conceptual Framework 69
3.4. Analytical Methods 73
3.4.1. Farmer's Profit Maximization 74
3.4.2. Processor's Profit Maximization (A Bi-level Optimization Problem) 76

3.4.3. Solution Approach 77
3.4.4. Calculation of LCA-based GHG Emissions 79
3.4.5. RJF Co-products and RIN Credits 80
3.4.6. Welfare Analysis of RJF 81
3.4.7. Carbon Credits Scenarios 82
3.5. Data 83
3.6. Results and Discussions 85
3.6.1. Solutions of the Baseline Stackelberg Model 85
3.6.2. Comparison of Carbon Credit Scenarios with the Baseline 87
3.6.3. Costs of GHG Emission Abatement with RJF Use 89
3.7. Conclusions 91
References 94
Appendices 103
Chapter IV. Designing Cost-effective Payments for Forest-based Carbon Sequestration: An Auction-based Modeling Approach 115
Abstract 116
4.1. Introduction 117
4.2. Literature Review 122
4.3. Conceptual Framework 126
4.3.1. Discriminatory-price Auction 128
4.3.2. Correlation and Payment Design 129
4.4. Empirical Methods 135
4.4.1. Bid Simulation and Learning 136
4.4.2. Binary Linear Optimization 138
4.5. Data 140
4.6. Results and Discussions 141
4.6.1. Fixed-rate Payment and Discriminatory-price Auction in a Static Setting 141
4.6.2. BC and TC Discriminatory-price Auctions in a Dynamic Setting 142
4.6.3. Fixed-rate Payment and Discriminatory-price Auction in a Dynamic Setting 144

4.7. Conclusions 146
References 149
Appendices 154
Appendix 4-A. Tables and Figures 154
Appendix 4-B. Nash-equilibria Bids in Reverse Auctions 160
Chapter V. Conclusions 166
Vita 172

List of Tables

Table 2-A 1: Definitions of identifiers, parameters and variables 51
Table 2-A 2: Data source 53
Table 2-A 3: Yield scenario generation 54
Table 2-A 4: Optimal costs in Models 1 and 2 55
Table 2-A 5: Annualized cost components in Models 1 and 2 56
Table 3-A 1: Definitions of identifiers, parameters and variables 103
Table 3-A 2: Data source for feedstock-based ethanol production costs 105
Table 3-A 3: Data source for feedstock-based ethanol production emissions 106
Table 3-A 4: Data source for ethanol-to-RJF conversion 106
Table 3-A 5: Parametric assumptions for cellulosic ATJ conversion pathway 107
Table 3-A 6: Parameters on energy-equivalent substitutes to ATJ products 108
Table 3-A 7: RIN credits and parameters for CC scenarios 108
Table 3-A 8: Annualized variables for the baseline 111
Table 3-A 9: Welfare for the baseline 111
Table 3-A 10: Difference in annualized variables for carbon credit scenarios compared to Baseline 112
Table 3-A 11: GHG emission abatement costs with 2016-A RIN credit 114

List of Figures

Figure 2-A 1: Potential biorefinery location and feedstock cultivation site 55
Figure 2-A 2: Cumulative density function (CDF) of optimal costs in Models 1 and 2 56
Figure 2-A 3: Optimal investment decisions in Model 1..... 57
Figure 2-A 4: Optimal investment decisions in Model 2..... 57
Figure 2-A 5: Shortage in Models 1 and 2..... 58
Figure 2-A 6: Surplus in Models 1 and 2..... 58
Figure 2-A 7: Annualized cost components in Model 1 with and without BCAP 59
Figure 2-A 8: Optimal investment decisions in Model 1 with BCAP 59
Figure 2-A 9: Annualized cost components in Model 2 with and without BCAP 60
Figure 2-A 10: Optimal investment decisions in Model 2 with BCAP 60
Figure 2-A 11: Change in objective values with BCAP subsidies in Models 1 and 2 61
Figure 3-A 1: Potential facility locations and feedstock supply area 107
Figure 3-A 2: Optimal land use and facility locations..... 109
Figure 3-A 3: Margins of individual feedstock suppliers 109
Figure 3-A 4: Feedstock suppliers' break-even costs and margins 110
Figure 3-A 5: Reduction in objectives solutions between carbon credit scenarios and the Baseline 112
Figure 3-A 6: Difference in land use for carbon credit scenarios compared to Baseline 113
Figure 3-A 7: Difference in net welfare for carbon credit scenarios compared to Baseline 113
Figure 3-A 8: RJF break-even prices with RIN credits and revenues of co-products 114
Figure 4-A 1: Cost-efficiencies of the payment designs for the BC model 154
Figure 4-A 2: Cost-efficiencies of the payment designs for the TC model 154
Figure 4-A 3: Cost-efficiencies of the cost-ranked BC auction under multiple rounds (L1) 155
Figure 4-A 4: Cost-efficiencies of the cost-benefit-ranked BC auction under multiple rounds (L1) 155
Figure 4-A 5: Cost-efficiencies of the cost-ranked TC auction under multiple rounds (L1) 156
Figure 4-A 6: Cost-efficiencies of the cost-benefit-ranked TC auction under multiple rounds (L1) 156
Figure 4-A 7: Cost-efficiencies of cost-ranked BC auction under multiple rounds (L2) 157
Figure 4-A 8: Cost-efficiencies of cost-benefit-ranked BC auction under multiple rounds (L2)157

Figure 4-A 9: Cost-efficiencies of cost-ranked TC auction under multiple rounds (L2) 158
Figure 4-A 10: Cost-efficiencies of cost-benefit-ranked TC auction under multiple rounds (L2) 158
Figure 4-A 11: Cost-efficiency gains of cost-ranked BC auctions with L1 and L2 bidders 159
Figure 4-A 12: Cost-efficiency gains of cost-benefit-ranked BC auctions with L1 and L2 bidders 159

Chapter I. Introduction

Anthropogenic climate change, a consequence of long-standing increment in atmospheric greenhouse gas (GHG) concentrations attributed to fossil fuels use, deforestation, intensive farming, and land deterioration, remains a major global issue. Combustion of fossil fuels has been the largest contributor of global GHG emissions followed by aggregated emissions from agriculture, deforestation, and other land-use changes (Boden et al., 2017). It is estimated that more than 9,800 million metric tons of carbon was released from fossil fuels use globally in the year 2014 (Boden et al., 2017). In the United States (U.S.) alone, the estimated net GHG emissions accounting for terrestrial sequestration has reached 5,828 million metric tons of CO_2-equivalents (CO_2e) for the year 2015 (Environmental Protection Agency [EPA], 2017). For the same year, emissions from fossil fuels use in the transportation sector comprised of about 27 percent of total U.S. GHG emissions, making it second largest contributor of U.S. GHG emissions after the electricity sector. Conversely, land-use, land-use change, and forestry sector (LULUCF) sequestered about 12 percent of total U.S. GHG emissions which mostly includes CO_2 removed from the atmosphere (EPA, 2017).

It is well understood that terrestrial carbon sequestration is one of the ways to mitigate future adverse consequences of climate change achieved either through reduced rate of release of GHG emissions in the atmosphere, or carbon captured through ecosystem restoration, and rehabilitation (McCarl & Schneider, 2000). Renewable energy produced from agricultural commodities such as biofuels, and atmospheric carbon captured from land management practices such as afforestation, reforestation are long-term solutions to mitigating GHG emissions (Weiss et al., 2007). Forests are the major sinks of CO_2 emissions whereas biofuels can reduce substantial amount of emissions through substitution of fossil fuels (McCarl et al., 2005). Large-scale users of fossil fuels, especially transportation including aviation, have either drawn

increasing attention or are pressurized in complying with national and global environmental regulations on specific GHG emission targets. Furthermore, possibility of increased cost of extraction because of depleting reserves, disruption in the supply due to natural disasters, etc. resulting in increased prices and decreased availability of fossil fuels has always been a foreseeable issue for the concerned stakeholders (Ladanai & Vinterbäck, 2010).

Biofuels can either reduce or offset GHG emissions released into the atmosphere compared to fossil fuels (Johnson et al., 2007). They release lower net GHG emissions from combustion as the carbon accumulated in the biomass i.e. biogenic carbon, during the growth of feedstocks, is initially captured from the atmosphere (Wang et al., 2012). Reduced imports leading to sustainability and enhanced energy security along with regional economic expansion through increased labor demand for biofuel processing are some of the additional benefits (Demirbas, 2009). Large scale production of biofuels generated from non-edible feedstocks with less GHG emissions compared to fossil fuels, low-competition for resources with food crops, and socio-economic development of the rural community has been the focus of stakeholders involved in the research and development of biofuels. However, nascent nature of the feedstock-based conversion technologies along with investment risks hinder large-scale deployment of biofuels at present.

Ecosystem restoration programs such as afforestation, avoided deforestation, reforestation, etc., can store a large amount of atmospheric CO_2 into the soil, and standing trees (McCarl & Sands, 2007). These programs compensate landowners for their opportunity cost of providing ecosystem services, including carbon sequestration in the form of direct incentives, called payment for ecosystem services (PES). However, the most popular form of PES, fixed-rate payment (Zandersen et al., 2009), does not address spatial heterogeneity in opportunity costs

of providing ecosystem services (ES) resulting in inefficient allocation of limited conservation funds. Conservation programs around the world are adopting competitive bidding mechanism in the form of conservation auction to overcome information asymmetry in securing cost-efficiency of the conservation programs (Brown et al., 2011; Connor et al., 2008; Stoneham et al., 2003). But, the efficiency gains of auction-based payments remain doubtful as landowners learn to extract higher information rents from the conservation agency under multiple rounds of procurement (Hailu & Schilizzi, 2004; Hailu & Thoyer, 2007; Lennox & Armsworth, 2013).

Polices have been formulated stimulating production and consumption of renewable energy. In the U.S., Renewable Fuel Standard (RFS) proposed by EPA under the Energy Independence and Security Act (EISA) mandated 36 billion gallons of ethanol to be blended into gasoline and diesel by 2022, of which 16 billion gallons are from lignocellulosic biomass (EPA, 2007). In an effort to promote robust supply of biomass feedstock for meeting mandated levels of feedstock-based biofuel production, the Conservation and Energy Act of 2008 initiated the Biomass Crop Assistance Program (BCAP) that provides subsidies in the form of establishment, annual, and matching payments for feedstock producers. Renewable Identification Numbers (RINs) issued by EPA, is another policy instrument created to incentivize biofuel production. It does not only provide tradable credits for processing facilities but also ensures the compliance of RFS mandates by registered blenders. In response to the global carbon abatement goals and to achieve an environment friendly sustainable growth in the U.S. aviation sector, U.S. Federal Aviation Administration (FAA) has set a voluntary target of 1 billion gallons of renewable jet fuel (RJF) production and consumption beginning 2018 which includes targets specific to the U.S. Air Force, the U.S. Navy and the commercial aviation (FAA, 2011). The RJFs can qualify

as advanced biofuels under the RFS, and thus become eligible for RIN credits even though there are no regulatory mandates on RJF blending as of today.

As a potential means of reducing the buildup of GHG emissions in the atmosphere, forest-based carbon sequestration has been widely implemented which relies on incentive payments to landowners for achieving the desired goals. Cap-and-trade program adopted by California includes provision of emission offset credits to the landowners for forest-based carbon sequestration (National Conference of State Legislatures [NCSL], 2018). Forest projects that sequester CO_2 are eligible for offset allowances through the Regional Greenhouse Gas Initiative (RGGI) program which covers states of Connecticut, Delaware, Maine, Maryland, Massachusetts, New Hampshire, New York, Rhode Island, and Vermont (NCSL, 2018). Recent years has shown involvement of other U.S. states such as West Virginia, Tennessee, North Carolina, Pennsylvania, and Oregon for carbon sequestration through reforestation projects based on incentive payments for farmers (EPA, 2012). In many developing countries, Reducing Emissions from Deforestation and forest Degradation (REDD+) program has been adopted under the United Nations Framework Convention on Climate Change (UNFCCC) which provides financial incentives for enhancing carbon stocks through sustainable forest management practices (International Climate Initiative [IKI], 2017).

This dissertation aims to assess the effect of policy supports and incentive programs on renewable fuel production and afforestation. Driven by the impacts of variation in biomass feedstock availability on the investment and operations of the biofuel industry, a growing number of studies have examined the optimization of biomass to biofuel supply chain considering the uncertainty related to feedstock supply (Chen & Fan, 2012; Gebreslassie et al., 2012; Huang et al., 2014). These studies, however, do not address land use decision for feedstock

production which seeks special attention because of the non-existence of market for large scale supply of biomass. Other studies dealing with uncertainty in biomass-biofuel supply chains are based on impractical assumption of risk neutrality (Azadeh et al., 2014; Kim et al., 2011). Bioethanol from lignocellulosic feedstock, such as switchgrass, has potential to mitigate the indirect negative consequences of food-crop based ethanol production (Sivakumar et al., 2010). However, feedstock yield uncertainty and high production costs are significant barriers to invest in a switchgrass-based bioethanol (SB) supply chain for biofuel production (Schnepf, 2011). Importantly, uncertainty in biomass yield creates difficulties in the assessment of investment decisions such as land use for feedstock cultivation (Gouzaye & Epplin, 2016). Federal subsidies, on the other hand, can have varying degree of impacts on investment decisions consistent with risk perception of the biofuel industry under uncertain environment.

The first essay evaluates impact of BCAP on optimal decisions of a bioethanol industry with different risk preferences in presence of feedstock yield uncertainty. A systematic approach to SB production is utilized wherein the impact of BCAP on optimal land-use and biorefinery configuration decisions are looked at while addressing yield uncertainty and the associated risk preferences of the biofuel sector. A two-stage stochastic mixed integer linear programming (MILP) model is developed initially to optimize the expected integrated cost of the supply chain based on the assumption of risk neutrality of the biofuel industry. The stochastic model is later expanded to a risk management model to incorporate the financial risk assuming the biofuel sector is risk averse. Conditional Value-at-Risk (CVaR) is optimized considering the risk associated with investment decisions under feedstock uncertainty. Applicability of the stochastic model is illustrated through a case study in west Tennessee.

Recent literature has also paid increasing attention to the techno-economic analysis of potential conversion technologies for RJF due to environmental regulations, increased demand for air traffic, and the instability of the energy prices (Diederichs et al., 2016; Mawhood et al., 2014; Natelson et al., 2015; Tao et al., 2017; Yao et al., 2017). Some of the studies have primarily focused on economic assessment of the existing conversion technologies (Bann et al., 2017; Reimer & Zheng, 2016), while others have assessed environmental performance alone (de Jong et al., 2017; Han et al., 2017). Few have attempted to combine life cycle analysis (LCA) with economic assessment in the evaluation of RJF (Staples et al., 2014; Winchester et al., 2015; Winchester et al., 2013). These studies, however, have generally neglected the economic interaction between the individual decision-makers, and thus have not paid attention to the welfare implication of RJF production. Net welfare analysis is specifically important in this context since reduction of aviation emissions is the primary goal of using RJF, and the GHG reductions achieved through large-scale RJF deployment with or without policy supports should justify the investments made in the RJF sector.

The second essay determines economics, and welfare implications of RJF produced from a lignocellulosic feedstock while addressing the economic motives of the participating actors. Specifically, GHG emissions reduction and welfare implication of policy supports in the form of carbon credits, needed to promote large-scale production of RJF, is evaluated while internalizing environmental costs of aviation emissions. A bi-level game theoretic competition between the farmers and the processor is designed to address the economic and environmental viability of the RJF production. As a leader, the processor chooses a capacity and spatial configuration for the potential plant with a price offer to the farmers that minimizes its feedstock procurement and the processing costs while acknowledging the spatial distribution of the potential feedstock

suppliers, their opportunity costs of supplying feedstock, and the spatial yield variability. The mixed-integer non-linear bi-level model is solved by converting into a single-level problem by replacing the original constraints of the lower-level problem (farmer's profit maximization) with its corresponding Karush-Kuhn-Tucker (KKT) conditions. Availability of RIN credits, and revenues from co-products are considered while analyzing the commercial feasibility of cellulosic RJF production. Applicability of the game-theoretic model is illustrated through a case study in west Tennessee.

In the research of economic incentives for afforestation program, landowners' willingness to accept for offering land into the program and the information on associated carbon gains of land use change are primarily focused in designing an optimal payment for forest-based carbon storage. However, commonly used fixed-rate system fails to address the information asymmetry between the conservation agency and the landowners with payments delivered far more than their opportunity costs (Ferraro, 2008; Persson & Alpízar, 2013) resulting in inefficient allocation of the limited conservation funds. Conservation auctions can reveal the approximate opportunity costs of land use change for the landowners which can then be effectively combined with the carbon sequestration benefits to design a cost-effective payment system. Furthermore, the degree of correlation between the opportunity costs and the environmental benefits shapes the relative gains of incorporating cost-benefit information in an optimally determined payment system (Babcock et al., 1997; Ferraro, 2003). Conclusions drawn from these studies that integrated cost and benefit are helpful in assisting conservation agencies for ensuring efficiency gain in a single-round conservation auction. However, the impact of integrating costs and benefits information on ensuring efficiency gain or ensuring minimal

efficiency loss in a multi-round conservation auction where landowners learn to extract information rents, has not been explored yet.

The third essay determines cost-efficiency of voluntary incentive payments for forest-based carbon sequestration when opportunity costs of land use change are correlated with carbon sequestration gains. Cost-efficiency of cost-ranked and cost-benefit-ranked auction-based payment designs is examined for forest-based carbon storage with varying degree of correlation between opportunity costs of afforestation and carbon sequestration capacities in a static as well as dynamic setting. Conservation auction is introduced to reveal the opportunity costs of conservation before ranking them, and then conceptualize the bid learning behavior of the participants in a multi-round conservation auction through an agent-based model. Bids are simulated using a stochastic term that denotes the amount of overbidding mimicking discriminatory-price auction. Based on whether the program is constrained by limited conservation fund or a specified conservation target, either budget-constrained (BC) or target-constrained (TC) format of auction is designed. The outcomes from the models are analyzed for cost-efficiency gains against an equivalent fixed-rate payment, while estimating magnitude of efficiency losses when bidders learn in a dynamic setting.

References

Azadeh, A., Arani, H. V., & Dashti, H. (2014). A stochastic programming approach towards optimization of biofuel supply chain. *Energy*, *76*, 513-525.

Babcock, B. A., Lakshminarayan, P., Wu, J., & Zilberman, D. (1997). Targeting tools for the purchase of environmental amenities. *Land Economics*, 325-339.

Bann, S. J., Malina, R., Staples, M. D., Suresh, P., Pearlson, M., Tyner, W. E., . . . Barrett, S. (2017). The costs of production of alternative jet fuel: A harmonized stochastic assessment. *Bioresource technology*, *227*, 179-187.

Boden, T., Marland, G., & Andres, R. (2017). Global, Regional, and National Fossil-Fuel CO2 Emissions in TRENDS: a Compendium of Data on Global Change. *Carbon Dioxide Information Analysis Center, Oak Ridge National Laboratory, US Department of Energy, Oak Ridge*, *20*.

Brown, L. K., Troutt, E., Edwards, C., Gray, B., & Hu, W. (2011). A uniform price auction for conservation easements in the Canadian prairies. *Environmental and Resource Economics*, *50*(1), 49-60.

Chen, C.-W., & Fan, Y. (2012). Bioethanol supply chain system planning under supply and demand uncertainties. *Transportation Research Part E: Logistics and Transportation Review*, *48*(1), 150-164.

Connor, J. D., Ward, J. R., & Bryan, B. (2008). Exploring the cost effectiveness of land conservation auctions and payment policies. *Australian journal of agricultural and resource economics*, *52*(3), 303-319.

de Jong, S., Antonissen, K., Hoefnagels, R., Lonza, L., Wang, M., Faaij, A., & Junginger, M. (2017). Life-cycle analysis of greenhouse gas emissions from renewable jet fuel production. *Biotechnology for Biofuels, 10*(1), 64.

Demirbas, A. (2009). Political, economic and environmental impacts of biofuels: A review. *Applied Energy, 86*, S108-S117.

Diederichs, G. W., Mandegari, M. A., Farzad, S., & Görgens, J. F. (2016). Techno-economic comparison of biojet fuel production from lignocellulose, vegetable oil and sugar cane juice. *Bioresource technology, 216*, 331-339.

Ferraro, P. J. (2003). Assigning priority to environmental policy interventions in a heterogeneous world. *Journal of Policy Analysis and Management, 22*(1), 27-43.

Ferraro, P. J. (2008). Asymmetric information and contract design for payments for environmental services. *Ecological economics, 65*(4), 810-821.

Gebreslassie, B. H., Yao, Y., & You, F. (2012). Design under uncertainty of hydrocarbon biorefinery supply chains: multiobjective stochastic programming models, decomposition algorithm, and a comparison between CVaR and downside risk. *AIChE Journal, 58*(7), 2155-2179.

Gouzaye, A., & Epplin, F. M. (2016). Land requirements, feedstock haul distance, and expected profit response to land use restrictions for switchgrass production. *Energy Economics, 58*, 59-66.

Hailu, A., & Schilizzi, S. (2004). Are auctions more efficient than fixed price schemes when bidders learn? *Australian Journal of Management, 29*(2), 147-168.

Hailu, A., & Thoyer, S. (2007). Designing Multi-unit Multiple Bid Auctions: An Agent-based Computational Model of Uniform, Discriminatory and Generalised Vickrey Auctions. *Economic Record*, *83*(s1), S57-S72.

Han, J., Tao, L., & Wang, M. (2017). Well-to-wake analysis of ethanol-to-jet and sugar-to-jet pathways. *Biotechnology for Biofuels*, *10*(1), 21.

Huang, Y., Fan, Y., & Chen, C.-W. (2014). An integrated biofuel supply chain to cope with feedstock seasonality and uncertainty. *Transportation Science*, *48*(4), 540-554.

International Climate Initiative (IKI). (2017). *Conservation, Restoration and Sustainable Use of Natural Carbon Sinks – REDD+*. Retrieved from https://www.international-climate initiative.com/fileadmin/Dokumente/2017/171107_IKI_FS_REDD_.pdf

Johnson, J. M., Coleman, M. D., Gesch, R., Jaradat, A., Mitchell, R., Reicosky, D., & Wilhelm, W. (2007). Main content area Biomass-Bioenergy Crops in the United States: A Changing Paradigm. *Americas Journal of Plant Science and Biotechnology*, *1*(1), 1-28.

Kim, J., Realff, M. J., & Lee, J. H. (2011). Optimal design and global sensitivity analysis of biomass supply chain networks for biofuels under uncertainty. *Computers & Chemical Engineering*, *35*(9), 1738-1751.

Ladanai, S., & Vinterbäck, J. (2010). Biomass for energy versus food and feed, land use analyses and water supply.

Lennox, G. D., & Armsworth, P. R. (2013). The ability of landowners and their cooperatives to leverage payments greater than opportunity costs from conservation contracts. *Conservation Biology*, *27*(3), 625-634.

Mawhood, R., Cobas, A. R., Slade, R., & Final, S. (2014). Establishing a European renewable jet fuel supply chain: the technoeconomic potential of biomass conversion technologies. *Biojet fuel supply Chain Development and Flight Operations (Renjet)*.

McCarl, B. A., Gillig, D., Lee, H.-C., El-Halwagi, M., Qin, X., & Cornforth, G. C. (2005). Potential for biofuel-based greenhouse gas emission mitigation: rationale and potential. *Agriculture as a Producer and Consumer of Energy. Cambridge, MA: CABI Publishers*.

McCarl, B. A., & Sands, R. D. (2007). Competitiveness of terrestrial greenhouse gas offsets: are they a bridge to the future? *Climatic Change, 80*(1-2), 109-126.

McCarl, B. A., & Schneider, U. A. (2000). US agriculture's role in a greenhouse gas emission mitigation world: An economic perspective. *Review of Agricultural economics, 22*(1), 134-159.

Natelson, R. H., Wang, W.-C., Roberts, W. L., & Zering, K. D. (2015). Technoeconomic analysis of jet fuel production from hydrolysis, decarboxylation, and reforming of camelina oil. *Biomass and Bioenergy, 75*, 23-34.

National Conference of State Legislatures (NCSL). (2018). *State Forest Carbon Incentives and Policies*. Retrieved from http://www.ncsl.org/research/environment-and-natural-resources/state-forest-carbon-incentives-and-policies.aspx#Forestandcarbon

Persson, U. M., & Alpízar, F. (2013). Conditional cash transfers and payments for environmental services—a conceptual framework for explaining and judging differences in outcomes. *World Development, 43*, 124-137.

Reimer, J. J., & Zheng, X. (2016). Economic analysis of an aviation bioenergy supply chain. *Renewable and Sustainable Energy Reviews*.

Schnepf, R. (2011). Cellulosic ethanol: Feedstocks, conversion technologies, economics, and policy options. *Asia Pacific Journal of Life Sciences, 5*(3), 171.

Sivakumar, G., Vail, D. R., Xu, J., Burner, D. M., Lay, J. O., Ge, X., & Weathers, P. J. (2010). Bioethanol and biodiesel: Alternative liquid fuels for future generations. *Engineering in Life Sciences, 10*(1), 8-18.

Staples, M. D., Malina, R., Olcay, H., Pearlson, M. N., Hileman, J. I., Boies, A., & Barrett, S. R. (2014). Lifecycle greenhouse gas footprint and minimum selling price of renewable diesel and jet fuel from fermentation and advanced fermentation production technologies. *Energy & Environmental Science, 7*(5), 1545-1554.

Stoneham, G., Chaudhri, V., Ha, A., & Strappazzon, L. (2003). Auctions for conservation contracts: an empirical examination of Victoria's BushTender trial. *Australian journal of agricultural and resource economics, 47*(4), 477-500.

Tao, L., Markham, J. N., Haq, Z., & Biddy, M. J. (2017). Techno-economic analysis for upgrading the biomass-derived ethanol-to-jet blendstocks. *Green Chemistry, 19*(4), 1082-1101.

U.S. Environmental Protection Agency (EPA). (2007). *Renewable Fuel Standard Program: Overview for Renewable Fuel Standard*. Retrieved from https://www.epa.gov/renewable-fuel-standard-program/overview-renewable-fuel-standard

U.S. Federal Aviation Administration (FAA). (2011). *Destination 2025*. Retrieved from https://www.faa.gov/about/plans_reports/media/Destination2025.pdf

U.S. Environmental Protection Agency (EPA). (2012). *Carbon Sequestration through Reforestation: A Local Solution with Global Implications*. Retrieved from https://semspub.epa.gov/work/HQ/176034.pdf

U.S. Environmental Protection Agency (EPA). (2017). *Inventory of U.S. Greenhouse Gas Emissions and Sinks: 1990-2015*. Retrieved from https://www.epa.gov/ghgemissions/inventory-us-greenhouse-gas-emissions-and-sinks

Wang, M., Han, J., Dunn, J. B., Cai, H., & Elgowainy, A. (2012). Well-to-wheels energy use and greenhouse gas emissions of ethanol from corn, sugarcane and cellulosic biomass for US use. *Environmental research letters, 7*(4), 045905.

Weiss, M., Patel, M., Heilmeier, H., & Bringezu, S. (2007). Applying distance-to-target weighing methodology to evaluate the environmental performance of bio-based energy, fuels, and materials. *Resources, Conservation and Recycling, 50*(3), 260-281.

Winchester, N., Malina, R., Staples, M. D., & Barrett, S. R. (2015). The impact of advanced biofuels on aviation emissions and operations in the US. *Energy Economics, 49*, 482-491.

Winchester, N., McConnachie, D., Wollersheim, C., & Waitz, I. A. (2013). Economic and emissions impacts of renewable fuel goals for aviation in the US. *Transportation Research Part A: Policy and Practice, 58*, 116-128.

Yao, G., Staples, M. D., Malina, R., & Tyner, W. E. (2017). Stochastic techno-economic analysis of alcohol-to-jet fuel production. *Biotechnology for Biofuels, 10*(1), 18.

Zandersen, M., Bråten, K. G., & Lindhjem, H. (2009). *Payment for and management of ecosystem services*: Nordic Council of Ministers.

Chapter II. Economic Impact of Government Subsidies on a Cellulosic Biofuel Sector Assimilating Its Risk Preferences toward Feedstock Yields Uncertainty

Abstract

The urgency to reduce dependence on fossil fuels and minimize green-house gas emissions has led to research on environment friendly as well as socio-economically sustainable renewable energy source. However, commercial level of production of bioenergy is severely constrained by investment risk and uncertainty. This study uses an integrated approach to evaluate the impacts of policy supports on the optimal supply chain decisions driven primarily by yield uncertainty and associated investment risk. As an instance of federal subsidies, the impact of Biomass Crop Assistance Program (BCAP) is evaluated under different risk preferences of the biofuel sector. A two-stage stochastic mixed integer linear programming is developed to model a risk neutral biofuel sector that minimizes the expected cost considering investment in switchgrass cultivation along with biorefinery establishment. Alternatively, the Conditional Value-at-Risk (CVaR) is optimized under the risk averse case considering the financial risk associated with investment decisions under feedstock yield uncertainty. Results of a case study in west Tennessee suggest that CVaR minimization case converts more land for switchgrass cultivation compared to the expected cost minimization to lower the high costs of low yield conditions. With the availability of BCAP payments, expected cost and investment risk are improved for both risk averse and risk neutral biofuel sector. However, both the expected cost and investment risk are reduced by a higher percent for the risk averse biofuel sector than the risk neutral one that optimizes expected cost.

Keywords Risk-averse, risk-neutral, stochastic, two-stage, uncertainty

2.1. Introduction

Growing concerns over future energy security and need for sustainable renewable energy source have directed formulation of government policies to stimulate production and consumption of biofuels. For instance, Renewable Fuel Standard (RFS) under the Energy Independence and Security Act (EISA) in 2007 mandated 36 billion gallons of ethanol to be blended into gasoline and diesel by 2022, of which 16 billion gallons are from lignocellulosic biomass (U.S. Congress, 2007). Biofuel produced from lignocellulosic biomass (LCB) feedstock is suggested as a potential form of socio-economically sustainable renewable energy source (Dale et al., 2011). Amongst the LCB feedstock category, switchgrass has been considered as one of the most promising bioenergy crops given net negative life cycle greenhouse gas (GHG) emissions of switchgrass derived ethanol compared to gasoline (U.S. Department of Energy, 2010). In addition, switchgrass' adaptability to the less fertile land could reduce resource competition against the food crops, hence lessen the "food vs fuel" debate (Carriquiry et al., 2011; Naik et al., 2010; Sims et al., 2010; Sokhansanj et al., 2009).

Considerable research effort has been made to explore the potentials of producing large scale biofuels derived from switchgrass (McLaughlin & Kszos, 2005; Perlack et al., 2011; Schmer et al., 2008; Schnepf, 2011; Wang et al., 2012; Wright, 2007). However, the commercial production of switchgrass-based biofuel (SB) remains moderate currently. One of the challenges in designing and implementing an efficient SB supply chain is the uncertainty associated with strategic and operational decisions of the biofuel industry. Strategic uncertainties are primarily related with climate and weather, technological innovation; whereas operational uncertainties typically involve variations in biofuel demand and prices. Variations in biomass availability due to diverse climatic conditions not only hinder the operations of the biofuel industry but also

create difficulties in the assessment of strategic investment decisions. Morrow et al. (2014) simulated the impact of droughts using climate models and suggested that yield reduction by drought could bring economic disruption to many biorefineries planned in the U.S. Thus, addressing feedstock supply uncertainty and associated investment risks is very crucial in determining SB supply chain for large scale biofuel production.

To mitigate the impact of feedstock supply uncertainly on biofuel industry and expedite the path to reach the mandated biofuel level, the Conservation and Energy Act of 2008 initiated the Biomass Crop Assistance Program (BCAP) (USDA, 2015). The BCAP provides incentives for the supply of dedicated energy crops in the form of three different payments: establishment, annual (land rent) and matching payments. Recent studies have documented the impacts of BCAP and other insurance programs on investment risk associated with land use change into perennial energy crops (Dolginow et al., 2014; Larson, 2008; Luo & Miller, 2017; Skevas et al., 2016). These studies evaluated BCAP subsidies with respect to improving profitability distribution of bioenergy crops for potential feedstock producers under uncertain yields and prices. In addition to enhancing individual farmer's decision for feedstock production, BCAP presumably improves the economics as well as risk of biofuel supply chain since the biomass suppliers and conversion facility must meet the BCAP program objectives set by USDA to be eligible for specific payments (USDA, 2015). However, the potential impacts of BCAP subsidies in the design of a biofuel supply chain under feedstock yield uncertainty, is lacking in the literature.

A large number of studies have attempted to determine the economic optimization of biofuel supply chain considering the uncertainty related to feedstock supply (Azadeh et al., 2014; Chen & Fan, 2012; Dal-Mas et al., 2011; Huang et al., 2014; Kim et al., 2011). A key

assumption made in these stochastic studies is that biomass feedstock with uncertain availability can be acquired from the markets. However, markets do not presently exist for large-scale use of the biomass feedstock and such assumption ignores the necessity to make a beforehand investment decision in the production of biomass. Except for Osmani and Zhang (2013), allocation of land for feedstock cultivation was excluded from strategic investment in previous studies. The land use choice for biomass feedstock production or supply considering the variation in the yield of feedstocks, especially perennial energy crops, should be included in the design of biomass-biofuel supply chain.

The standard approach to address strategic uncertainties is to incorporate them in investment decisions by optimizing average economic performance under the probabilistic anticipation of future conditions. Expected economic optimization, which assumes risk-neutrality, may fail to account for the risk minimizing behavior of biofuel sector under uncertain future. Instead of economic performance, implementing and optimizing risk measures provides effective risk mitigating strategies, particularly for the risk averse decision makers. A few studies have considered the financial risks associated with the operational level decisions in biofuel supply chain optimization (Dal-Mas et al., 2011; Gebreslassie et al., 2012; Giarola et al., 2013; Kazemzadeh & Hu, 2013; You et al., 2009). However, similar to the expected economic optimization studies, the uncertainty of feedstock supply and associated land use choice in the strategic level decisions while minimizing risk has not been addressed.

The present study thus aims to enhance the existing literature of biofuel supply chain in two dimensions: first, it assesses the impacts of BCAP on SB supply chain in the presence of feedstock yield uncertainty. Presumably, such subsidies have different impacts on land use and biorefinery investment decisions in the supply chain subject to the risk preference of the biofuel

sector. Second, the land use choice and biorefinery facility location is added in investment decisions regarding the presence of feedstock yield variability in an optimal SB supply chain. A two-stage stochastic model is employed wherein investment decisions are driven by expected cost minimization (assuming risk neutral) and Conditional Value-at-Risk (CVaR) minimization (assuming risk averse) of the biofuel sector.

2.2. Literature Review

Few studies outside integrated biomass-biofuel supply chain optimization literature, but relevant to the individual farmer's decision to switch to perennial bioenergy crops, have assessed the impacts of federally subsidized biomass programs while addressing the profitability requirements of the potential feedstock producers. Dolginow et al. (2014) compared the profitability range and associated investment risk of the bioenergy crops including switchgrass against the food-grain crops simultaneously incorporating the subsidies available from BCAP, and the uncertainty in prices and the yields of the bioenergy crops. Luo and Miller (2017) designed a model based on game-theoretic competition between the potential switchgrass producers to estimate the standard BCAP subsidies and the more efficient incentive levels required to realize the production of cellulosic biomass in view of meeting the RFS mandates. Skevas et al. (2016) incorporated the BCAP payments and a hypothetical revenue insurance program in modeling stochastic prices and yields of perennial cellulosic bioenergy crops to generate mean break-even levels, and the probability distribution of profitability while assuming different risk preferences of the farmers. Similarly, Larson (2008) evaluated the impact of BCAP as a risk management strategy where growth specific yields, weather influenced logistics, and inputs costs were identified as potential sources of risk determining the profitability distribution of switchgrass.

There is a rich literature on deterministic supply-chain optimization studies addressing economic costs as well as environmental objectives of GHG emission reduction. Akgul et al. (2012) designed an optimal hybrid first/second generation ethanol supply chain driven by the mechanism of total supply chain cost minimization. Zhang et al. (2013) implemented switchgrass-based supply chain optimization framework for integrated system cost reduction through a case study in North Dakota. A bicriterion feedstock cost and GHG emission minimization objective is considered in Yu et al. (2014) for determining optimal switchgrass supply system in Tennessee. Zhong et al. (2016) applied a multiobjective optimization model to determine the tradeoffs among the feedstock cost, GHG emission, and soil erosion minimization objectives in the design of a switchgrass-based supply chain in Tennessee. A multiobjective supply chain optimization extending to a dynamic planning horizon over a decade is developed in Huang and Xie (2015) to minimize the total system cost and GHG emission. Melo et al. (2006) proposed a dynamic facility location framework driven by cost minimization capturing essential strategic level supply chain decisions. You and Wang (2011) addressed the optimization of biomass to liquid supply chains from a life cycle perspective under a bicriterion objective of cost and GHG reduction.

A growing number of stochastic studies have also examined the impact of feedstock supply related uncertainty on the optimal economic performance, and the associated financial risk of the integrated biofuel supply chains. Uncertainty related with demand of biofuel and supply of feedstock are considered by Chen and Fan (2012) in an expected system cost minimization framework. Optimization problem associated with hydrocarbon biorefinery supply chain under supply and demand uncertainties is addressed by Gebreslassie et al. (2012) where they simultaneously minimized the expected annualized cost and the financial risk. Seasonal

variations and uncertainties of feedstock supply are considered in designing an efficient supply chain system by Huang et al. (2014) where they proposed an algorithm based on scenario decomposition to minimize the expected supply chain cost. Kim et al. (2011) adopted combined scenarios using most influential parameters affecting profit into stochastic framework to maximize the expected profit of the supply chain. Kazemzadeh and Hu (2013) modeled supply chain uncertainties in fuel market price, feedstock supply, and logistic costs considering expected value of profit and CVaR of profit as optimization objectives. A multi-period optimization framework is used in Dal-Mas et al. (2011) where expected NPV and CVaR are considered for economic performance and risk measurement, respectively, under stochastic scenarios.

2.3. Conceptual Framework

In this section, specific conditions defining the range of lands in terms of opportunity costs for switchgrass cultivation are derived given BCAP subsidies while ensuring the expected system cost of the biofuel sector under feedstock yield uncertainty matches what it would have been before BCAP is introduced. The biofuel sector in this study refers to an autonomous decision maker consisting of two coordinating supply chain participants i.e. biomass producers and biofuel processors. Similarly, the costs associated with supply chain decisions from biomass cultivation through biofuel delivery to the blending facility are cumulatively defined as the system (integrated) cost.

Consider a biomass and a biofuel producer decide on the optimal location of the biorefinery and the switchgrass draw area to achieve the minimum system cost under a biofuel contract with an exogenous biofuel price.

$$Minimize: \eta = (\alpha + \beta)x + \varphi q + \theta q + \rho\sigma q + \mu + \Omega(D - \sigma q), \qquad (2-1)$$

where α denotes switchgrass establishment cost in \$/hectare (ha), β denotes opportunity cost in \$/ha, x denotes hectares of switchgrass harvested, φ denotes switchgrass production cost in \$/Mega gram (Mg), q denotes biomass production in Mg, θ denotes transportation cost between switchgrass harvest site and biorefinery in \$/Mg, ρ denotes production cost for biorefinery in \$/Liter (L), μ denotes annualized investment cost for biorefinery in \$, σ denotes the biomass-biofuel conversion efficiency in L/Mg, D denotes the biofuel demand in liters by the blending facility, and Ω denotes penalty cost when the contracted biofuel demand was not met in \$/L.

Let us introduce yield uncertainty: $y_1 > y > y_2$ with corresponding production $q_1 > q > q_2$ where y Mg/ha be the real yield of switchgrass unknown at the time investment decisions are made.

Then, the cost minimization problem becomes:

$$Minimize: \eta = \ (\alpha + \beta)x + \varphi(\lambda q + (1-\lambda)q_2) + \theta(\lambda q + (1-\lambda)q_2) + \rho\sigma(\lambda q + (1-\lambda)q_2)$$

$$+\mu + \ \gamma\lambda(q_1 - q) + \Omega\sigma(1-\lambda)(q - q_2), \qquad (2-2)$$

where γ denotes inventory associated cost in \$/Mg, $\lambda = 1$ for $y_1 > y$, and $\lambda = 0$ for $y_2 < y$

Under the assumption of risk neutrality, objective function in equation (2-2) can be written as:

$$E(\eta) = Prob(y_1 > y)[(\alpha + \beta)x + \varphi q + \theta q + \rho\sigma q + \gamma(q_1 - q) + \mu]$$

$$+ Prob(y_2 < y)[(\alpha + \beta)x + \varphi q_2 + \theta q_2 + \rho\sigma q_2 + \Omega\sigma(q - q_2) + \mu], \qquad (2-3)$$

$$E(\eta) = Prob(y_1 > y)[(\alpha + \beta)x + (\varphi + \theta + \rho\sigma)yx + \gamma(y_1 - y)x + \mu]$$

$$+ Prob(y_2 < y)[(\alpha + \beta)x + (\varphi + \theta + \rho\sigma)y_2x + (\alpha + \beta)x + \Omega\sigma(y - y_2)x + \mu]. \qquad (2-4)$$

Let us assume for simplicity: $Prob(y_1 > y) = Prob(y_2 < y) = 1/2$.

$$E(\eta) = \frac{[(\alpha+\beta)x + (\varphi+\theta+\rho\sigma)yx + \gamma(y_1 - y)x + \mu]}{2}$$

$$+ \frac{[(\alpha+\beta)x + (\varphi+\theta+\rho\sigma)y_2x + \Omega\sigma(y - y_2)x + \mu]}{2}, \qquad (2-5)$$

$$E(\eta) = \frac{(2(\alpha+\beta) + (\varphi+\theta+\rho\sigma)(y+y_2) + \gamma y_1 - \Omega\sigma y_2 + (\Omega\sigma - \gamma)y)x + 2\mu}{2}. \qquad (2-6)$$

Let x^* be the optimal land use that minimizes the expected system cost under yield uncertainty.

$$E(\eta) = \frac{(2(\alpha+\beta) + (\varphi+\theta+\rho\sigma+\Omega\sigma-\gamma)y + (\varphi+\theta+\rho\sigma-\Omega\sigma)y_2 + \gamma y_1)x^* + 2\mu}{2}.$$

$$(2-7)$$

Under the condition of an optimal land use x^*, we obtain:

$$(2(\alpha+\beta) + (\varphi+\theta+\rho\sigma+\Omega\sigma-\gamma)y + (\varphi+\theta+\rho\sigma-\Omega\sigma)y_2 + \gamma y_1) = 0, \qquad (2-8)$$

$$y = \frac{(\Omega\sigma - g - \theta - \rho\sigma)y_2 - 2(\alpha+\beta) - \gamma y_1}{(\varphi+\theta+\rho\sigma+\Omega\sigma-\gamma)}. \qquad (2-9)$$

$$\theta = \frac{(\Omega\sigma - \varphi - \rho\sigma)y_2 - 2(\alpha+\beta) - (g+\rho\sigma+\Omega\sigma-\gamma) - \gamma y_1}{(y+y_2)}. \qquad (2-10)$$

Assuming the optimal land used for switchgrass cultivation x^*remains the same with BCAP subsidies, which cut annualized establishment cost by 50%, i.e. $\alpha^{bcap} = \frac{\alpha}{2}$, and lower annualized opportunity cost (land rent or profit of current agricultural practice) by 50%, i.e. $\beta^{bcap} = \frac{\bar{\beta}}{2}$, let us look at conditions defining the range of opportunity costs, i.e. $\bar{\beta}$ of available land that can be selected with BCAP subsidies while the expected system cost remains the same.

Case 1

Let us assume the selected land for switchgrass production given BCAP subsidies has identical spatial yields but less proximity to biorefinery.

$$\theta' < \theta \ (y' = y, y_2{}' = y_2 \ \& \ y_1{}' = y_1),$$

$$\frac{(\Omega\sigma - \varphi - \rho\sigma)y_2{}' - 2\left(\frac{\alpha}{2} + \frac{\bar{\beta}}{2}\right) - (\varphi + \rho\sigma + \Omega\sigma - \gamma) - \gamma y_1{}'}{(y' + \ y_2{}')}$$

$$< \frac{(\Omega\sigma - \varphi - \rho\sigma)y_2 - 2(\alpha + \beta) - (\varphi + \rho\sigma + \Omega\sigma - \gamma) - \gamma y_1}{(y + y_2)},$$

$$\bar{\beta} > \alpha + 2\beta.$$

Case 2

Let us assume the selected land for switchgrass production after BCAP subsidies has higher spatial yields but identical proximity to the biorefinery.

$$y' > y \ (\ \theta' = \theta, y_2{}' > y_2 \ \& \ y_1{}' > y_1),$$

$$\frac{(\Omega\sigma - \varphi - \theta' - \rho\sigma)y_2{}' - 2\left(\frac{\alpha}{2} + \frac{\bar{\beta}}{2}\right) - \gamma y_1{}'}{(\varphi + \theta' + \rho\sigma + \Omega\sigma - \gamma)} > \frac{(\Omega\sigma - \varphi - \theta - \rho\sigma)y_2 - 2(\alpha + \beta) - \gamma y_1}{(\varphi + \theta + \rho\sigma + \Omega\sigma - \gamma)},$$

$$\bar{\beta} < \alpha + 2\beta + (\Omega\sigma - \varphi - t - \rho\sigma)(y_2{}' - y_2) - \gamma(y_1{}' - y_1).$$

Under both the cases, farmers can select that range of high opportunity cost lands which facilitate the expected cost of the SB supply chain to be lesser than the one without the BCAP subsidies.

2.4. Analytical Methods

2.4.1. Expected Cost Minimization Model (Model 1)

A two-stage mixed integer linear programming (MILP) model is developed considering the yield uncertainty, and the computation of optimal first-stage (investment/strategic) and second-stage (operational) level variables is driven by the mechanism of the expected integrated cost minimization. Availability of secondary feedstock is not considered allowing biomass deficit, and any shortage in fulfilling the final demand is penalized which can be interpreted as cost of procuring biofuel from alternative sources to meet the contractual demand of the blending facility. Consequently, surplus production, if any is managed as an inventory for future incurring storage cost which can be regarded as the penalty for overproduction. Stochastic model used in this study is an extension of Yu et al. (2014).

Total system cost minimization under yield uncertainty gives rise to a typical two-stage structure which minimizes the sum of scenario independent (first-stage) costs and expected value of scenario dependent (second-stage) costs (Ahmed, 2010; Shapiro & Philpott, 2007). Equation (2-11) represents the objective function of the expected cost minimization model (referred as Model 1 hereafter). All the identifiers, parameters and variables used in the stochastic model are defined in Table 2-A1.

$$Minimize: E(Cost) = Cost_{1st-stage} + E\left(Cost_{2nd-stage}\right). \qquad (2-11)$$

Equation (2-12) presents the investment related costs which includes annualized investment cost of conversion facilities (C_{inv}^{fac}) and annualized establishment cost of switchgrass (C_{est}^{swi}). Similarly, opportunity cost of switchgrass (C_{opc}^{swi}) also enters the first-stage as it is proportional to switchgrass coverage. Computation of these investment cost components are expressed in equations (2-13)-(2-15).

$$Cost_{1st-stage} = C_{inv}^{fac} + C_{est}^{swi} + C_{opc}^{swi}. \quad (2-12)$$

$$C_{inv}^{fac} = \sum_{j \in J} \sum_{g \in G} (\mu_g \times z_{jg}). \quad (2-13)$$

$$C_{est}^{swi} = \sum_{i \in I} \sum_{h \in H} (\alpha \times X_{ih}). \quad (2-14)$$

$$C_{opc}^{swi} = \sum_{i \in I} \sum_{h \in H} (\beta_{ih} \times X_{ih}), \quad (2-15)$$

where

$$\beta_{ih} = \begin{cases} P_{ih} \times Y_{ih} - C_{ih} & if \ (P_{ih} \times Y_{ih} - C_{ih}) \geq R_{ih} \\ R_{ih} & if \ (P_{ih} \times Y_{ih} - C_{ih}) < R_{ih} \end{cases}.$$

Operational cost depends upon the operational uncertainty induced by yield uncertainty and thus is the expected cost under all considered yield scenarios (equation (2-16)). Switchgrass production (C_{pro}^{swi}), switchgrass storage (C_{stg}^{swi}), switchgrass transportation (C_{trans}^{swi}), biofuel conversion (C_{conv}^{bio}), biofuel transportation (C_{tran}^{bio}) and biofuel shortage (C_{short}^{bio}) costs all are defined under expectations. Each of these expected costs are calculated in equations (2-17)-(2-22).

$$E\left(Cost_{2nd-stage}\right) = E(C_{pro}^{swi}) + E(C_{stg}^{swi}) + E(C_{trans}^{swi}) + E(C_{conv}^{bio}) + E(C_{trans}^{bio}) + E(C_{short}^{bio}). \quad (2-16)$$

$$E(C_{pro}^{swi}) = \sum_{i \in I} \sum_{h \in H} \sum_{s \in S} (AM + \omega) \times X_{ih} \times prob\ (s). \quad (2-17)$$

$$E(C_{stg}^{swi}) = \sum_{i \in I} \sum_{s \in S} XS_{is} \times \gamma \times prob\ (s). \quad (2-18)$$

$$E(C_{tran}^{swi}) = \sum_{m\in M}\sum_{i\in I}\sum_{s\in S} XQ_{mis} \times \theta \times prob\ (s)\,. \qquad (2-19)$$

$$E\left(C_{conv}^{bio}\right) = \sum_{m\in M}\sum_{j\in J}\sum_{b\in B}\sum_{s\in S} XO_{mjbs} \times \rho \times prob\ (s). \qquad (2-20)$$

$$E\left(C_{tran}^{bio}\right) = \sum_{m\in M}\sum_{j\in J}\sum_{b\in B}\sum_{s\in S} XO_{mjbs} \times \delta \times prob\ (s)\,. \qquad (2-21)$$

$$E(C_{short}^{bio}) = \sum_{m\in M}\sum_{s\in S} Shortage_{ms} \times \Omega \times prob\ (s). \qquad (2-22)$$

Equations (2-23)-(2-30) define the constraints imposed on the cost minimization problem. Equation (2-23) limits feedstock production in each spatial unit to the available agricultural land. Equation (2-24) assures that total biomass available in each site equals total biomass production in that site. Equations (2-25)-(2-28) are mass balance/flow constraints. Biomass produced is directly transported to biorefinery in harvest season and remaining is stored for off-harvest season (equation (2-25)). Equation (2-26) ensures cumulative switchgrass delivered to the facility plus the surplus feedstock at the end of the off-harvest period equals the total biomass stored at the harvest season. Equation (2-27) ensures that the amount of biomass transported during each season is all converted into ethanol by biorefinery. Equation (2-28) guarantees any shortage plus the bioethanol sent to blending facility each season equals the demand of biofuel by blending facility. Equation (2-29) limits the number of biorefinery at each site. Equation (2-30) denotes the domain of the binary decision variable. Non-negativity constraints imposed on the continuous decision variables are listed in equation (2-31).

$$X_{ih} \leq A_{ih}\ \forall\ i, h. \qquad (2-23)$$

$$\sum_{h \in H} Y_{ixs} \times X_{ih} \ = XNS_{is} + XS_{is} \ \ \forall\, i, s. \qquad (2-24)$$

$$XNS_{is} \ = \sum_{m \in M_{on}} \sum_{j \in J} \frac{XQ_{mijs}}{(1-DT)} \ \ \forall\, , i, s. \qquad (2-25)$$

$$XS_{is} = \sum_{m \in M_{off}} \sum_{j \in J} \frac{XQ_{mijs}}{(1-DS) \times (1-DT)} + \frac{Surplus_{is}}{(1-DS)} \quad \forall\, i, s. \qquad (2-26)$$

$$\sigma \sum_{i \in I} \sum_{j \in J} XQ_{mijs} \ = \sum_{j \in J} \sum_{b \in B} XO_{mjbs} \ \forall\, m, s. \qquad (2-27)$$

$$\sum_{j \in J} \sum_{b \in B} XO_{mjbs} + Shortage_{ms} = D_m \ \ \forall\, m, s. \qquad (2-28)$$

$$\sum_{g \in G} z_{jg} \leq \ 1 \ \forall\, j. \qquad (2-29)$$

$$z_{jg} \in \{0, 1\} \ \ \forall \ j, g. \qquad (2-30)$$

$$X, XNS, XS, XQ, XO, Surplus, Shortage \geq 0. \qquad (2-31)$$

2.4.2. CVaR Minimization Model (Model 2)

Feedstock supply is a main source of uncertainty in the biofuel supply chain driven by the fluctuations in the yield, which is highly dependent on weather, disease and pest-incidence. Consequently, the system may not be able to meet the demand, or there might be excess production resulting in inventory accumulation. The associated risk can be quantified using standard stochastic procedure optimizing economic performance, but its management calls for integrating risk management metrics in the framework.

Value-at-Risk (VaR) and CVaR are commonly used risk aversion metrics in supply chain optimization under uncertainties. Within a given confidence interval ϑ, VaR_{ϑ} of a random variable is defined as the lowest value *t* such that with probability ϑ the loss will not be greater than *t* (Rockafellar & Uryasev, 2000). Similarly, $CVaR_{\vartheta}$ is the conditional expectation of the loss above the value *t*. In this study, random variable is replaced by integrated cost (Cost) and VaR_{ϑ} is the minimum value *t* such that the cost is less or equal to *t* with probability ϑ. $CVaR_{\vartheta}$ is the conditional expectation of the integrated cost above the value *t*. For a discrete distribution of the costs under different yield scenarios, CVaR is more generally defined as the weighted average of the VaR and the costs strictly exceeding VaR (Krokhmal et al., 2002).

$$CVaR_{\vartheta}(Cost, \vartheta\ ) = \frac{\sum_{s \in S} \emptyset(s) \times prob(s)}{1 - \vartheta} + VaR_{\vartheta}(Cost).$$

where

$$VaR_{\vartheta}(Cost) = Infimum\{t: Probability(Cost \leq t) \geq \vartheta\},$$

$$\emptyset(s) \geq Cost(s) - VaR_{\vartheta}(Cost), \emptyset(s) \geq 0, VaR_{\vartheta}(Cost) \geq 0.$$

The non-negativity constraint of $\emptyset(s)$ makes sure it is set to zero if $Cost(s)$ is below $VaR_{\vartheta}(Cost)$ while computing $CVaR_{\vartheta}(Cost, \vartheta)$.

Certain undesirable mathematical properties make VaR a non-coherent measure of risk (Artzner et al., 1999; Rockafellar & Uryasev, 2000). In addition, VaR is often criticized for offering no information on the risks above the defined percentile (Kidd, 2012). Thus, CVaR is minimized with the defined ϑ in this study using the stochastic model developed in section 2.4.1. Equation (2-32) represents the objective function of the CVaR minimization model (referred as Model 2 hereafter).

$$Minimize: CVaR_{\vartheta}(Cost, \vartheta) = \frac{\sum_{s \in S} \emptyset(s) \times prob(s)}{1 - \vartheta} + VaR_{\vartheta}(Cost). \qquad (2-32)$$

Subject to

$$\emptyset(s) \geq Cost(s) - VaR_{\vartheta}(Cost), \emptyset(s) \geq 0, VaR_{\vartheta}(Cost) \geq 0. \qquad (2-33)$$

$$Equations\ (2-23) - (2-31). \qquad (2-34)$$

General Algebraic Modeling System (GAMS) is used to solve two-stage stochastic MILP for two different objectives (Rosenthal, 2008).

2.4.3. Estimating Impact of BCAP Subsidies

The subsidies corresponding to 50% of amortized establishment costs and amortized value of 5-year annual subsidies corresponding to land rents are introduced as offered in the BCAP. The matching payment is documented ineligible for switchgrass in the BCAP. Stochastic optimization outputs with and without BCAP are compared to see the effect of incentives on optimal land allocation and biorefinery configuration. A discount rate (r_1) of 15% for annualizing establishment cost (Yu et al., 2014), and another discount rate (r_2) of 7.5% for annualizing land rent payment (Dolginow et al., 2014) for a time-period (*T*) of 10 years is used.

$$AEP = \frac{1}{2}\left[\frac{A \times r_1}{1 - [1 + r_1]^{-T}}\right],$$

where *AEP* is the annualized establishment payment, and *A* is the per hectare establishment cost.

$$ARP_{ih} = \frac{5 \times R_{ih} \times r_2}{1 - [1 + r_2]^{-T}},$$

where ARP_{ih} is the annualized land rent payment, and R_{ih} is the per hectare land rent for land unit *i* with crop type *h*.

2.5. Data

Optimization framework for establishing switchgrass-based bioethanol industry in west Tennessee uses high resolution 5 square mile level data showing considerable spatial variation in yield with uncertain feedstock yields. Table 2-A2 presents the sources of cost[1] related data on switchgrass-based ethanol production in west Tennessee.

The primary purpose of this study is to model yield variability in switchgrass corresponding to weather uncertainty. Statistical analysis of the field trial datasets suggests that there is considerable variability in switchgrass yields corresponding to variation in weather variables (Fike et al., 2006; Gunderson et al., 2008; Heaton et al., 2004; Jager et al., 2010; Thomson et al., 2009; Wullschleger et al., 2010). Matured yield of switchgrass from field trials between 2006 and 2011 at west Tennessee (Boyer et al., 2013; Boyer et al., 2012) is considered to generate yield uncertainty scenarios. Equally spaced yield intervals are created, and each interval is assumed a scenario with probability obtained from the frequency distribution of yield under that scenario. Taking each interval's mean and standard deviation together with the truncation limits, yields are simulated assuming normal distribution to match the number of spatial units under each scenario.

Fifteen different yield scenarios are used in optimization for each of the two-stage stochastic models (Table 2-A3). An increased number of scenarios (sample size) allows flexibility of choosing the risk-aversion parameter (ϑ-percentile) and improves reliability of the CVaR estimate as CVaR is more sensitive to estimation errors than the corresponding VaR (Yamai & Yoshiba, 2005).

[1] All the monetary values are defined in 2015 U.S. dollars.

Spatial yield variation under each yield scenario is mapped per the simulated spatial variation in switchgrass yields across U.S. (Jager et al., 2010). Potential sites for biorefinery and switchgrass establishment are shown in Figure 2-A1. A total of 18 land resource units (industrial parks) are identified as candidates for establishing biorefineries. Each spatial unit can have a biorefinery with either 189 million liters per year (MLY) or 378 MLY capacity. Similarly, 1936 spatial units (existing agricultural lands) are eligible for switchgrass cultivation replacing current crops. An annual demand of 1.1 billion L ethanol for west Tennessee is considered (Yu et al., 2016). A biomass-to-ethanol conversion efficiency of 304 L/Mg for switchgrass is used in the analysis. Configuration of biorefinery with pre-determined capacity is the first-stage binary decision variable whereas amount of land required for switchgrass cultivation is the first-stage continuous decision variable in the model. All the first-stage (strategic) and second-stage (operational) decisions are driven by the biofuel demand constrained by yield uncertainty.

2.6. Results and Discussions

2.6.1. Influence of Risk Preference over Supply Chain Decisions

Stochastic optimization incorporating feedstock yield uncertainty in terms of E(cost) minimization under the assumption of risk neutrality and CVaR(cost) minimization under the assumption of risk averse nature of biofuel industry are evaluated for the optimal supply chain decisions. The optimal costs and related yield uncertainty by scenario for both the models is presented in Table 2-A4. The lowest costs for the E(cost) minimization model (Model 1) correspond to yield scenarios with highest probabilities i.e. S5 and S6, as the investment decisions are based on risk neutrality assumption. On the other hand, scenarios with lower yields but higher costs in Model 1 i.e. S3 and S4, are prioritized in CVaR(cost) minimization model (Model 2) considering the cost risks associated with those scenarios (Table 2-A4).

The CVaR(Cost) minimization is implemented with ϑ equal to 95% where VaR(Cost) represents the value corresponding to 95th percentile of the cost distribution. The number of yield scenarios at and above VaR(Cost) of the cost distribution under Model 1 and Model 2 is three and seven, respectively (Figure 2-A2). The increased number of scenarios at and above the 95th percentile implies the risk associated with scenarios with high costs has been effectively reduced when the system risk is minimized in the stochastic model. Since Model 2 minimizes the weighted average of the cost at defined percentile and the expectation of the costs exceeding that percentile, VaR(Cost) is simultaneously determined in CVaR(Cost) minimization. In addition, several scenarios have identical optimal cost in Model 2 as it only minimizes the risk at and above VaR(Cost) with less control over the scenarios that fall below the 95th percentile of the distribution (Yamout et al., 2007).

The E(Cost) from Model 1 is $1,124 million compared to $1,249 million from Model 2. The VaR(Cost) under Model 1 and Model 2 is $1,360 million and $1,243 million, respectively. Although the E(Cost) is higher in Model 2 but its VaR(Cost) is $117 million lesser than the same in Model 1 (see Figure 2-A2). Consequently, CVaR(Cost) is reduced to $1,358 million in Model 2 through risk minimization compared to $1,441 million in Model 1.

2.6.1.1. Optimal Investment Decisions in Models 1 and 2

Optimal land allocation for switchgrass cultivation and configuration of biorefinery under E(Cost) and CVaR(Cost) minimization are shown in Figures 2-A3 and 2-A4, respectively. Considerable spatial variation in switchgrass yield appears across potential cultivation sites in all yield scenarios. Configuring biorefineries near the high yield sites reduces the biomass transportation cost but increases the biofuel transportation cost to blending facility which is one

of the plausible explanation for the observed optimal locations for the biorefineries under both the objectives.

An important consideration in land selection is the opportunity cost of each crop which determines the specific area under each crop and pasture (or hay) land that goes into switchgrass cultivation. Selection of land under food crops entails higher opportunity costs compared to pasture which explains the reason behind both models selecting considerable hectares from pasture land. Land under proximal food crops is selected only after the difference in biomass transportation costs between distant pasture fields and proximal crop lands exceeds the opportunity costs difference between the crop and pasture land.

Model 2 selected more land for switchgrass cultivation compared to Model 1 because CVaR(Cost) minimization reduces the risk associated with unfavorable scenarios (low yield scenarios in general). Land usage under crop lands increased from 14 to 43 thousand hectares whereas land usage under pasture lands increased from 265 to 324 thousand hectares after risk minimization. In other words, cost associated with low yield scenarios is minimized by lowering the penalty on biofuel shortage. Model 1, on the other hand, simply minimizes the cost on average given the yield scenarios and does not necessarily prioritize the unfavorable scenarios since the investment decisions are based on risk neutrality assumption.

Since Model 2 tried to minimize the high supply-chain costs associated with low yield scenarios by allocating more land for feedstock production, it incurred higher opportunity, and maintenance costs proportional with higher establishment costs as well as higher expected harvest, and storage costs compared to Model 1 (Table 2-A5). However, Model 1 has higher expected biomass (and biofuel) transportation costs, grinding costs associated with feedstock

conversion, and biorefinery operation costs. Model 2 incurred larger expected penalty on biofuel shortage compared to Model 1.

2.6.1.2. Optimal Operational Decisions in Models 1 and 2

The model with the objective of CVaR(Cost) minimization reduced shortage associated with high costs corresponding to low yield scenarios (at and above 95th percentile cost distribution from E(Cost) minimization). Higher costs corresponding to larger shortages[2] in Model 1 are lowered down considerably by CVaR(Cost) minimization in Model 2 (Figure 2-A5). To achieve these reductions, more hectares of switchgrass are cultivated as biofuel shortages correspond to lower feedstock yields.

Land selection for switchgrass cultivation is a strategic level decision variable and more of it under Model 2 automatically increased storage costs and surpluses associated with individual scenarios except for the low yields (Figure 2-A6). Shortages or surpluses under alternate cost scenarios in Model 1 are mutually exclusive (see Figures 2-A5 and 2-A6), which however is not necessary under Model 2.

2.6.2. Influence of BCAP Subsidies over Supply Chain Decisions

2.6.2.1. Model 1 Output with and without BCAP Subsidies

With BCAP subsidies in effect, E(Cost), VaR(Cost), and CVaR(Cost) in Model 1 decreased to $1,081 million, $1,318 million, and $1,399 million, respectively. Cost components affected by BCAP subsidies in E(Cost) minimization model are presented in Figure 2-A7. Gross[3] opportunity cost of land use increased from $20 million to $30 million under subsidies. A

[2] A penalty of $1.32/L is applied on the biofuel shortage. This parameter is carefully chosen to avoid non-optimal outcomes such as no production or forced production.
[3] If opportunity cost has not been subsidized with annualized land rent payment from BCAP.

considerable drop is shown in expected biomass transportation cost, from $62 million to $56 million, with a slight decrease in expected biofuel transportation cost with BCAP.

The selection of biorefinery locations and land use in the strategic level decision varied with and without BCAP (Figure 2-A8 vs. Figure 2-A3). It is cost effective to select proximal crop lands if the difference between the opportunity cost from crop lands and the opportunity cost from pasture fields is smaller than the difference between biomass transportation cost from distant pasture fields and the biomass transportation cost from proximal crop lands. With BCAP's annual land rent payments, the difference in the net[4] opportunity costs became smaller than the difference in the opportunity costs without the BCAP subsidies. Consequently, more hectares under proximal crop lands with higher gross opportunity costs is selected (Figure 2-A8) which lowered E(Cost) primarily because of the reduced biomass transportation costs (Case 1 in conceptual framework). Land usage under crop lands increased from 14 to 73 thousand hectares whereas land usage under pasture lands decreased from 265 to 205 thousand hectares with BCAP subsidies.

2.6.2.2. Model 2 Output with and without BCAP Subsidies

The E(Cost), VaR(Cost), and CVaR(Cost) of Model 2 lowered to $1,181 million, $1,175 million, and $1,299 million, respectively, when BCAP subsides are incorporated in decision-making. The relevant cost components from CVaR(Cost) minimization under BCAP are summarized in Figure 2-A9. An increment in gross opportunity cost of land use from $31 million to $58 million is observed with BCAP subsidies. Expected biorefinery operation cost increased from $332 million to $342 million with subsequent increase in expected biofuel transportation cost from

[4] Difference between gross opportunity cost and annualized land rent payment.

$23 million to $30 million under BCAP. A major drop in the expected biofuel shortage cost from $153 million to $115 million is achieved through substantial reduction in biofuel shortage across the low-yield scenarios with BCAP subsidies.

With the BCAP subsidies considered in strategic level decisions, biorefinery locations as well land use choice for feedstock cultivation appeared vastly different compared to the one without it (Figure 2-A10 vs. Figure 2-A4). The land use selection concentrated in the northern region with higher feedstock yields with a major increment in the crop land use under BCAP. An increment in crop land use from 43 to 152 thousand hectares is accompanied by a decrement in pasture land use from 324 to 208 thousand hectares with the BCAP subsidies. Since the higher feedstock yields correspond to higher gross opportunity cost lands (northern region of west Tennessee), Model 2 under BCAP subsidies facilitated land selection with higher yields even though they correspond to higher gross opportunity costs (Figure 2-A10). As the shortage associated with low yield scenarios is minimized by selecting land with higher yields, there is subsequent reduction in CVaR(Cost) which represents the expected cost at and above 95th percentile of distribution (Case 2 in conceptual framework). The tradeoff of the difference between biomass transportation costs and the difference between net opportunity costs amongst the crop and pasture lands is still relevant as in the case of Model 1.

2.6.3. Comparison of Models with and without BCAP Subsidies

Figure 2-A11 shows BCAP subsidies lowered E(Cost) by 3.86 and 5.41 percent in Models 1 and 2, respectively. Similarly, CVaR(Cost) associated with Models 1 and 2 reduced by 2.89 and 4.36 percent, respectively. Model 2 minimized the high costs associated with lower yield scenarios, which led to use of more land for feedstock cultivation. Additional land use in Model 2 ensured more establishment and annual land rent payments to the biofuel sector under BCAP. Thus, both

the E(Cost) and CVaR(Cost) are lowered by a higher percent in Model 2 compared to Model 1 (Figure 2-A11).

2.7. Conclusions

This study evaluated impacts of federally subsidized BCAP on optimal decisions of a switchgrass-based biofuel sector under feedstock yield uncertainty while addressing both the risk neutral and more conventional risk averse nature in terms of supply-chain cost minimization. A two-stage stochastic MILP is developed to minimize the expected system cost which considers allocation of land for switchgrass cultivation together with biorefinery facility location in the strategic level investment decisions. Furthermore, the E(Cost) minimization model, which assumes risk neutrality, is extended to CVaR(Cost) minimization model considering the risk averse nature of the biofuel sector under uncertainty of high costs.

Applicability of the stochastic model is illustrated through a case study in west Tennessee. The CVaR(Cost) minimization model selected more land for switchgrass cultivation compared to the E(Cost) minimization model as CVaR(Cost) minimization reduces the cost associated with unfavorable (low yield) scenarios. With the introduction of BCAP subsidies, crop land use increased whereas pasture land selection decreased. However, land selection is more responsive to BCAP subsidies in CVaR(Cost) minimization model compared to E(Cost) minimization model. The necessity to reduce shortage associated with high costs in CVaR(Cost) minimization model is favored by allowing land selection with higher spatial yields. Furthermore, higher spatial yields mostly correspond to lands with higher opportunity costs which are effectively reduced after BCAP land rent payments. More land usage for feedstock cultivation in CVaR(Cost) minimization model meant larger subsidies under BCAP.

Consequently, both the E(Cost) and CVaR(Cost) are reduced by a higher percent in CVaR(Cost) minimization model compared to E(Cost) minimization model with the BCAP subsidies.

The expected costs of supplying biomass to the biorefinery are $80 and $102/Mg for E(Cost) and CVaR(Cost) minimization models, respectively, which are lowered down to $68 and $89/Mg, respectively, with the BCAP subsidies. From the supply-chain perspective, the expected costs of biofuel delivery to the blending facility are $1.02 and $1.13/L for E(Cost) and CVaR(Cost) minimization models, respectively. With the BCAP subsidies, the expected biofuel delivery costs reduced to $0.98 and $1.07/L for E(Cost) and CVaR(Cost) minimization models, respectively. The costs in this study are higher compared to the findings in other stochastic studies mainly because of the incorporated risk, feedstock type, storage (including surplus) cost and shortage penalty. For example, Huang et al. (2014) and Chen & Fan (2012) estimated expected delivery price of biofuel using corn stover (and forest residue) to be $2.05/gallon ($0.54/L) and using cellulosic waste around $1.20/gallon ($0.32/L), respectively.

In this study, BCAP subsidies induced crop land into feedstock cultivation improving both the economics and the associated risk of the biofuel sector. More importantly, the annual land rent payments sufficiently lowered the opportunity costs of crop land thus making its conversion economically feasible. One major environmental benefit of using crop land for switchgrass cultivation instead of pasture land is the reduced GHG emissions associated with net carbon sequestration (Yu et al., 2016; Zhong et al., 2016). However, one of the reasons for exploring switchgrass as a bioenergy source is its potential to adapt to less fertile soils with minimal competition with the food crops. The agricultural land used for switchgrass cultivation has its demerits with respect to resource competition and increased food prices as consistently raised in “food vs fuel” debates for crop-based energy production (Fargione et al., 2008; Mallory

et al., 2011; Searchinger et al., 2008). The crop land use decisions of the biofuel sector with the BCAP subsidies are amplified in this study which is a major unintended consequence of such policy supports.

Considering the investment risk associated with switching well-established agricultural crops into perennial energy crops for achieving cellulosic biofuel mandates, this study provided economic assessment of the impacts of federally subsidized biomass programs on the investment decisions (including land allocation) of a risk-sensitive biofuel industry under feedstock supply uncertainty. One novel feature of this study is the use of experimental data collected from field trials in west Tennessee for generating probabilistic yield scenarios rather than assuming a random uniform distribution, common in stochastic optimization. However, field data has its caveat in limiting number of scenarios which is a compromise on the accuracy of decisions under Conditional Value-at-Risk minimization. On the other hand, computational complexity reduced the scope of the study to an annualized two-stage analysis i.e. perennial nature of the feedstock could not be modeled. A multi-stage expansion of the adopted modeling framework exploiting the dynamics of the logistic operations under uncertainties over a planning horizon capturing the entire life cycle of switchgrass will be an insightful improvement of this work.

References

Ahmed, S. (2010). Two-Stage Stochastic Integer Programming: A Brief Introduction. *Wiley Encyclopedia of Operations Research and Management Science*. doi: 10.1002/9780470400531.eorms0092

Akgul, O., Shah, N., & Papageorgiou, L. G. (2012). Economic optimisation of a UK advanced biofuel supply chain. *Biomass and Bioenergy, 41*, 57-72.

American Agricultural Economics Association. (2000). *Commodity cost and returns handbook*. Ames, IA.

American Society of Agricultural and Biological Engineers. (2006). *Agricultural machinery standards*. St. Joseph, MI.

Artzner, P., Delbaen, F., Eber, J. M., & Heath, D. (1999). Coherent measures of risk. *Mathematical finance, 9*(3), 203-228.

Azadeh, A., Arani, H. V., & Dashti, H. (2014). A stochastic programming approach towards optimization of biofuel supply chain. *Energy, 76*, 513-525.

Bowling, R. G., McKinley, T. L., & Rawls, E. L. (2006). *Tennessee Forage Budgets*. UT extension. The University of Tennessee. Retrieved from http://economics.ag.utk.edu/budgets/PB1658ForageBudgets07.pdf

Boyer, C. N., Roberts, R. K., English, B. C., Tyler, D. D., Larson, J. A., & Mooney, D. F. (2013). Effects of soil type and landscape on yield and profit maximizing nitrogen rates for switchgrass production. *Biomass and Bioenergy, 48*, 33-42.

Boyer, C. N., Tyler, D. D., Roberts, R. K., English, B. C., & Larson, J. A. (2012). Switchgrass yield response functions and profit-maximizing nitrogen rates on four landscapes in Tennessee. *Agronomy Journal, 104*(6), 1579-1588.

Carriquiry, M. A., Du, X., & Timilsina, G. R. (2011). Second generation biofuels: Economics and policies. *Energy Policy, 39*(7), 4222-4234.

Chen, C.-W., & Fan, Y. (2012). Bioethanol supply chain system planning under supply and demand uncertainties. *Transportation Research Part E: Logistics and Transportation Review, 48*(1), 150-164.

Dal-Mas, M., Giarola, S., Zamboni, A., & Bezzo, F. (2011). Strategic design and investment capacity planning of the ethanol supply chain under price uncertainty. *Biomass and Bioenergy, 35*(5), 2059-2071.

Dale, V. H., Kline, K. L., Wright, L. L., Perlack, R. D., Downing, M., & Graham, R. L. (2011). Interactions among bioenergy feedstock choices, landscape dynamics, and land use. *Ecological Applications, 21*(4), 1039-1054.

Dolginow, J., Massey, R. E., Kitchen, N. R., Myers, D. B., & Sudduth, K. A. (2014). A stochastic approach for predicting the profitability of bioenergy grasses. *Agronomy Journal, 106*(6), 2137-2145.

Fargione, J., Hill, J., Tilman, D., Polasky, S., & Hawthorne, P. (2008). Land clearing and the biofuel carbon debt. *Science, 319*(5867), 1235-1238.

Fike, J. H., Parrish, D. J., Wolf, D. D., Balasko, J. A., Green, J. T., Rasnake, M., & Reynolds, J. H. (2006). Switchgrass production for the upper southeastern USA: influence of cultivar and cutting frequency on biomass yields. *Biomass and Bioenergy, 30*(3), 207-213.

Gebreslassie, B. H., Yao, Y., & You, F. (2012). Design under uncertainty of hydrocarbon biorefinery supply chains: multiobjective stochastic programming models, decomposition algorithm, and a comparison between CVaR and downside risk. *AIChE Journal, 58*(7), 2155-2179.

Giarola, S., Bezzo, F., & Shah, N. (2013). A risk management approach to the economic and environmental strategic design of ethanol supply chains. *Biomass and Bioenergy, 58*, 31-51.

Gunderson, C. A., Davis, E. B., Jager, H., West, T. O., Perlack, R. D., Brandt, C. C., . . . Downing, M. (2008). Exploring potential US switchgrass production for lignocellulosic ethanol. *ORNL/TM-2007/183, Oak Ridge National Laboratory: Oak Ridge, Tennessee*.

Heaton, E., Voigt, T., & Long, S. P. (2004). A quantitative review comparing the yields of two candidate C 4 perennial biomass crops in relation to nitrogen, temperature and water. *Biomass and Bioenergy, 27*(1), 21-30.

Huang, Y., Fan, Y., & Chen, C.-W. (2014). An integrated biofuel supply chain to cope with feedstock seasonality and uncertainty. *Transportation Science, 48*(4), 540-554.

Huang, Y., & Xie, F. (2015). Multistage Optimization of Sustainable Supply Chain of Biofuels. *Transportation Research Record: Journal of the Transportation Research Board*(2502), 89-98.

Jager, H. I., Baskaran, L. M., Brandt, C. C., Davis, E. B., Gunderson, C. A., & Wullschleger, S. D. (2010). Empirical geographic modeling of switchgrass yields in the United States. *GCB Bioenergy, 2*(5), 248-257.

Kazemzadeh, N., & Hu, G. (2013). Optimization models for biorefinery supply chain network design under uncertainty. *Journal of Renewable and Sustainable Energy, 5*(5), 053-125.

Kidd, D. (2012). Value at risk and conditional value at risk: A comparison. *Investment Risk and Performance Feature Articles, 2012*(1), 1-4.

Kim, J., Realff, M. J., & Lee, J. H. (2011). Optimal design and global sensitivity analysis of biomass supply chain networks for biofuels under uncertainty. *Computers & Chemical Engineering, 35*(9), 1738-1751.

Krokhmal, P., Palmquist, J., & Uryasev, S. (2002). Portfolio optimization with conditional value-at-risk objective and constraints. *Journal of risk, 4*, 43-68.

Larson, J. A. (2008). Risk and uncertainty at the farm level. *Proceedings of the conference: Risk, Infrastructure and Industry Evolution USDA Office of Energy Policy and New Uses*, 42-52.

Larson, J. A., Yu, T.-H., English, B. C., Mooney, D. F., & Wang, C. (2010). Cost evaluation of alternative switchgrass producing, harvesting, storing, and transporting systems and their logistics in the Southeastern USA. *Agricultural Finance Review, 70*(2), 184-200.

Luo, Y., & Miller, S. A. (2017). Using Game Theory to Resolve the "Chicken and Egg" Situation in Promoting Cellulosic Bioenergy Development. *Ecological economics, 135*, 29-41.

Mallory, M. L., Hayes, D. J., & Babcock, B. A. (2011). Crop-based biofuel production with acreage competition and uncertainty. *Land Economics, 87*(4), 610-627.

McLaughlin, S. B., & Kszos, L. A. (2005). Development of switchgrass (Panicum virgatum) as a bioenergy feedstock in the United States. *Biomass and Bioenergy, 28*(6), 515-535.

Melo, M. T., Nickel, S., & Da Gama, F. S. (2006). Dynamic multi-commodity capacitated facility location: a mathematical modeling framework for strategic supply chain planning. *Computers & Operations Research, 33*(1), 181-208.

Morrow, W. R., Gopal, A., Fitts, G., Lewis, S., Dale, L., & Masanet, E. (2014). Feedstock loss from drought is a major economic risk for biofuel producers. *Biomass and Bioenergy, 69*, 135-143.

Naik, S. N., Goud, V. V., Rout, P. K., & Dalai, A. K. (2010). Production of first and second generation biofuels: a comprehensive review. *Renewable and Sustainable Energy Reviews, 14*(2), 578-597.

Osmani, A., & Zhang, J. (2013). Stochastic optimization of a multi-feedstock lignocellulosic-based bioethanol supply chain under multiple uncertainties. *Energy, 59*, 157-172.

Perlack, R. D., Eaton, L. M., Turhollow Jr, A. F., Langholtz, M. H., Brandt, C. C., Downing, M. E., . . . Shamey, A. M. (2011). US billion-ton update: biomass supply for a bioenergy and bioproducts industry.

Rockafellar, R. T., & Uryasev, S. (2000). Optimization of conditional value-at-risk. *Journal of risk, 2*, 21-42.

Rosenthal, E. (2008). *GAMS-A user's guide.* Paper presented at the GAMS Development Corporation.

Schmer, M. R., Vogel, K. P., Mitchell, R. B., & Perrin, R. K. (2008). Net energy of cellulosic ethanol from switchgrass. *Proceedings of the National Academy of Sciences, 105*(2), 464-469.

Schnepf, R. (2011). Cellulosic ethanol: Feedstocks, conversion technologies, economics, and policy options. *Asia Pacific Journal of Life Sciences, 5*(3), 171.

Searchinger, T., Heimlich, R., Houghton, R. A., Dong, F., Elobeid, A., Fabiosa, J., . . . Yu, T.-H. (2008). Use of US croplands for biofuels increases greenhouse gases through emissions from land-use change. *Science, 319*(5867), 1238-1240.

Shapiro, A., & Philpott, A. (2007). *A tutorial on stochastic programming*. Retrieved from https://www2.isye.gatech.edu/people/faculty/Alex_Shapiro/TutorialSP.pdf

Sims, R. E., Mabee, W., Saddler, J. N., & Taylor, M. (2010). An overview of second generation biofuel technologies. *Bioresource technology, 101*(6), 1570-1580.

Skevas, T., Swinton, S. M., Tanner, S., Sanford, G., & Thelen, K. D. (2016). Investment risk in bioenergy crops. *GCB Bioenergy, 8*(6), 1162–1177.

Sokhansanj, S., Mani, S., Turhollow, A., Kumar, A., Bransby, D., Lynd, L., & Laser, M. (2009). Large-scale production, harvest and logistics of switchgrass (Panicum virgatum L.)–current technology and envisioning a mature technology. *Biofuels, Bioproducts and Biorefining, 3*(2), 124-141.

Thomson, A. M., Izarrualde, R. C., West, T. O., Parrish, D. J., Tyler, D. D., & Williams, J. R. (2009). Simulating potential switchgrass production in the United States. *Pacific Northwest National Laboratory, Richland, WA*. doi: 10.2172/972974

Ugarte, D. G. D. L. T., & Ray, D. E. (2000). Biomass and bioenergy applications of the POLYSYS modeling framework. *Biomass and Bioenergy, 18*(4), 291-308.

University of Tennessee. (2015). *Field crop budgets.* Retrieved from http://economics.ag.utk.edu/budgets.html

U.S. Congress. (2007). *Energy independence and security act of 2007*. Retrieved from https://www.gpo.gov/fdsys/pkg/BILLS-110hr6enr/pdf/BILLS-110hr6enr.pdf

U.S. Department of Agriculture (USDA). (2015). *Biomass crop assistance program.* Retrieved from https://www.fsa.usda.gov/Assets/USDA-FSA-Public/usdafiles/Energy/ccc_2015_0001_0001

U.S. Department of Agriculture ERS. (2015). *Commodity costs and returns*. Retrieved from

https://www.ers.usda.gov/data-products/commodity-costs-and-returns/

U.S. Department of Agriculture NASS. (2011). *CropScape-cropland data layer.* Retrieved from http://nassgeodata.gmu.edu/CropScape

U.S. Department of Agriculture NASS. (2013-15). *Crop values annual summary*. Retrieved from http://usda.mannlib.cornell.edu/MannUsda/viewDocumentInfo.do?documentID=1050

U.S. Department of Agriculture NASS. (2013-15). *Cash rents by county.* Retrieved from https://www.nass.usda.gov/Surveys/Guide_to_NASS_Surveys/Cash_Rents_by_County/

U.S. Department of Agriculture NRCS. (2012). *SSURGO structural metadata*. Retrieved from https://www.nrcs.usda.gov/wps/portal/nrcs/detail/soils/survey/geo/?cid=nrcs142p2_053631

U.S. Department of Energry (DOE). (2010). *Alternative Fuels Data Center*. Retrieved from https://www.afdc.energy.gov/data/categories/emissions--2

Wang, M., Han, J., Dunn, J. B., Cai, H., & Elgowainy, A. (2012). Well-to-wheels energy use and greenhouse gas emissions of ethanol from corn, sugarcane and cellulosic biomass for US use. *Environmental research letters, 7*(4), 045905.

Wright, L. L. (2007). Historical perspective on how and why switchgrass was selected as a" model" high-potential energy crop: Oak Ridge National Laboratory (ORNL).

Wullschleger, S. D., Davis, E. B., Borsuk, M. E., Gunderson, C. A., & Lynd, L. (2010). Biomass production in switchgrass across the United States: database description and determinants of yield. *Agronomy Journal, 102*(4), 1158-1168.

Yamai, Y., & Yoshiba, T. (2005). Value-at-risk versus expected shortfall: A practical perspective. *Journal of Banking & Finance, 29*(4), 997-1015.

Yamout, G. M., Hatfield, K., & Romeijn, H. E. (2007). Comparison of new conditional value-at-risk-based management models for optimal allocation of uncertain water supplies. *Water Resources Research, 43*(7). doi: 10.1029/2006WR005210

You, F., & Wang, B. (2011). Life cycle optimization of biomass-to-liquid supply chains with distributed–centralized processing networks. *Industrial & Engineering Chemistry Research, 50*(17), 10102-10127.

You, F., Wassick, J. M., & Grossmann, I. E. (2009). Risk management for a global supply chain planning under uncertainty: models and algorithms. *AIChE Journal, 55*(4), 931-946.

Yu, T. E., English, B. C., He, L., Larson, J. A., Calcagno, J., Fu, J. S., & Wilson, B. (2016). Analyzing Economic and Environmental Performance of Switchgrass Biofuel Supply Chains. *BioEnergy Research, 9*(2), 566-577.

Yu, T. E., Wang, Z., English, B. C., & Larson, J. A. (2014). Designing a dedicated energy crop supply system in Tennessee: a multiobjective optimization analysis. *Journal of Agricultural and Applied Economics, 46*(3), 357-373.

Zhang, J., Osmani, A., Awudu, I., & Gonela, V. (2013). An integrated optimization model for switchgrass-based bioethanol supply chain. *Applied Energy, 102*, 1205-1217.

Zhong, J., Yu, T. E., Larson, J. A., English, B. C., Fu, J. S., & Calcagno, J. (2016). Analysis of environmental and economic tradeoffs in switchgrass supply chains for biofuel production. *Energy, 107*, 791-803.

Appendices

Table 2-A 1: Definitions of identifiers, parameters and variables

Category	Unit	Definition
Identifiers		
$i \epsilon I$		location of switchgrass production field
$j \epsilon J$		location of the biorefinery facility
$b \epsilon B$		location of the blending facility
$g \epsilon G$		annual capacity of conversion facility
$m \epsilon M$		season of the year
$M_{on} \epsilon M$		harvest season of the year
$M_{off} \epsilon M$		off-harvest season of the year
$h \epsilon H$		crop (pasture/hay, corn, soybean, wheat, sorghum, cotton)
$s \epsilon S$		uncertainty scenario for switchgrass yield
x		switchgrass
Parameters		
P_{ih}	\$/Mg	crop price
Y_{ih}	Mg/ha	crop yield
C_{ih}	\$/ha	production cost of crop
Y_{ixs}	Mg/ha	yield of switchgrass in each hexagon
R_{ih}	\$/ha	land rent of crop
α	\$/ha	amortized establishment cost of switchgrass field
β_{ih}	\$/ha	opportunity cost of switchgrass cultivation
AM	\$/ha	annual maintenance cost of switchgrass field
μ_g	\$/plant	amortized investment cost of conversion facility
ω	\$/ha	annual harvest cost for switchgrass
γ	\$/Mg	cost per unit of storing switchgrass
θ	\$/Mg	cost per unit of transporting switchgrass
ρ	\$/L	biorefinery operation cost
δ	\$/L	biofuel transportation cost

Table 2- A1 Continued

Category	**Unit**	**Definition**
DT	%	dry matter loss during transportation
A_{ih}	ha	cropland available in each hexagon for each crop
DS	%	dry matter loss during storage
σ	L/Mg	switchgrass-ethanol conversion rate
Δ_{mjg}	L/season	seasonal biofuel production capacity of biorefinery
D_m	L/season	seasonal demand for ethanol
Ω	$/L	penalty on biofuel shortage
$Prob(s)$		probability associated with each yield scenario
<u>Variables</u>		
z_{jg}		binary variable: 1 for biorefinery selection, 0 otherwise
X_{ih}	ha	switchgrass area harvested during harvest season
XNS_{is}	Mg	switchgrass not stored at the harvest site after harvest
XS_{is}	Mg	switchgrass stored at the harvest site after harvest
XO_{mijs}	Mg	switchgrass delivered to the biorefinery each season
$Surplus_{is}$	Mg	switchgrass stored as harvest surplus after meeting demand
$Shortage_{ms}$	L	demand shortage of biofuel in each season
XO_{mjbs}	L	fuel transported from biorefinery to blending facility

Table 2-A 2: Data source

Category	**Source**
Land conversion to switchgrass	
Land rents	USDA NASS (U.S. Department of Agriculture, 2013-2015)
Crop yields	USDA, SSURGO (U.S. Department of Agriculture Nature Resources Conservation Service, 2012)
Crop price and area	USDA NASS (U.S. Department of Agriculture, 2013-2015)
Crop production cost	USDA ERS (U.S. Department of Agriculture, 2015), POLYSIS (Ugarte & Ray, 2000)
Switchgrass yield	Boyer et al. (2013), Boyer et al. (2012), Jager et al. (2010)
Switchgrass production and harvest cost	Larson et al. (2010), University of Tennessee (2015)
Production	
Establishment	American Agricultural Economics Association (2000)
Annual maintenance	American Society of Agricultural and Biological Engineers (2006)
Harvest	
Fuels and labors	University of Tennessee (2015)
Storage	
Covers and pallets	University of Tennessee (2015)
Transport	
Trailer, fuel and labor	University of Tennessee (2015)

Table 2-A 3: Yield scenario generation

Scenario	Yield (Mg/ha)	Prob.
S1	$2.22 \leq \psi^{*} < 4.67$	0.005
S2	$4.67 \leq \psi < 7.12$	0.016
S3	$7.12 \leq \psi < 9.59$	0.067
S4	$9.59 \leq \psi < 12.03$	0.124
S5	$12.03 \leq \psi < 14.48$	0.159
S6	$14.48 \leq \psi < 16.93$	0.220
S7	$16.93 \leq \psi < 19.37$	0.183
S8	$19.37 \leq \psi < 21.84$	0.118
S9	$21.84 \leq \psi < 24.29$	0.063
S10	$24.29 \leq \psi < 26.69$	0.023
S11	$26.69 \leq \psi < 29.16$	0.009
S12	$29.16 \leq \psi < 31.63$	0.007
S13	$31.63 \leq \psi < 34.10$	0.002
S14	$34.10 \leq \psi < 36.57$	0.002
S15	$36.57 \leq \psi \leq 39.04$	0.002

*Denotes spatial yield.

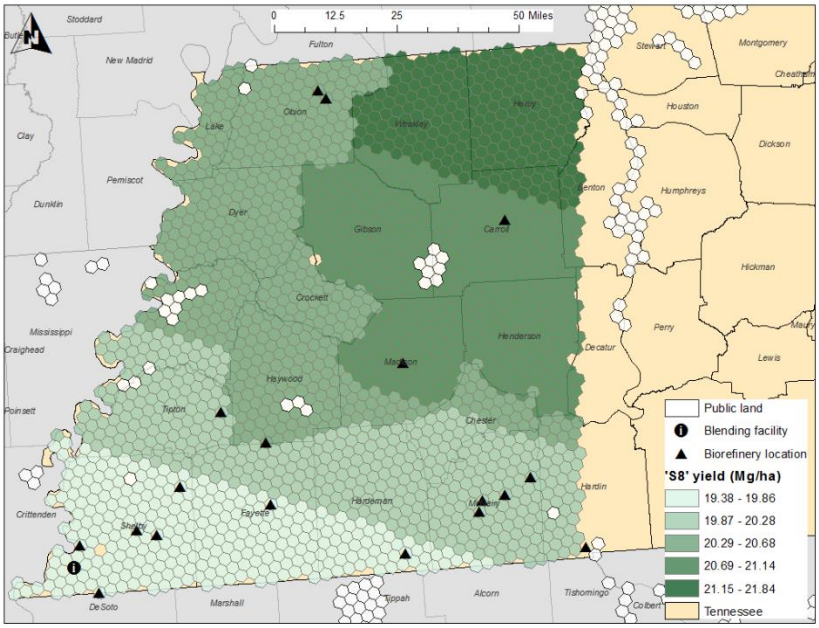

Figure 2-A 1: Potential biorefinery location and feedstock cultivation site

Table 2-A 4: Optimal costs in Models 1 and 2

Cost*	C1	C2	C3	C4	C5	C6	C7	C8	C9	C10	C11	C12	C13	C14	C15
Model 1	S5	S6	S7	S8	S9	S10	S11	S12	S13	S14	S4	S15	S3	S2	S1
Model 2	S3	S4	S5	S6	S7	S8	S9	S10	S11	S12	S13	S14	S15	S2	S1

* Ranked in the ascending order.
Note: Models 1 and 2 represent E(Cost) and CVaR(Cost) minimization models, respectively.

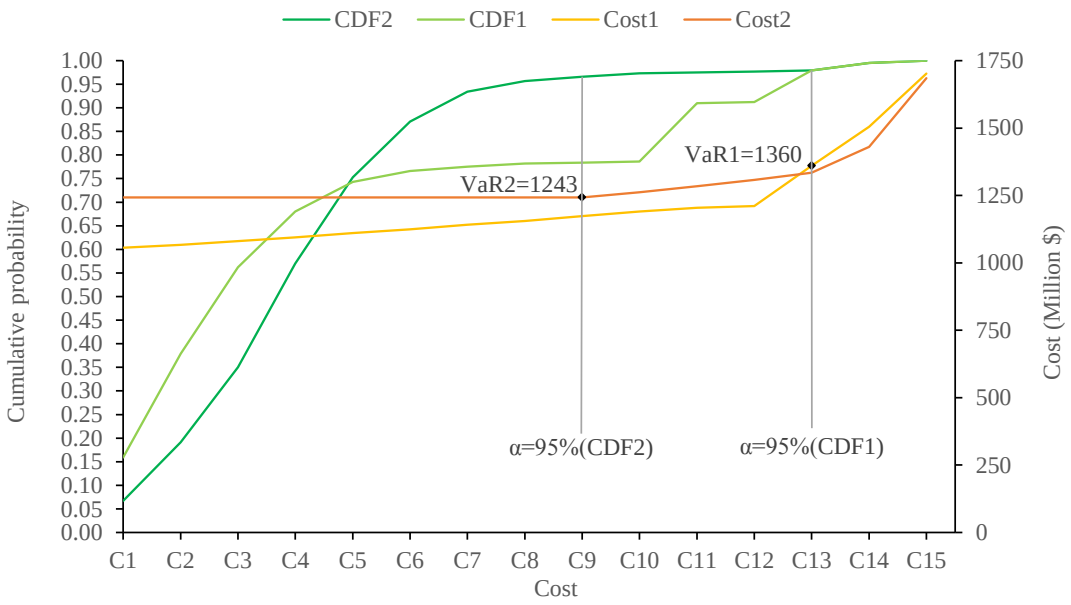

Figure 2-A 2: Cumulative density function (CDF) of optimal costs in Models 1 and 2
Note: Cost1 and Cost2 denotes optimal costs associated with yield scenarios for the Models 1 and 2, respectively. CDF1 and CDF2 denotes cumulative density of the optimal costs for the Models 1 and 2, respectively where Models 1 and 2 represent E(Cost) and CVaR(Cost) minimization models, respectively.

Table 2-A 5: Annualized cost components in Models 1 and 2

Annualized variables	**Unit**	**Model 1**	**Model 2**
Biorefinery investment cost	Million $	326	326
Feedstock establishment cost	Million $	49	64
Opportunity cost	Million $	20	31
Maintenance cost	Million $	36	47
E(Harvest cost)	Million $	101	133
E(Storage cost)	Million $	22	32
E(Grinding cost)	Million $	49	47
E(Biomass transportation cost)	Million $	62	61
E(Biofuel transportation cost)	Million $	25	23
E(Biorefinery operation cost)	Million $	350	332
E(Shortage penalty cost)	Million $	85	153

Note: Models 1 and 2 represent E(Cost) and CVaR(Cost) minimization models, respectively. E is the expectation operator.

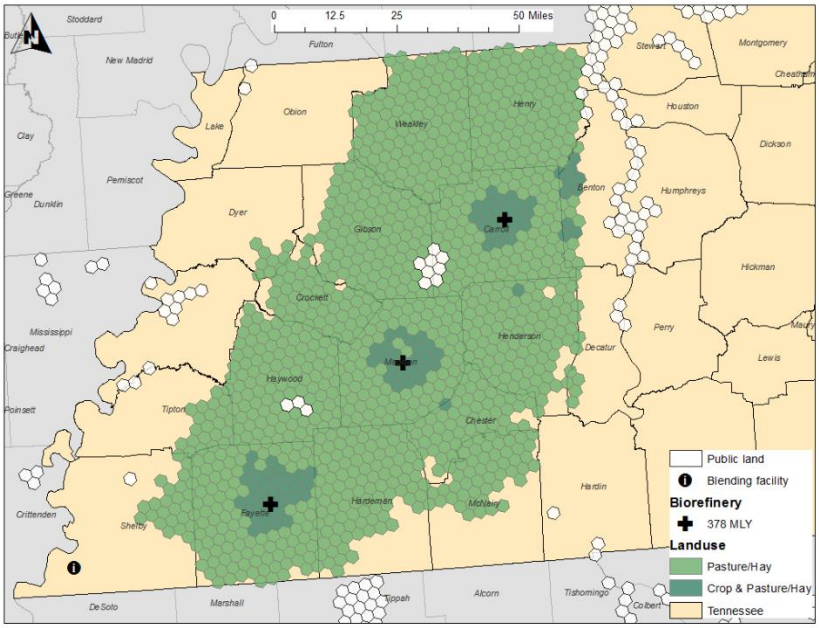

Figure 2-A 3: Optimal investment decisions in Model 1
Note: Model 1 represents E(Cost) minimization model.

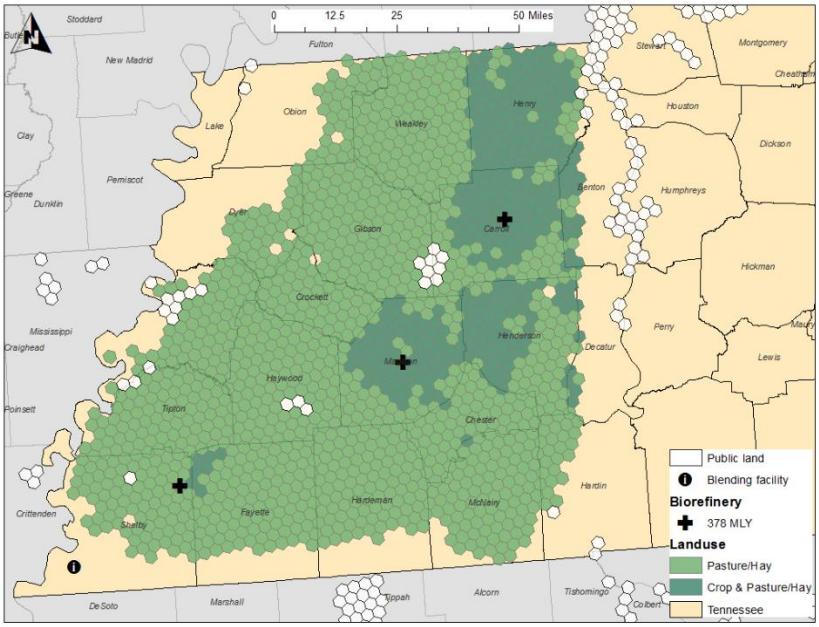

Figure 2-A 4: Optimal investment decisions in Model 2
Note: Model 2 represents CVaR(Cost) minimization model.

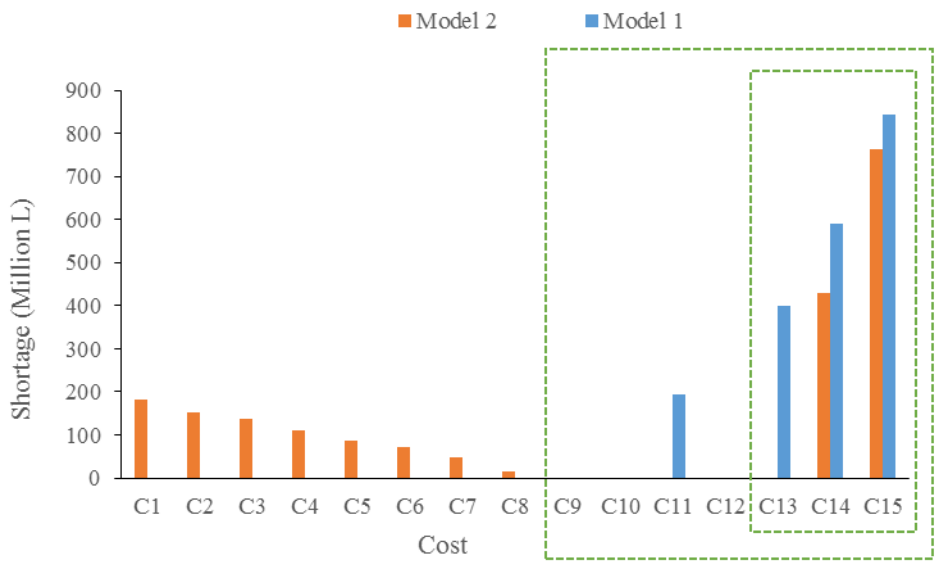

Figure 2-A 5: Shortage in Models 1 and 2
Note: Small and large insets capture 95th percentile and above cost distribution for Models 1 and 2, respectively where Models 1 and 2 represent E(Cost) and CVaR(Cost) minimization models, respectively.

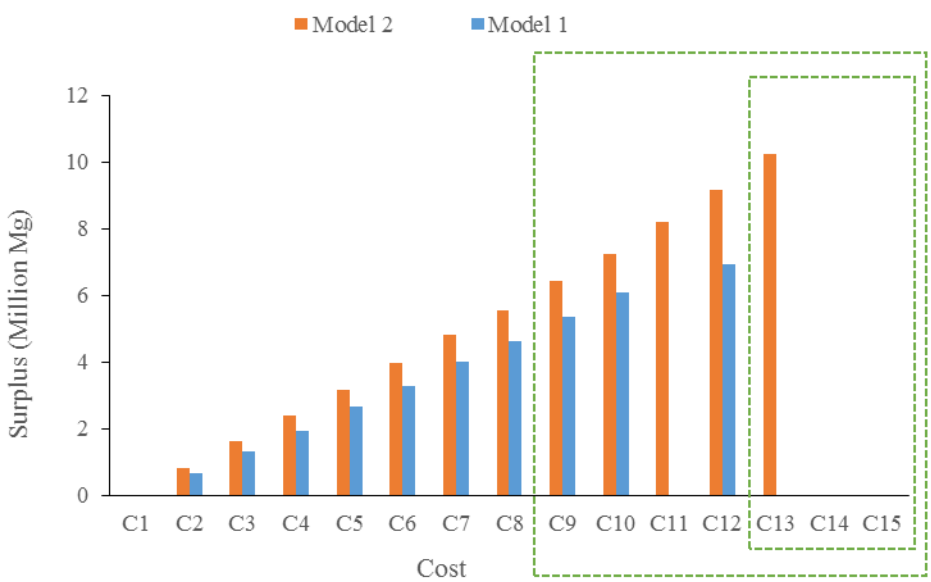

Figure 2-A 6: Surplus in Models 1 and 2
Note: Small and large insets capture 95th percentile and above cost distribution for Models 1 and 2, respectively where Models 1 and 2 represent E(Cost) and CVaR(Cost) minimization models, respectively.

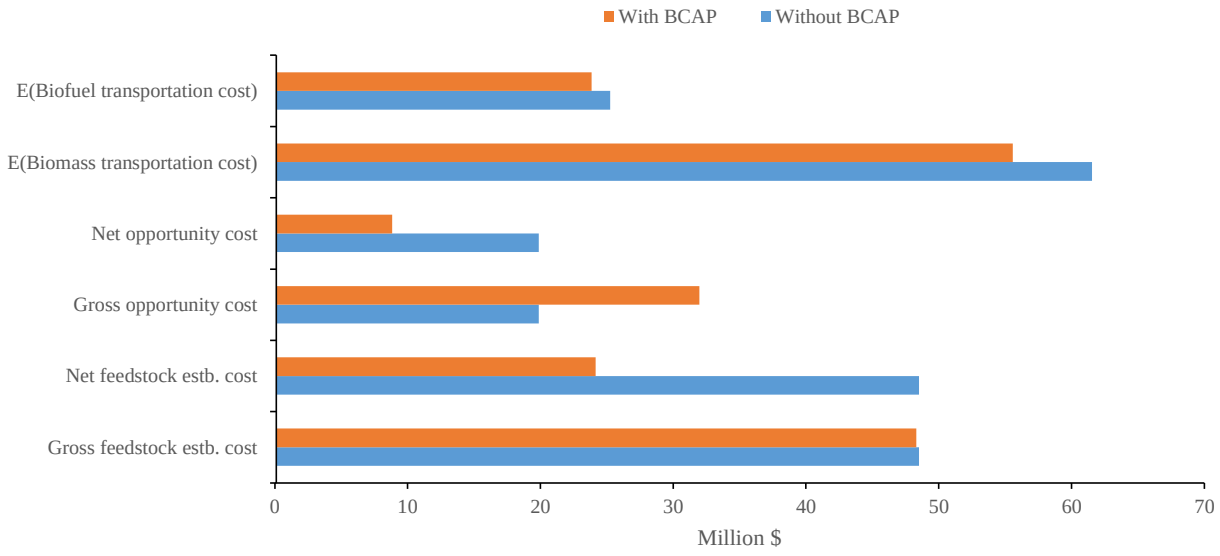

Figure 2-A 7: Annualized cost components in Model 1 with and without BCAP
Note: Gross opportunity and feedstock establishment costs refers to the costs if establishment and opportunity costs have not been subsidized with annual establishment and land rent payments, respectively, from BCAP. Model 1 represents E(Cost) minimization model. E is the expectation operator.

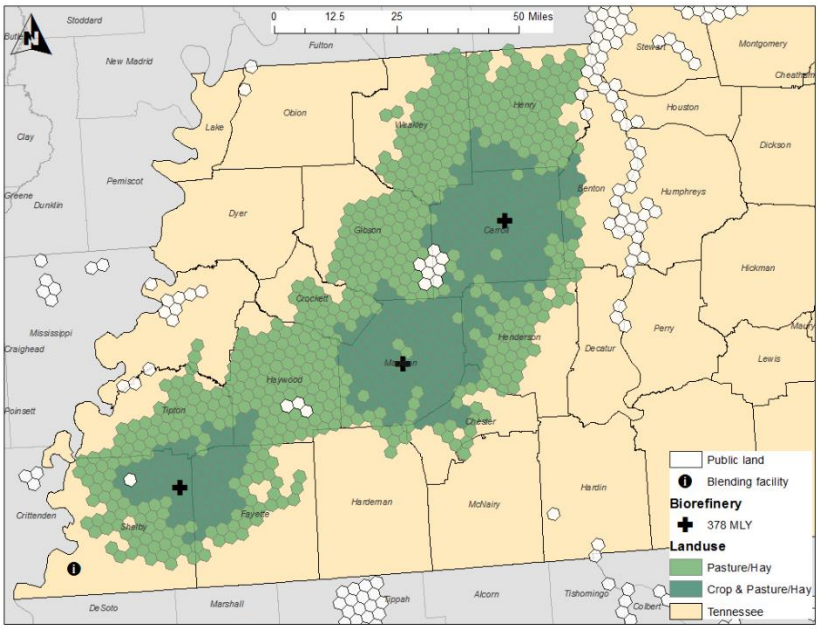

Figure 2-A 8: Optimal investment decisions in Model 1 with BCAP
Note: Model 1 represents E(Cost) minimization model.

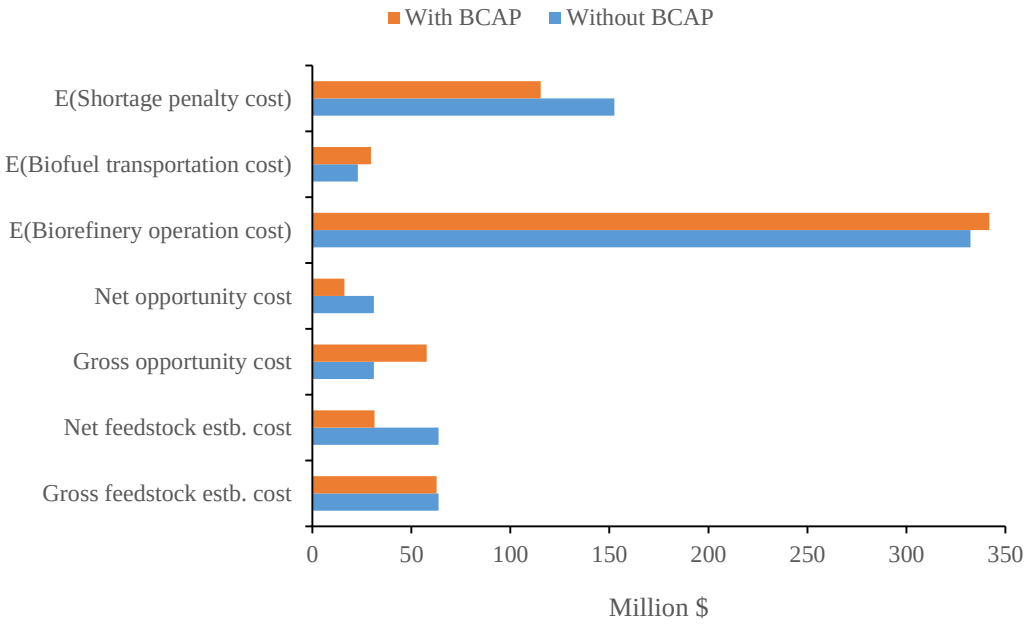

Figure 2-A 9: Annualized cost components in Model 2 with and without BCAP
Note: Gross opportunity and feedstock establishment costs refers to the costs if establishment and opportunity costs have not been subsidized with annual establishment and land rent payments, respectively, from BCAP. Model 2 represents CVaR(Cost) minimization model. E is the expectation operator.

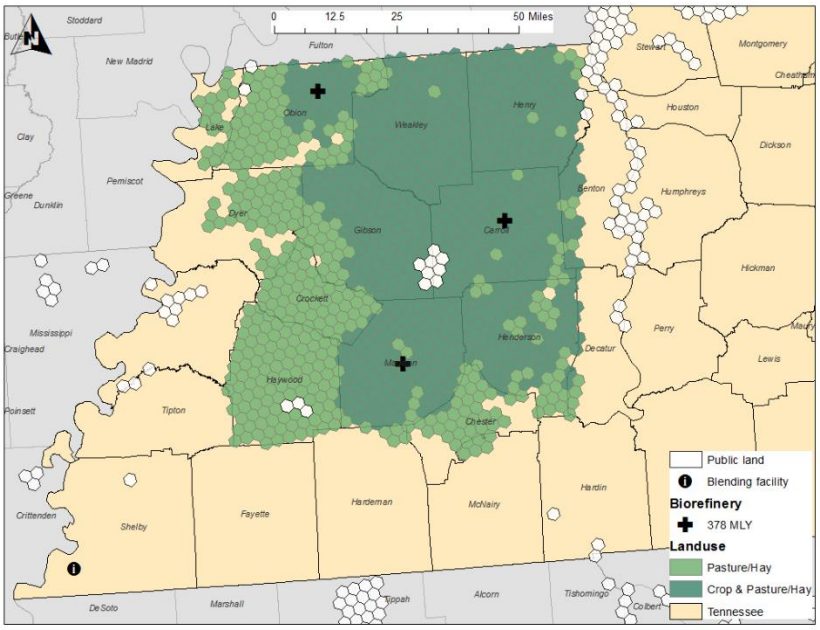

Figure 2-A 10: Optimal investment decisions in Model 2 with BCAP
Note: Model 2 represents CVaR(Cost) minimization model.

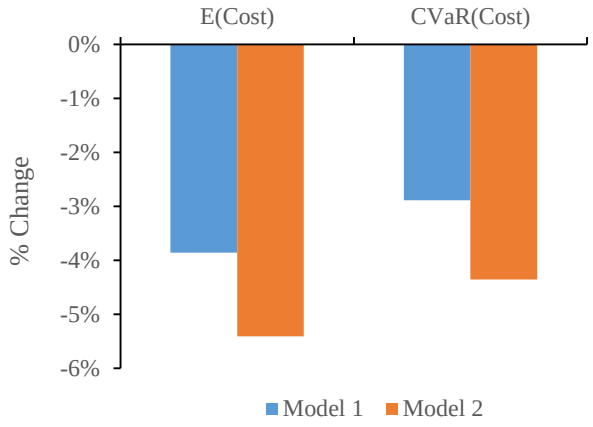

Figure 2-A 11: Change in objective values with BCAP subsidies in Models 1 and 2
Note: Models 1 and 2 represent E(Cost) and CVaR(Cost) minimization models, respectively.

Chapter III. Welfare Analysis of Carbon Credits to the Renewable Jet Fuel Sector: A Game-theoretic Perspective

Abstract

Renewable jet fuel (RJF) has been considered as a potential approach to mitigate greenhouse gas (GHG) emissions from the aviation sector; however, development of a commercial scale RJF sector still needs more stimulus. Provision of tradable carbon credits could be one of the ways for promoting an emerging environment friendly product like RJF. This study presents economic and environmental analysis of commercial scale RJF production from switchgrass-based alcohol-to-jet (ATJ) pathway in west Tennessee using a game-theoretic model that accounts for potential economic interaction between feedstock producers and RJF processor. Results indicate supplying 136 million gallons of RJF to the Memphis International Airport annually can potentially reduce 62.5% of GHG emissions compared to conventional jet fuel (CJF), with a net welfare of $4.3 million. In addition, GHG emissions could be lowered by about 65% from displacing CJF given hypothetical carbon credits of $11.58 to 42.56 per ton of CO_2-equivalent (CO_2e), which generated an estimated net welfare ranging between $17 and 55 million.

Keywords Carbon credit, GHG emissions, renewable jet fuel, Stackelberg, welfare

3.1. Introduction

Increasing air transportation driven by globalization has led to substantial increase in aviation fuel consumption and subsequent GHG emissions (Singh & Sharma, 2015). The International Air Transport Association (IATA) (2017a) estimates that about 815 million tons of CO_2e emissions were produced from global aviation in 2016 and predicts the passenger travel by air will double between 2016 and 2035. Given the continuously increasing consumption of jet fuel, the aviation industry is under political and public pressure to alleviate its GHG emissions. Therefore, IATA (2015) has set up clear aviation targets of carbon neutral growth by 2020 and reduction of GHG emissions by 50% by 2050 compared to the 2005 level. Members of the International Civil Aviation Organization (ICAO) have agreed to a new global market-based measure to achieve the short-term goals on carbon neutrality and the long-run goals of reduced global carbon emissions (Wyman, 2017).

Among various potential approaches to mitigate GHG emissions from the aviation sector, utilization of RJFs produced from agricultural and forestry residues, energy crops, or municipal wastes has a crucial role in meeting the ambitious goal of GHG emissions reduction (Fellet, 2016). The potentials of using RJF for GHG emissions mitigation have also been examined in various technical reports (Elgowainy et al., 2012; Wang et al., 2016). The “drop-in” nature of the RJF allows safe deployment with existing aircrafts without modifying engine designs or other engineering aspects (IATA, 2017b). In addition, Moore et al. (2017) showed that using jet biofuels can reduce the volatile and non-volatile particle number and mass emissions by 50-70% compared to CJF. Some commercial airlines have already adopted RJF in their flights and the volume of RJF purchased by the U.S. commercial aviation sector has increased from nearly none in 2015 to over a million gallons in 2016 (FAA, 2017).

Despite the potentials for GHG emissions reduction from adopting RJF, development of a commercial scale RJF sector still needs more stimulus to expedite the pace of abating GHG emissions from the aviation sector. Provision of tradable carbon credits could be one of the ways for promoting an emerging environment friendly product like RJF (Luo & Miller, 2013). Carbon credits can be allocated in ways similar to the emission offset credits issued by California Cap-and-Trade program or the RIN credits provisioned by the U.S. EPA. Those carbon credits can work like the RIN credits that are bought by registered blenders to ensure the compliance of a target or mandates. Alternatively, the federal agency may issue GHG emission permits to the processors of RJF and those permits can be traded in the hypothetical carbon market to generate carbon credits.

Current studies related to RJF have primarily focused on holistic approach of economic assessment of various conversion technologies of RJF (Bann et al., 2017; Diederichs et al., 2016; Mawhood et al., 2014; Natelson et al., 2015; Reimer & Zheng, 2016; Tao et al., 2017; Yao et al., 2017). Several researches have examined the environmental metrics related to the life cycle of RJF (de Jong et al., 2017; Han, Tao, & Wang, 2017). Only a few have attempted to integrate life cycle analysis (LCA) with economic assessment in the evaluation of RJF (Staples et al., 2014; Winchester et al., 2015; Winchester et al., 2013). Except for Reimer and Zheng (2016), the impact of policy or provision, such as carbon credits, on GHG emissions and costs of RJF production have not been addressed in those studies. Understanding the economic and environmental impacts of carbon credits provide important insights of policy mechanism on aviation GHG emissions reduction.

One key element that has been generally neglected in the previous economic or integrated analysis of RJF is the potential interaction between renewable feedstock producers and RJF

processors along with its welfare implication. The biomass feedstock, such as perennial grass, cover crops, or forest residues, are typically not traded in the market. Therefore, it is important to incorporate feedstock producers' decision process in allocating their scarce resources, such as land, when assessing the economics of RJF. Economic objectives of individual feedstock suppliers determine the feedstock acquisition costs for the processor, which accounts for a large portion of processor's variable cost of supplying RJF (Agusdinata et al., 2011). Eventually, the processor's profitability shapes its decision to negotiate a price with the interested airlines before agreeing on the amount of RJF to be produced and delivered. As a result, the market price of RJF produced from a given feedstock-based conversion technology is a consequence of individual decisions and probable competition amongst the supply chain participants.

Since the advent of RJF is primarily a response of the aviation industry to the goal of reduced GHG emissions, assessment of the welfare associated with RJF needs to account for the environmental benefits of reduced emissions. The feedstock and RJF prices, an outcome of economic motives and market interaction between decision-makers along the supply chain, is imperative in determining the welfare while internalizing the social costs of aviation GHG emissions (Reimer & Crandall, 2018). In addition, taking into account the spatial characteristics of the feedstock production and transportation is crucial to the estimation of GHG emissions as GHG footprint in the supply chain may vary greatly given different geographic conditions such as soil quality and road network (Jäppinen et al., 2011; Yu et al., 2016). Thus, incorporating high resolution spatial information for the RJF supply chain can better realize its environmental outcome and associated welfare.

The objective of this study has three-folds: first, the impacts of the commercial-scale RJF production on farmland allocation, processing facility configuration, and GHG emissions is

determined considering competitive interaction among the feedstock producers and the RJF processors. Second, the welfare of a hypothetical carbon credit as a policy instrument for incentivizing the GHG emission reductions from the RJF section is identified. Third, the abatement cost of LCA-based GHG emissions from displacing CJF with RJF is assessed. This study improved on the relevant literature by estimating economic and environmental metrics of commercial-scale RJF production accounting for the potential economic interaction between the supply-chain participants. Furthermore, land allocation of the feedstock producers is explicitly evaluated by using a high spatial resolution data. The findings will provide researchers, the industry and policy makers more insights of the potential economic and environmental impacts of developing a commercial scale RJF for aviation industry.

3.2. Literature Review

Renewable jet fuel literature has primarily focused on assessing the economic performance of the conversion technologies while estimating the incentives required to make RJF cost-competitive with the CJF. The break-even price or minimum selling price (MSP) varies greatly given different conversion technologies. Using stochastic dominance approach, Yao et al. (2017) found the mean break-even prices of $3.65 to 5.21 per gallon from various feedstock using the ATJ pathway; whereas Tao et al. (2017) estimated the MSP of $4.20 to 6.14 per gallon of RJF associated with the ethanol-to-jet (ETJ) upgrading technique. Bann et al. (2017) calculated the MSPs of Hydro-processed Esters and Fatty Acids (HEFA) and Fischer-Tropsch (FT) conversion pathways, and determined the price ranging between $0.66 and 1.42 per liter ($2.50 and 5.38 per gallon) of RJF. Zhao, Brown, and Tyner (2015) applied stochastic dominance rank study to identify the lowest break-even price for RJF at $3.11 per gallon of gasoline equivalent. Reimer and Zheng (2016) evaluated potential policy mechanisms to make RJF price competitive with

CJF, and concluded that a 17% subsidy on RJF, a 20% tax on CJF, or a combined 9% subsidy on RJF and 9% tax on CJF would make RJF price equivalent to CJF.

With regard to estimating the potential environmental gains of using RJF, other studies have used LCA methodology alone or in conjunction with economic analysis. Han et al. (2017) and de Jong et al. (2017) estimated the GHG reduction potential of various feedstock conversion pathways to be in the range of 16 to 80% compared to CJF. Staples et al. (2014) calculated GHG footprint of RJF produced from Advanced Fermentation (AF) pathway and suggested RJF's GHG emissions in the range of -27.0 to 89.8 gCO_2e/MJ given the MSPs of \$0.61 to 6.30 per liter (\$2.31 to 23.85 per gallon) from different feedstocks, compared to 90.0 gCO_2e/MJ of CJF. Winchester et al. (2013) and Winchester et al. (2015) assessed the implicit subsidy required for RJF production from oilseed rotation crops and perennial energy crops via HEFA and AF, respectively, and suggested the cost of aviation emission reduction ranging from \$42 to 652/tonCO_2e.

Although existing literature on renewable jet fuel has analyzed economic feasibility of RJF production along with emission abatement costs, possible economic interaction among the supply chain decision-makers and the related welfare has not been considered. The market-oriented approach accounting for competitive interaction between the supply chain participants, however, has been applied to the literature of the supply chain optimization of biofuels (Bai, Ouyang, & Pang, 2012; Yue & You, 2014, 2017). In addition, few studies have analyzed the welfare implications of alternative government policies on biomass, biofuel and RIN markets accounting for probable interactions between the supply chain participants (Bai, Ouyang, & Pang, 2016; Wang et al., 2013). Those studies provided better insights on the economics of biofuels by addressing more realistic interactions of the supply-chain participants compared to

the integrated approach in the existing literature of biofuels. However, they did not consider the environmental performance of biofuels in terms of LCA-based GHG emissions estimation, which is crucial in justifying the use of biomass-based renewable energy. On the other hand, those studies primarily used aggregated geospatial data assuming counties as the individual decision makers supplying feedstock in response to the market prices.

3.3. Conceptual Framework

Assuming both feedstock producers (farmers) and the RJF processor aim to maximize their respective profits in a non-cooperative manner, the RJF processer decides on the optimal number and configuration of the processing facilities considering the profit maximizing behavior of the spatially distributed farmers. This leads to a non-cooperative Stackelberg game (bi-level profit maximization) where the processer acts as a leader with farmers as multiple followers. The underlying assumption of the leader-follower game is that the processor anticipates that the farmers act rationally, implying each farmer maximizes its profits in response to the feedstock prices offered at the processing facilities while anticipating similar responses of other farmers.

Considering a lignocellulosic feedstock without a well-established market (switchgrass in this study), the profit maximization problem of the farmers is formulated as follows:

$$\underbrace{Maximize:}_{\substack{\boldsymbol{x_i}=[x_{hi}]_{h\in H} \\ \boldsymbol{q_i}=[q_{ijm}]_{j\in Jm\in M}}} \ \pi_i = \sum_{j\in J}\sum_{m\in M}(p_j - \varphi_i - \theta_{ij})\, q_{ijm} - \sum_{h\in H}(\alpha + \beta_{hi})x_{hi}. \qquad (3-1)$$

Subject to

$$x_{hi} \leq f_{hi} \ \forall \ h, i, \qquad (3-2)$$

$$\sum_{j\in J}\sum_{m\in M} q_{ijm} = y_i \sum_{h\in H} x_{hi} \ \forall \ i, \qquad (3-3)$$

$$\sigma\left(q_{ijm} + Q_{-ijm}\right) \leq \Delta_{jm}\, z_j \ \forall \ j, m, \qquad (3-4)$$

where p_j denotes feedstock price (\$/ton) offered at the processing facility j , φ_i denotes feedstock production cost (\$/ton) at site i, θ_{ij} denotes transportation cost (\$/ton) between i and j, q_{ijm} denotes feedstock supply quantity (tons) from i to j at time m, α denotes annualized feedstock establishment cost (\$/acre), x_{hi} denotes acreage of harvested feedstock from replacing existing crop h at site i, β_{hi} denotes opportunity cost (\$/acre) for land use h at site i f_{hi} denotes available acreage under existing crop h at site i, y_i denotes spatial feedstock yield (ton/acre) at site i, σ denotes the feedstock-RJF conversion efficiency (gallon/ton), and Δ_{jm} denotes production capacity (gallons) of the processing facility j at time m.

Similarly, the profit maximization problem of the processor is solved by determining feedstock procurement price and configuration of the processing facility.

$$\underbrace{Maximize}_{\substack{\boldsymbol{p_j}=[p_j]_{j\in J} \\ \boldsymbol{z_j}=[z_j]_{j\in J}}} : \Pi = \sum_{k\in K}\left(\sum_{j\in J}\sum_{m\in M}\left(\left(p_k-\delta_{jk}\right)\sigma\sum_{i\in I} q_{ijm}\right)\right) - \sum_{j\in J}\sum_{m\in M}\left(p_j\sum_{i\in I} q_{ijm}\right)$$

$$-\rho\sigma\sum_{j\in J}\sum_{m\in M}\left(\sum_{i\in I} q_{ijm}\right) - \sum_{j\in J} z_j\mu_j. \qquad (3-5)$$

Subject to

$$z_j \in \{0,1\}\ \forall\ j, \qquad (3-6)$$

$$Equations\ (3-1)\ to\ (3-4)\ \forall\ i, \qquad (3-7)$$

where p_k denotes the RJF price (\$/gallon) the processor received at airport k, δ_{jk} denotes transportation cost (\$/gallon) between j and k, ρ denotes production cost (\$/gallon) for processing facility, z_j denotes binary variable of processing facility establishment at j, and μ_j denotes amortized investment cost for processing facility j.

The break-even cost for the farmer i delivering feedstock to processing facility j is:

$$p_{ij}^{BE} = \frac{\sum_{m\in M}(\varphi_i + \theta_i)q_{im}^* + \sum_{h\in H}(\alpha + \beta_{hi})x_{hi}^*}{\sum_{m\in M} q_{im}^*}.$$

Assuming the farmer *i* supplies feedstock only if the profit is at least r_1 % greater than either net returns from existing land use, or land rent, whichever is higher (i.e. opportunity cost), the price offered by the processing facility *j* that satisfies i^{th} profit-maximizing farmer is:

$$p_j{}^* \geq \frac{\sum_{m\in M}(\varphi_i + \theta_i)q_{im}^* + \alpha \sum_{h\in H} x_{hi}^* + (1 + r_1) \sum_{h\in H} \beta_{hi} x_{hi}^*}{\sum_{m\in M} q_{im}^*}. \qquad (3-8)$$

Consequently, the break-even price for processing facility *j* delivering RJF to airport *k* is:

$$p_{jk}^{BE} = \frac{p_j{}^* \sum_{m\in M} \sum_{i\in I} q_{im}^* + \rho\sigma \sum_{m\in M} \sum_{i\in I} q_{im}^* + \delta_j \sigma \sum_{m\in M} \sum_{i\in I} q_{im}^* + z_j{}^* \mu_j}{\sigma \sum_{m\in M} \sum_{i\in I} q_{im}^*}. \qquad (3-9)$$

Let us further assume that the processing facility *j* produces RJF only if the price received from the airlines includes a premium at least \$ r_2 above the break-even. Given the price-offer satisfies the processor's profit margins, the net welfare is then determined as follows while internalizing environmental costs of GHG emissions based on LCA methodology:

$$Welfare = CS_{FS} + PS_{FS} + CS_{RJF} + PS_{RJF} - c_e E_{LCA}, \qquad (3-10)$$

where c_e is the environmental cost of emission in \$/tonCO_2e, and E_{LCA} denotes field to wake emission from RJF in tonCO_2e. PS_{FS} and PS_{RJF} are surpluses of feedstock (FS) producer and RJF processor whereas CS_{FS} and CS_{RJF} are surpluses of FS and RJF consumers respectively.

The impacts of processor-based carbon credit can be further evaluated based on the processor's updated profit objective:

$$Maximize: \Pi = \sum_{k\in K} \left(\sum_{j\in J} \sum_{m\in M} \left((p_k - \delta_{jk}) \sigma \sum_{i\in I} q_{ijm} \right) \right) - \sum_{j\in J} \sum_{m\in M} \left(p_j \sum_{i\in I} q_{ijm} \right)$$

$$-\rho\sigma\sum_{j\in J}\sum_{m\in M}\left(\sum_{i\in I}\ q_{ijm}\right)-\sum_{j\in J}z_j\mu_j\ +\ p_e\left(\Phi_{LCA}\sigma\sum_{j\in J}\sum_{m\in M}\left(\sum_{i\in I}\ q_{ijm}\right)-\ E_{LCA}^{CC}\right),$$

$$(3-5.1)$$

where p_e is the carbon credit in \$/tonCO_2e, Φ_{LCA} denotes well-to-wake (WTW) emission from energy-equivalent CJF in tonCO_2e/gallon, and E_{LCA}^{CC} denotes total field-to-wake (FTW) emission from RJF in tonCO_2e as a result of processor's optimal decisions under carbon credit (CC) scenario.

The total carbon credit is proportional to the GHG emission reductions achieved compared to equivalent CJF based on the LCA methodology. A higher carbon credit encourages the processor for greater reduction in GHG emissions. Consequently, the break-even price for processing facility *j* delivering RJF to airport *k* is reduced:

$$p_{jk}^{BE^{CC}}=\frac{p_j{}^*\sum_{m\in M}\sum_{i\in I}q_{im}^*+\rho\sigma\sum_{m\in M}\sum_{i\in I}q_{im}^*+\delta_j\sigma\sum_{m\in M}\sum_{i\in I}q_{im}^*+z_j{}^*\mu_j-p_e(\Phi_{LCA}(\sigma\sum_{m\in M}\sum_{i\in I}q_{im}^*)-\ E_{LCA}^{CC})}{\sigma\sum_{m\in M}\sum_{i\in I}q_{im}^*}.\qquad(3-11)$$

Stackelberg nature of the game allows processor to influence the optimal decisions of the farmers through its own decisions under carbon credit, which will change the net welfare of the RJF market.

$$Welfare^{CC}=CS_{FS}^{CC}+PS_{FS}^{CC}+CS_{RJF}^{CC}+PS_{RJF}^{CC}-c_eE_{LCA}^{CC},\qquad(3-12)$$

where PS_{FS}^{CC} and PS_{RJF}^{CC} are surpluses of feedstock producer and RJF processor, respectively, while CS_{FS}^{CC} and CS_{RJF}^{CC} are respective surpluses of feedstock and RJF consumers, under the carbon credit scenario. The total carbon credit given by $p_e(\Phi_{LCA}(\sigma\sum_{m\in M}\sum_{i\in I}q_{im}^*)-\ E_{LCA}^{CC})$, lowers the break-even for the processor, and the subsequent contract price between the airlines

and the processor for the RJF production resulting in changes in the welfare. Similarly, the net welfare changes as the total environmental costs are lowered through reduced GHG emissions.

3.4. Analytical Methods

A supply chain framework entailing game-theoretic competition between the farmers and the RJF processor is designed to analyze the economic feasibility of the RJF supply chain. The famers maximize their individual profits competing amongst each other in fulfilling the derived demand (the demand for feedstock is proportional to the RJF demand faced by the processer). The feedstock processor, on the other hand, maximizes its profits nesting the profit maximizing behavior of the individual farmers, and thus acts as a leader which is modeled as a sequential single leader-multiple follower Stackelberg game.

The individual farmers are assumed profit-maximizing rational agents who will take the risk of growing lignocellulosic energy crops such as switchgrass if they are likely to receive a better payoff compared to what they are getting under current crop production. A potential investor interested in RJF processing determines the break-even price level for the negotiated product delivery to foresee its profits before accepting the airlines' offered price leading to an offtake agreement[5]. The RJF processor decides the price offered to the farmers, and the farmer's decision is whether to accept the offered price or not. The processor does not price discriminate and offers all farmers in the region the same price. An individual farmer's decision to land use change and feedstock supply is shaped by whether the offered price meets its minimal profits expectation or not. Essentially, the processor chooses a processing capacity for the potential

[5] Offtake agreements are contracts between fuel consumers and producers specifying the procurement of specified fuel volumes for a period, and have recently been agreed upon with several airlines (Commercial Aviation Alternative Fuels Initiative [CAAFI], 2016).

plant with its spatial configuration along with a price offered to the farmers that minimizes its feedstock procurement and the RJF processing costs. Finally, a premium above the break-even price obtained from the processor's bi-level optimization is used as the contract price between airlines and RJF processor to satisfy the profitability of the processor.

3.4.1. Farmer's Profit Maximization

Switchgrass producer (farmer) decides on biomass supply quantities to maximize its profits considering feedstock price offered at the processing facility subject to land availability and the processing facility capacity constraints. Feedstock price is exogenous to the farmers and is endogenously determined by the processor. The definition for variables, notations and parameters for equations (3-13)-(3-35) is presented in Table 3-A1.

$$\underbrace{Maximize:}_{\substack{\boldsymbol{X_i}=[X_{ih}]_{h\in H} \\ \boldsymbol{XQ_i}=[XQ_{mij}]_{m\in M, j\in J}}} \quad \pi_i = \sum_{j\in J}\sum_{m\in M_{on}} (P_j - \theta) \times XQ_{mij} + \sum_{j\in J}\sum_{m\in M_{off}} (P_j - \gamma - \theta) \times XQ_{mij}$$

$$- \sum_{h\in H} (\alpha + \omega + AM + \beta_{ih}) \times X_{ih}. \qquad (3-13)$$

Subject to

$$X_{ih} \leq A_{ih} \; \forall \; i, h, \qquad (3-14)$$

$$\sum_{j\in J} (XNS_{ij} + XS_{ij}) = Y_{ix} \times \sum_{h\in H} X_{ih} \; \forall \; i, \qquad (3-15)$$

$$\sigma \times \left(XQ_{mij} + \sum_{-i} XQ_{mij} \right) \leq \Delta_{mjg} \times z_{jg} \; \forall \; m, j, \qquad (3-16)$$

$$XNS_{ij} = \sum_{m\in M_{on}} \frac{XQ_{mij}}{(1-DT)} \; \forall \; i, j, \qquad (3-17)$$

$$XS_{ij} = \sum_{m \in M_{off}} \frac{XQ_{mij}}{(1 - DS) \times (1 - DT)} \quad \forall\, i, j, \tag{3 - 18}$$

$$X_{ih} \in \mathbb{R}^{+} \quad \forall\ i, h, \tag{3 - 19}$$

$$XQ_{mij} \in \mathbb{R}^{+} \quad \forall\ m, i, j, \tag{3 - 20}$$

Equation (3-13) defines the profit maximization problem of the individual farmer where the first summation term presents the difference between revenues from feedstock supply and transportation costs incurred during harvest season, while the second term represents the profit subtracting feedstock transportation and storage costs at off-harvest. The third component sums up annualized feedstock establishment, harvest, maintenance, and the opportunity costs of land use change. Opportunity cost is defined as either net returns from existing land use, or land rent, whichever is higher:

$$\beta_{ih} = \begin{cases} P_{ih} \times Y_{ih} - C_{ih} & if\ \ (P_{ih} \times Y_{ih} - C_{ih}) \geq R_{ih} \\ R_{ih} & if\ \ (P_{ih} \times Y_{ih} - C_{ih}) < R_{ih} \end{cases}.$$

Equations (3-14)-(3-20) define the constraints imposed on the profit maximization problem. Equation (3-14) limits feedstock production area to the available agricultural land. Equation (3-15) assures that total biomass available to each farmer equals the total biomass production. Equation (3-16) allows the competitive relationship between the individual farmers. It assures that total biomass supplied by the profit maximizing farmer and all other farmers does not exceed the production capacity of the processing facility. Equations (3-17)-(3-18) are mass balance/flow constraints accounting for the dry matter loss during harvest, storage, and transportation. Equations (3-19)-(3-20) are the non-negativity constraints imposed on the continuous decision variables.

3.4.2. Processor's Profit Maximization (A Bi-level Optimization Problem)

Since the RJF market price is assumed as a contract between the processor and the airlines once the RJF processor identifies its break-even price, the processor's profit maximization is essentially a cost minimization problem. Thus, the RJF processor decides on biomass procurement price and the configuration of facilities to minimize its costs subject to the anticipated optimal behavior of the farmers.

$$\underbrace{Minimize}_{\substack{\boldsymbol{XO}=[XO_{mj}]_{m\in M, j\in J} \\ \boldsymbol{P}=[P_j]_{j\in J} \\ \boldsymbol{Z}=[z_{jg}]_{j\in J, g\,\epsilon\, G}}}: \quad \eta = \sum_{j\in J}\sum_{m\in M}(\rho+\delta)\times XO_{mj} + \sum_{j\in J}\sum_{g\in G}(\mu_g \times z_{jg})$$

$$+\sum_{j\in J}\sum_{m\in M}\left(P_j \times \sum_{i\in I} XQ_{mij}\right). \qquad (3-21)$$

Subject to

$$XO_{mj} = \sigma \times \sum_{i\in I} XQ_{mij} \;\forall\, m, j, \qquad (3-22)$$

$$\sum_{j\in J} XO_{mj} = D_m \;\; \forall\, m, \qquad (3-23)$$

$$\sum_{g\in G} z_{jg} \leq \; 1 \;\forall\, j, \qquad (3-24)$$

$$z_{jg} \in \{0,1\} \;\; \forall \;\; j, g, \qquad (3-25)$$

$$XO_{mj} \in \mathbb{R}^+ \;\; \forall \;\; m, j, \qquad (3-26)$$

$$\pi_i \geq \; r_1 \times \sum_{h\in H} \beta_{ih} \times X_{ih} \;\forall \;\; i, \qquad (3-27)$$

$$Equations\ (3-13) \text{ to } (3-20)\ \forall\ i, \qquad (3-28)$$

Equation (3-21) defines the cost minimization problem of the processor where the first component denotes the total of feedstock-to-RJF conversion and RJF transportation costs. The second term presents the annualized investment costs of processing facilities, whereas the last component counts the feedstock procurement costs of the RJF processor. Equations (3-22)-(3-28) define the constraints imposed on its cost minimization problem. Equation (3-22) ensures that the amount of biomass transported during each season is all converted into RJF by processing facility. Equation (3-23) guarantees RJF sent to airport at each season meets the seasonal demand of RJF. Equation (3-24) limits the number of processing plants at each site. Equations (3-25) and (3-26) denote the domains of the binary and continuous decision variables. Equation (3-27) is an important constraint which assures that profit of individual farmer remains at least r_1 % greater than the opportunity costs. A minimum margin equal to 10% (r_1) is assumed in this study to fulfill the profitability expectations of the potential feedstock suppliers. Finally, equation (3-28) guarantees that the objective function and all the constraints corresponding to individual farmer's profit maximization problem are satisfied.

3.4.3. Solution Approach

The profit maximization problem of the individual farmer is essentially a lower-level problem in this bi-level optimization given the sequential nature of the game with the RJF processor acting as a leader (upper-level problem). Since the lower-level problem is linear, the bi-level optimization can be solved by converting it into a single-level optimization replacing the original objective function and constraints of the lower-level by its corresponding Karush-Kuhn-Tucker (KKT) conditions. The KKT conditions guarantee the stationarity, primal-feasibility, dual-feasibility, and the complementary slackness of the lower-level problem.

$$0 \leq X_{ih} \perp -(\alpha + \omega + AM + \beta_{ih}) - \lambda_{ih}^{1} + Y_{ix} \times \lambda_{i}^{4} \geq 0 \ \forall \ i, h. \qquad (3-13.1)$$

$$0 \leq XQ_{mij} \perp (P_j - \theta) - \sigma \times \lambda_{mj}^{2} + \frac{\lambda_{ij}^{5}}{(1-DT)} \geq 0 \ \forall \ i, j, m \in M_{on}. \qquad (3-13.2)$$

$$0 \leq XQ_{mij} \perp (P_j - \gamma - \theta) - \sigma \times \lambda_{mj}^{3} + \frac{\lambda_{ij}^{6}}{(1-DS)\times(1-DT)} \geq 0 \ \forall \ i, j, m \in M_{off}. \qquad (3-13.3)$$

$$0 \leq \lambda_{ih}^{1} \perp (A_{ih} - X_{ih}) \geq 0 \ \forall \ i, h. \qquad (3-14.1)$$

$$0 \leq \lambda_{mj}^{2} \perp \left[\Delta_{mjg} \times z_{jg} - \sigma \times \left(XQ_{mij} + \sum_{-i} XQ_{mij} \right) \right] \geq 0 \ \forall \ j, m \in M_{on}. \qquad (3-16.1)$$

$$0 \leq \lambda_{mj}^{3} \perp \left[\Delta_{mjg} \times z_{jg} - \sigma \times \left(XQ_{mij} + \sum_{-i} XQ_{mij} \right) \right] \geq 0 \ \forall \ j, m \in M_{off}. \qquad (3-16.2)$$

$$\lambda_{ih}^{1}, \lambda_{mj}^{2}, \lambda_{mj}^{3} \in \mathbb{R}^{+} \ \forall \ i, h, j. \qquad (3-29)$$

$$\lambda_{i}^{4}, \lambda_{ij}^{5}, \lambda_{ij}^{6} \in \mathbb{R} \ \forall \ i, j. \qquad (3-30)$$

Equations (3-14)-(3-20), the primal feasibility constraints of the lower-level problem, remain unchanged. Similarly, equations (3-21)-(3-27), the cost minimization problem of the processor, remain the same. Those equations are thus not shown in the KKT transformation. Equations (3-13.1)-(3-13.3) are the stationarity constraints of the lower-level problem. Equation (3-14.1) presents the complementary condition of the inequality constraint (3-14) whereas equations (3-16.1) and (3-16.2) are the complementary conditions to the inequality constraint (3-16) of the lower-level problem. λ_{ih}^{1}, λ_{mj}^{2}, and λ_{mj}^{3} are the Lagrange multipliers for the inequality constraints (3-14) and (3-16) whereas $\lambda_{i}^{4}, \lambda_{ij}^{5}$, and λ_{ij}^{6} are the Lagrange multipliers for the

equality constraints (3-15), (3-17), and (3-18) respectively. The domains of the introduced Lagrange multipliers are shown in equations (3-29) and (3-30).

The KKT transformation presented above, because of the introduction of stationarity conditions and non-linear complementary constraints, is a non-convex non-linear problem which is often difficult to solve (Gümüş & Floudas, 2005). These constraints are reformulated as disjunctions with the introduction of slack variables, and converted into mixed-integer constraints using Big-M and binary variables (Garcia-Herreros et al., 2016; Gümüş & Floudas, 2005). The resulting problem is solved using the CPLEX solver of the General Algebraic Modeling System (GAMS) (Rosenthal, 2008).

3.4.4. Calculation of LCA-based GHG Emissions

LCA-based GHG emissions from RJF[6] used in determining environmental viability of RJF, is shown in equation (3-31).

$$E_{LCA} = (E_{luc} + E_{energy} + E_{trans} + E_{conv})/1000. \qquad (3-31)$$

$$E_{luc} = \sum_{i \in I} \sum_{h \in H} (\Delta E_{hN2O} + \Delta E_{hCO2} + \Delta E_{hCH4}) \times X_{ih}. \qquad (3-32)$$

$$E_{energy} = \sum_{i \in I} \sum_{h \in H} (ProE + HarE) \times X_{ih} + \sum_{m \in M_{off}} \sum_{i \in I} \sum_{j \in J} XQ_{mij} \times StorE\,. \qquad (3-33)$$

$$E_{trans} = \left(\sum_{m \in M} \sum_{i \in I} \sum_{j \in J} XQ_{mij} \;/Load_{FS} + \sum_{m \in M} \sum_{j \in J} XO_{mj} \,/Load_{RJF} \right) \times TransE. \qquad (3-34)$$

[6] The GHG emissions from feedstock production through RJF delivery to the airport is considered as the LCA-based emission since GHG emission from burning biomass-based renewable fuel is almost equal to the amount of CO_2 sequestered by the biomass during its growth i.e. biogenic carbon (Elgowainy et al., 2012; Wang et al., 2012).

$$E_{conv} = \sum_{m \in M} \sum_{j \in J} XO_{mj} \times OperE. \qquad (3-35)$$

Three categories of GHG emissions from land use change (E_{luc}) which depend on different types of existing land converted into switchgrass, namely CO_2 (ΔE_{hCO2}), N_2O (ΔE_{hN2O}), and CH_4 (ΔE_{hCH4}) are included (equation (3-32))[7]. Similarly, energy consumption emissions (E_{energy}) included emissions from switchgrass production ($ProE$), harvest ($HarE$), and storage ($StorE$). GHG emissions from energy consumption for production and harvest are based on per acre of switchgrass produced and GHG emissions from storage are based on per ton of switchgrass stored (equation (3-33)). GHG emissions from energy consumption during transportation (E_{trans}) of biomass from field to processing facility and of RJF from facility to airport (equation (3-34)) is calculated using the emission factor ($TransE$). Amount of produced RJF is used for calculating the emissions related with feedstock grinding and conversion (E_{conv}) in equation (3-35).

3.4.5. RJF Co-products and RIN Credits

The technical uncertainty related with a specific conversion pathway brings considerable variations in the amount of co-products (Yao et al., 2017). Since the ATJ pathway produces other hydrocarbon fuels as co-products in addition to the RJF, estimation of LCA-based GHG emission for the main-product should account for the contribution of its co-products (Wang, Huo, & Arora, 2011). GHG emissions from the co-products are calculated using allocation method based on their approximately equal energy contents (Han, Tao, & Wang, 2017). On the

[7] Each GHG is converted into carbon dioxide-equivalent (CO_2e) based on its global warming potential (GWP) i.e. releasing each ton of methane (CH_4), and nitrous oxide (N_2O) is equivalent to releasing 25 tons, and 298 tons of CO_2, respectively into the atmosphere.

other hand, the co-products themselves are handled using displacement method generating additional revenue while displacing the energy products at their market prices. Thus, revenues and GHG emission reductions from co-products are included in estimating the economic, environmental, and welfare impacts of RJF.

The RFS established in the Energy Policy Act of 2005 is a market-based compliance system that utilizes RIN credits as a mechanism to trace if biofuel refiners or terminal operators produce the mandated level of biofuels under the Energy Act. Two different RIN credits for cellulosic biofuel i.e. based on average price for 2016 (2016-A), and 2017 (2017-A) are considered to examine its impacts on economic feasibility of RJF. Specific RIN credits for each of the energy products are generated based on the total LCA-based GHG emission reductions (using allocation method) compared to their fossil fuel counterparts. The impact of revenues from ATJ co-products as well RIN credits is exogenous since they are taken as additional economic incentives for supporting RJF production.

3.4.6. Welfare Analysis of RJF

The RJF processor is the consumer of feedstock whereas airlines purchasing the RJF from the processor are considered as the primary consumers of the RJF. It is assumed that the airlines can effectively transfer their cost burden to air-passengers considering their willingness to bear the economic burden if they perceive environmental benefits associated with flying in a renewable fuel propelled aircraft. Given the price assumptions used in satisfying the economic objectives of the supply-chain participants, surpluses for feedstock producers and the RJF processor are equal to the total famer profit and processor's profit, respectively given by:

$$PS_{FS} = \sum_{i \in I} \pi_i.$$

$$PS_{RJF} = r_2 \times \sum_{m \in M} D_m.$$

A \$0.10/gallon (r_2) is assumed as the markup adding to the break-even price that could satisfy the profitability requirements of the RJF processor. There is no surplus for the feedstock consumer i.e. RJF processor since the processor pays what is required to satisfy the profit margins of the feedstock suppliers. Similarly, the consumer in the RJF market i.e. airlines have zero surplus assuming they are price taker based on the margin that satisfies the processor's profits. Finally, the net welfare associated with RJF market is assessed while internalizing the environmental (social) costs of aviation emissions based on the social cost of carbon.

3.4.7. Carbon Credits Scenarios

To estimate the economic, environmental and welfare implication of the hypothetical carbon credits on the RJF supply-chain, the system in equations (3-21)-(3-28) is defined as the reference (Baseline hereafter). The objective function of RJF processor in equation (3-21) is augmented as follows when carbon credits become available:

$$\underbrace{Minimize}_{\substack{\boldsymbol{XO}=[XO_{mj}]_{m\in M,j\in J}\\ \boldsymbol{P}=[P_j]_{j\in J}\\ \boldsymbol{Z}=[z_{jg}]_{j\in J,g\,\epsilon\,G}}}: \quad \eta = \sum_{j\in J}\sum_{m\in M}(\rho+\delta)\times XO_{mj} + \sum_{j\in J}\sum_{g\in G}(\mu_g \times z_{jg}) + \sum_{j\in J}\sum_{m\in M}\left(P_j \times \sum_{i\in I} XQ_{mij}\right)$$

$$-\ p_e\left(\Phi_{LCA}\times\left(\sum_{j\in J}\sum_{m\in M} XO_{mj}\right) - E_{LCA}^{CC}\right). \qquad (3-21.1)$$

Three different carbon credit scenarios corresponding to historical low and high carbon prices in the California Cap-and-Trade program (CalCaT-L and CalCaT-H respectively), and historical high carbon price in the European Union Emission Trading System (EUETS-H) are used to evaluate the impact of potential carbon markets in GHG emissions reduction and supply-chain welfare. These scenarios are intentionally selected to reflect the ranges of the U.S. as well as the global carbon prices in the emission trading market. For the scenarios considered, a r_3 %

of the total carbon credits per gallon of RJF is used as an additional margin in determining the RJF contract price. A 10% (r_3) of the total carbon credits per gallon of RJF is assumed in addition to the $0.10/gallon markup above the break-even for the Baseline in determining the RJF contract price across the carbon credit scenarios.

The leader-follower nature of the game merits the processor in a way that impacts the optimal land use decisions of the feedstock suppliers through its facility location decisions under carbon credits. The processor is able to simultaneously lower the break-even RJF price and GHG emissions since the total carbon credits is proportional to the GHG emission reductions compared to equivalent CJF. This results in changes in net welfare primarily through changes in the surpluses for feedstock suppliers, the processor, and the airlines, respectively given by:

$$PS_{FS}^{CC} = \sum_{i \in I} \pi_i^{CC}.$$

$$PS_{RJF}^{CC} = \left(r_2 + r_3 \times \frac{p_e\left(\Phi_{LCA} \sum_{m \in M} D_m - E_{LCA}^{CC}\right)}{\sum_{m \in M} D_m}\right) \times \sum_{m \in M} D_m.$$

$$CS_{RJF}^{CC} = \left\{\left(p_k^{BE} + r_2\right) - \left(p_k^{BE^{CC}} + r_2 + r_3 \times \frac{p_e\left(\Phi_{LCA} \sum_{m \in M} D_m - E_{LCA}^{CC}\right)}{\sum_{m \in M} D_m}\right)\right\} \times \sum_{m \in M} D_m.$$

3.5. Data

The data used for cellulosic ATJ conversion pathway is categorized into two groups: feedstock-based ethanol production data, and the data on potential conversion technology of ethanol to RJF. Table 3-A2 presents the sources of cost related data on feedstock-based ethanol production, while Table 3-A3 summarizes the data sources and models used to estimate GHG emissions of feedstock-based ethanol production. Table 3-A4 contains the sources of cost, yields including co-products, and GHG emissions corresponding to ethanol-to-RJF conversion, primarily based on recent techno-economic analysis of feedstock-based ATJ or ETJ conversion pathways. These

parameters are augmented with relevant feedstock-based ethanol production data in estimating the feedstock-to-RJF conversion parameters.

Data from switchgrass field trials between 2006 and 2011 at west Tennessee (Boyer et al., 2013; Boyer et al., 2012) is used to simulate feedstock yields across 5 sq. mile spatial units on existing agricultural lands. Mean yields obtained from normally distributed simulations are matched to the number of potential farmers supplying feedstock. Spatial yield variation is mapped following the simulated spatial variation in switchgrass yields in the region (Jager et al., 2010). Simulated yield and potential sites for processing facility and feedstock cultivation are shown in Figure 3-A1. A total of 18 industrial parks are identified as candidates for establishing processing facilities. Each location can have at most one facility with the capacity of either 50 million gallons per year (MGY) or 100 MGY. Similarly, 1936 spatial units are taken as potential feedstock suppliers opting to cultivate switchgrass replacing current crops. An annual RJF demand of 136 million gallons for the Memphis International Airport (MEM) is assumed which replaces 50% of the total jet fuel consumption for flights departing from the MEM airport in 2016[8]. The feedstock price offered to the suppliers for the entire region is assumed to be $75/ton following the simulated farm gate price of $60/ton for biomass feedstock in Perlack et al. (2011) and an average transportation cost in west Tennessee (Yu et al., 2016).

Table 3-A5 presents key conversion parameters used in the analysis including co-products i.e. cellulosic-gasoline and cellulosic-diesel. Conversion cost and GHG emission in the table refers to the parameters associated with feedstock-to-RJF conversion excluding feedstock

[8] Total jet fuel consumption in Tennessee (TN) for the year 2016 was around 13.5 million barrels (U.S. EIA, 2016). Jet fuel consumption at the MEM airport is calculated based on the proportion of departing flights at the MEM airport to the total number of departing flights from seven major TN airports (BTS, 2016a). RJF demand equal to 50% of the total jet fuel consumption reflects the current statutory blending limit for RJF.

grinding. The cost and GHG emission parameters on feedstock grinding are taken into account separately based on Yu et al. (2016). The LCA-based GHG emissions of displaced conventional energy products (fossil fuels) are shown in Table 3-A6. The market prices of fossil fuels displaced by corresponding ATJ products are also included in Table 3-A6. Finally, Table 3-A7 shows the levels of RIN credits used and carbon credits considered for specific carbon credit scenarios. The social cost of carbon at \$33.70/tonCO_2e of GHG emissions is adapted from Nordhaus (2017).

3.6. Results and Discussions

3.6.1. Solutions of the Baseline Stackelberg Model

3.6.1.1. Supply-chain Economic and GHG Emissions Outputs

The overall cost accrued by the RJF processor from the optimal game-theoretic model is \$1,155 million per year. The aggregate profit of individual farmers is around \$16.88 million. Optimal land use decisions for the individual feedstock producers, and the facility location decision for the feedstock processor are shown in Figure 3-A2. An important factor in farmers' decision on converting their land to a new operation is the opportunity cost of land use change. Selection of land for food crops entailed higher opportunity costs compared to pasture land. In addition to varying opportunity costs of supplying feedstock across the existing land uses, spatial variation in switchgrass yields across west Tennessee created comparative advantage to some of the potential feedstock suppliers. A total of 657 thousand acres of farmland is used for feedstock cultivation with 382 thousand acres converting from pasture land. Among converted crop land, soybeans and corn acreages are the primary source for switchgrass production.

Feedstock procurement decisions of the processor depended on rational expectation of the behavior of the profit maximizing farmers in responding to the offered feedstock price. As

such, the processor's facility configuration decisions are influenced by the spatial distribution of the potential feedstock suppliers, their opportunity costs of supplying feedstock, and the spatial yield variability. The processor decided on a larger processing facility i.e. of 100 MGY capacity with concentrated feedstock suppliers owning agricultural lands operating at low opportunity costs. On the other hand, feedstock suppliers with higher yields are pivotal in determining the location for the 50 MGY facility simultaneously securing their profit margins.

The margin over the opportunity cost gained by farmers from supplying feedstock in the study area is shown in the Figure 3-A3. Most of the feedstock suppliers (more than 57%) received a margin up to 47 % over their opportunity cost of converting the land, whereas a few feedstock producers secured substantial margins up to 658%. The observed gains are primarily dictated by the types of land used for feedstock cultivation. In general, the margin is higher for feedstock producers converting pasture land only; whereas less margin is acquired for the ones using either crop land alone or a mix of the pasture and crop land because of the increased opportunity costs of crop land use.

Figure 3-A4 depicts a negative relationship between feedstock suppliers' margin and their break-even costs. The break-even costs are influenced by spatial yield variations, and the proximity of the processing facility locations in addition to the opportunity costs of land use change. Higher break-even costs resulted in lower margin given the exogenous feedstock price ($75/ton) offered by the facilities.

The aggregate annualized costs and GHG emissions by operation in the bi-level supply-chain optimization for the Baseline are summarized in Table 3-A8. As expected, the largest contributor to the processor's economic feasibility is RJF conversion, with a cost of around $515 million. Similarly, feedstock procurement (approximately $382 million) consists of a sizeable

portion of the processor's cost. Given the conversion factor of 26.72 gallons per ton, a total of 5.09 million tons of feedstock is procured for fulfilling the RJF demand at the MEM airport. Feedstock harvest cost of nearly $114 million, followed by feedstock transportation cost of around $107 million, are the highest costs incurred by the feedstock suppliers in aggregate.

The RJF conversion has the highest GHG emissions, above 380 thousand tons of CO_2e with feedstock harvest producing around 265 thousand tons of CO_2e emissions. Land use change resulted in sequestration of around 57 thousand tons of CO_2e emissions primarily achieved when crop lands are used for switchgrass cultivation because of net carbon sequestration in the soil.

3.6.1.2. Supply-chain Welfare Analysis

The net welfare of RJF production for the Baseline is shown in Table 3-A9. The surpluses for feedstock producers (PS-FS) and the RJF processor (PS-RJF) are equal to the total famer profit and processor' profit, respectively, whereas there are no economic surpluses for both the feedstock (CS-FS) and RJF (CS-RJF) consumers. The feedstock suppliers' economic surplus is about $16.88 million with the RJF processor securing a surplus of $13.60 million. Internalized environmental costs of aviation GHG emissions of around $26.20 million resulted in net supply-chain welfare of approximately $4.29 million for the Baseline[9].

3.6.2. Comparison of Carbon Credit Scenarios with the Baseline

3.6.2.1. Change in Optimal Solutions for the Bi-level Objectives

The impact of carbon credits in terms of the change in objective solutions associated with carbon credit scenarios against the Baseline is shown in Figure 3-A5. Processor's cost declined along

[9] This study assumed that airlines agree to purchase the RJF from the feedstock processor at the price that satisfies processor's profit margins inclusive of RIN credits, whether 2016-A or 2017-A, which means the welfare estimates are insensitive to the levels of RIN credits used.

with the level of carbon credits, mainly because of the lessened GHG emissions. Given the availability of carbon credits, the processor' s cost decreased by $17.65, 32.57, and 59.50 million under the CalCaT-L, CalCaT-H, and EUETS-H scenarios, respectively, compared to the Baseline.

The difference in relevant variables between carbon scenarios and the Baseline is summarized in Table 3-A10. Total farmer profit declined by $5.88, 5.90, and 10.45 million for the CalCaT-L, CalCaT-H, and EUETS-H scenarios, respectively, compared to the Baseline level as the opportunity costs of land use increased along with the growth in crop land conversion (see Figure 3-A6). In addition, the processor chose to locate the facility more close to the MEM airport to reduce RJF transportation emissions in response to carbon credits. As a result, the processor's cost also declined as the RJF transportation distance decreased from the facility to the MEM airport. Thus, higher carbon credit i.e. EUETS-H scenario, triggered major changes in land use and facility location resulting in larger changes in objective variables compared to the Baseline. Similarly, increased crop land use in response to proximity of the facility reduced the feedstock transportation costs by $1.72, 1.70, and 2.98 million for the CalCaT-L, CalCaT-H, and EUETS-H scenarios, respectively.

Major GHG emission reductions for the all carbon credit scenarios from the Baseline is associated with land use change. There are minor reductions in GHG emissions associated with feedstock and RJF transportation following the reductions in distance travelled. For the CalCaT-L and CalCaT-H scenarios, the changes in costs and GHG emissions are almost identical since the level of carbon credits do not vary by much between these two scenarios.

3.6.2.2. Change in Welfare Compared to the Baseline

The difference in net welfare for different carbon credit scenarios against the Baseline is illustrated in Figure 3-A7. With higher carbon credits, there is subsequent decrease in the RJF processor's break-even price. The RJF price, based on the profitability assumption under carbon credits, increased the surplus for the processor compared to the Baseline. Similarly, the RJF price at each carbon credit scenario is lower than the Baseline thus increasing the surplus for the RJF consumers i.e. airlines. The surplus for the feedstock producers, i.e. farmers, decreased as more crop land is converted to feedstock production due to carbon credits. The processor, as a leader in the supply-chain, influenced the optimal land use change decisions for the individual farmers through facility location and procurement contracts.

Subsequent abatements in the GHG emissions associated with higher carbon credits reduced the social cost of emissions compared to the Baseline in each carbon credit scenario. The net welfare increased largely across the carbon credit scenarios compared to the Baseline mainly because of the increment in the consumer surplus of the airlines. The net supply-chain welfare increased by $12.71, 27.61, and 50.62 million corresponding to the $16.12, 29.55, and 53.79 million increments in the airlines' surpluses for the CalCaT-L, CalCaT-H, and EUETS-H scenarios, respectively, compared to the Baseline. The welfare gains across scenarios are based on the existence of a potential carbon trading market with assumed carbon prices.

3.6.3. Costs of GHG Emission Abatement with RJF Use

The inclusion of cellulosic RIN credits has substantial impact in lowering the break-even RJF price as well as the cost of aviation emission abatement. Figure 3-A8 depicts the break-even

prices[10] for the RJF considering two levels of cellulosic RIN credits (2016-A and 2017-A) along with revenues from the co-products in the Baseline and three carbon credit scenarios. With the 2017-A RIN credit ($2.69/RIN), the feedstock processor's break-even for the RJF ($1.65/gallon) is lower than the market price of the CJF ($1.76/gallon) regardless of the availability of carbon credits. The RJF remained price-competitive with 2017-A RIN credits after implementing the markup of $0.10/gallon. If the RIN credit remained at the level 2016-A ($1.85/RIN), the break-even price of RJF for the Baseline and three carbon credit scenarios is higher than CJF.

The differences in GHG emissions between the energy products from the ATJ-pathway (RJF, cellulosic-diesel and cellulosic-gasoline) and the displaced fossil fuels (CJF, diesel and gasoline) in the Baseline and all carbon credit scenarios are estimated to evaluate the environmental benefits of ATJ products. For the Baseline, the total LCA-based GHG emission reduction through displacement of the fossil fuels with the ATJ products is 62.5% which lies within the range of 16 to 80% estimated in Han et al. (2017) and de Jong et al. (2017) for various feedstock conversion pathways. With carbon credits, the total GHG emission reduction from using RJF and its co-products is 64% for the CalCaT-L and CalCaT-H scenarios, and 65% for the EUETS-H scenario, compared to the CJF and the displaced fuels.

Cost associated with the LCA-based GHG emissions reduction using RJF including the ATJ co-products varied across the Baseline and carbon credit scenarios. With 2017-A RIN credit, the RJF price ($1.75/gallon) is lower than the market price of the CJF even without the carbon credits, thus no additional cost of GHG emission abatement. However, if the RIN credit

[10] The RJF break-even price level without the RIN credits remained above $7.5/gallon which is generally higher compared to the ones estimated in the recent RJF studies (e.g. Yao et al., 2017; Tao et al., 2017) as the minimal profitability expectation of the individual feedstock suppliers are satisfied given the game-theoretic interaction between the feedstock suppliers and the processor.

remained at 2016-A, the implicit subsidy from the airlines to the processor is $1.89/gallon for the Baseline which decreased to $1.77, $1.67, and $1.49/gallon for the CalCaT-L, CalCaT-H, and EUETS-H scenarios, respectively (Table 3-A11).

Table 3-A11 provides the estimates of GHG emission abatement costs incurred by the airlines under various carbon credit scenarios for the 2016-A RIN credit. The abatement costs correspond to total LCA-based GHG emission reductions from RJF including the ATJ co-products compared to the LCA-based GHG emissions from the displaced CJF. The implicit cost of abatement for the airlines is $198/ton$CO_2$e for the Baseline, which falls in between $42 to 652/ton$CO_2$e estimated in Winchester et al. (2013) and Winchester et al. (2015) for RJF produced from oilseed rotation crops and perennial energy crops. The estimate for the abatement costs further decreased to $182, $172, and $151/ton$CO_2$e for the CalCaT-L, CalCaT-H, and EUETS-H scenarios, respectively.

3.7. Conclusions

This study presents economic and environmental analysis of commercial-scale RJF production using ATJ technology capturing possible interaction amongst the market participants. Impacts of RJF production from switchgrass on farmland allocation, processing facility configuration, and GHG emissions are estimated assuming a bi-level Stackelberg interaction between the feedstock suppliers and the processor in response to fulfilling the RJF demand at the MEM airport in west Tennessee. As a market-based incentive approach to promote RJF production, potential impacts of hypothetical carbon credits on the optimal decisions of the feedstock suppliers and the processor are evaluated primarily in terms of changes in the LCA-based GHG emissions and net supply-chain welfare implications.

The feedstock suppliers' economic surplus is about $16.88 million for the Baseline with the majority of the feedstock suppliers receiving a margin up to 47 % over their opportunity costs of land conversion. Given the availability of carbon credits, the processor's cost decreased by $17.65 to 59.50 million compared to the Baseline. A large portion of the GHG emission reductions, for the processor is achieved when switchgrass is cultivated replacing the crop land because of net carbon sequestration. Consequently, feedstock suppliers having crop lands with high opportunity costs are induced into feedstock production. As a leader of the supply-chain, the processor influenced the land use decisions of the individual farmers through its facility location decisions resulting in a surplus decline of $5.88 to 10.45 million for the feedstock suppliers, compared to the Baseline. The additional markup increased the surplus for the processor compared to the Baseline with increasing carbon credits. On the other hand, airlines secured economic surplus as RJF price decreased when the carbon trading price increased in the hypothetical carbon market. The net supply-chain welfare increased by $12.71 to 50.62 million corresponding to the $16.12 to 53.79 million increments in the airlines' surpluses for the increasing carbon credit scenarios, compared to the Baseline.

Broader environmental impacts of the ATJ products include a 62.5 to 65% LCA-based GHG emission reductions through displacement of the fossil fuels. With the 2017-averaged cellulosic RIN credits, the RJF processor could break-even at lower than the CJF price even for the Baseline. If 2016-averaged cellulosic RIN credits are assumed, the break-even price for the RJF processor is high enough to be price-competitive against the CJF irrespective of the availability of hypothetical carbon credits. Satisfying the assumed profit margins of the processor needed an implicit subsidy from the airlines, of $1.49 to $1.89/gallon if the cellulosic RIN credits

remain at 2016 average. These subsidies are equivalent to GHG emission abatement costs of \$151 to 198/tonCO_2e for the airlines.

This study provided useful insights into economic and environmental impacts of large-scale RJF production in context to the increasing interest shown by the U.S. aviation sector with respect to achieving GHG emissions reduction goals. As a market-based incentive approach, carbon credits are found influential in reducing aviation GHG emissions while simultaneously improving net welfare of RJF sector whereas RIN credits largely determined the economic feasibility. The major limitation of this study is that RJF prices used in the welfare analysis are based on the margins above the break-even prices assumed to satisfy the processor's profits. Similarly, air-passengers are assumed to bear the economic burden of increased airfare conditional on their higher willingness to pay if they perceive environmental benefits from RJF propelled flights. Land use for feedstock cultivation and feedstock processing costs are highly sensitive to the variation in feedstock yield and conversion technology. An improvement in the feedstock yield along with conversion efficiency not only lowers the break-even prices but also reduces the GHG emissions. Future research can focus on incorporating these strategic uncertainties in decision-making process for the development of feedstock-based RJFs while simultaneously addressing the economic motives of the market participants.

References

Agusdinata, D. B., Zhao, F., Ileleji, K., & DeLaurentis, D. (2011). Life cycle assessment of potential biojet fuel production in the United States. *Environmental science & technology*, *45*(21), 9133-9143.

Alternative Fuels Data Center (AFDC). (2017). *Alternative Fuel Price Report*. U.S. Department of Energy, Washington, DC. Retrieved from https://www.afdc.energy.gov/uploads/publication/alternative_fuel_price_report_oct_2017.pdf

Argone National Laboratory. (2013). *The Greenhouse Gases, Regulated Emissions, and Energy Use in Transportation Model (GREET)*. Retrieved from http://www.transportation.anl.gov/publications/index.html

Argone National Laboratory. (2017). *The Greenhouse Gases, Regulated Emissions, and Energy Use in Transportation Model (GREET)*. Retrieved from http://www.transportation.anl.gov/publications/index.html

American Agricultural Economics Association. (2000). *Commodity Cost and Returns Handbook*. Ames, IA.

American Society of Agricultural and Biological Engineers. (2006). *Agricultural Machinery Standards*. St. Joseph, MI.

Bai, Y., Ouyang, Y., & Pang, J.-S. (2012). Biofuel supply chain design under competitive agricultural land use and feedstock market equilibrium. *Energy Economics*, *34*(5), 1623-1633.

Bai, Y., Ouyang, Y., & Pang, J.-S. (2016). Enhanced models and improved solution for competitive biofuel supply chain design under land use constraints. *European Journal of Operational Research*, *249*(1), 281-297.

Bann, S. J., Malina, R., Staples, M. D., Suresh, P., Pearlson, M., Tyner, W. E., . . . Barrett, S. (2017). The costs of production of alternative jet fuel: A harmonized stochastic assessment. *Bioresource technology*, *227*, 179-187.

Bowling, R. G., McKinley, T. L., & Rawls, E. L. (2006). *Tennessee Forage Budgets*. UT extension. The University of Tennessee. Retrieved from http://economics.ag.utk.edu/budgets/PB1658ForageBudgets07.pdf

Boyer, C. N., Roberts, R. K., English, B. C., Tyler, D. D., Larson, J. A., & Mooney, D. F. (2013). Effects of soil type and landscape on yield and profit maximizing nitrogen rates for switchgrass production. *Biomass and Bioenergy*, *48*, 33-42.

Boyer, C. N., Tyler, D. D., Roberts, R. K., English, B. C., & Larson, J. A. (2012). Switchgrass yield response functions and profit-maximizing nitrogen rates on four landscapes in Tennessee. *Agronomy Journal*, *104*(6), 1579-1588.

Bureau of Transportation Statistics (BTS). (2016a). *Airlines and Airports*. U.S. Department of Transportation, Washington, DC. Retrieved from https://www.transtats.bts.gov/NewAirportList.asp?xpage=airports.asp&flag=FACTS

Bureau of Transportation Statistics (BTS). (2016b). *Airline Fuel Cost and Consumption.* U.S. Department of Transportation, Washington, DC. Retrieved from https://www.transtats.bts.gov/fuel.asp?pn=1

California Carbon Dashboard. (2018). *Carbon Price.* Retrieved from http://calcarbondash.org/csv/output.csv

Commercial Aviation Alternative Fuels Initiative (CAAFI). (2016). *2016 Biennial General Meeting*. Retrieved from http://caafi.org/information/pdf/Biennial_Meeting_Oct252016_Opening_Remarks.pdf

Congressional Research Service. (2013). *Renewable Fuel Standard: Overview and Issues*. Retrieved from https://www.ifdaonline.org/IFDA/media/IFDA/GR/CRS-RFS-Overview-Issues.pdf

de Jong, S., Antonissen, K., Hoefnagels, R., Lonza, L., Wang, M., Faaij, A., & Junginger, M. (2017). Life-cycle analysis of greenhouse gas emissions from renewable jet fuel production. *Biotechnology for Biofuels*, *10*(1), 64. doi: 10.1186/s13068-017-0739-7

Diederichs, G. W., Mandegari, M. A., Farzad, S., & Görgens, J. F. (2016). Techno-economic comparison of biojet fuel production from lignocellulose, vegetable oil and sugar cane juice. *Bioresource technology*, *216*, 331-339.

El Takriti, S., Pavlenko, N., & Searle, S. (2017). MITIGATING INTERNATIONAL AVIATION EMISSIONS.

Elgowainy, A., Han, J., Wang, M., Carter, N., Stratton, R., Hileman, J., . . . Balasubramanian, S. (2012). Life-cycle analysis of alternative aviation fuels in GREET: Argonne National Laboratory (ANL).

Fellet, M. (2016). Now Boarding: Commercial Planes Take Flight with Biobased Jet Fuel. *Chemical & Engineering News*, *94*(37), 16-18.

Fribourg, H. A., & Loveland, R. W. (1978). Seasonal Production, Perloline Content, and Quality of Fescue After N Fertilization 1. *Agronomy Journal*, *70*(5), 741. doi: 10.2134/agronj1978.00021962007000050011x

Garcia-Herreros, P., Zhang, L., Misra, P., Arslan, E., Mehta, S., & Grossmann, I. E. (2016). Mixed-integer bilevel optimization for capacity planning with rational markets. *Computers & Chemical Engineering, 86*, 33-47.

Gümüş, Z. H., & Floudas, C. A. (2005). Global optimization of mixed-integer bilevel programming problems. *Computational Management Science, 2*(3), 181-212.

Han, J., Tao, L., & Wang, M. (2017). Well-to-wake analysis of ethanol-to-jet and sugar-to-jet pathways. *Biotechnology for Biofuels, 10*(1), 21. doi: 10.1186/s13068-017-0698-z

International Air Transport Association (IATA). (2015). *IATA Sustainable Aviation Fuel Roadmap*. Retrieved from https://www.iata.org/whatwedo/environment/Documents/safr-1-2015.pdf

International Air Transport Association (IATA). (2017a). *Fact Sheet: Climate Change & CORSIA*. Retrieved from https://www.iata.org/pressroom/facts_figures/fact_sheets/Documents/fact-sheet-climate-change.pdf

International Air Transport Association (IATA). (2017b). *Fact Sheet: Alternative Fuels.* Retrieved from https://www.iata.org/pressroom/facts_figures/fact_sheets/Documents/fact-sheet-alternative-fuels.pdf

Jager, H. I., Baskaran, L. M., Brandt, C. C., Davis, E. B., Gunderson, C. A., & Wullschleger, S. D. (2010). Empirical geographic modeling of switchgrass yields in the United States. *GCB Bioenergy, 2*(5), 248-257.

Jäppinen, E., Korpinen, O. J., & Ranta, T. (2011). Effects of local biomass availability and road network properties on the greenhouse gas emissions of biomass supply chain. *ISRN Renewable Energy*. doi:10.5402/2011/189734

Larson, J. A., Yu, T.-H., English, B. C., Mooney, D. F., & Wang, C. (2010). Cost evaluation of alternative switchgrass producing, harvesting, storing, and transporting systems and their logistics in the Southeastern USA. *Agricultural Finance Review, 70*(2), 184-200.

Luo, Y., & Miller, S. (2013). A game theory analysis of market incentives for US switchgrass ethanol. *Ecological economics, 93*, 42-56.

Mawhood, R., Cobas, A. R., Slade, R., & Final, S. (2014). Establishing a European renewable jet fuel supply chain: the technoeconomic potential of biomass conversion technologies. *Biojet fuel supply Chain Development and Flight Operations (Renjet)*.

Moore, R. H., Thornhill, K. L., Weinzierl, B., Sauer, D., D'Ascoli, E., Kim, J., ... & Barrick, J. (2017). Biofuel blending reduces particle emissions from aircraft engines at cruise conditions. *Nature*, *543*(7645), 411-415.

Muir, J. P., Sanderson, M. A., Ocumpaugh, W. R., Jones, R. M., & Reed, R. L. (2001). Biomass Production of 'Alamo' Switchgrass in Response to Nitrogen, Phosphorus, and Row Spacing. *Agronomy Journal, 93*(4), 896. doi: 10.2134/agronj2001.934896x

Natelson, R. H., Wang, W.-C., Roberts, W. L., & Zering, K. D. (2015). Technoeconomic analysis of jet fuel production from hydrolysis, decarboxylation, and reforming of camelina oil. *Biomass and Bioenergy, 75*, 23-34.

Nordhaus, W. D. (2017). Revisiting the social cost of carbon. *Proceedings of the National Academy of Sciences, 114*(7), 1518-1523.

Perlack, R. D., Eaton, L. M., Turhollow Jr, A. F., Langholtz, M. H., Brandt, C. C., Downing, M. E., ... & Nelson, R. G. (2011). US billion-ton update: biomass supply for a bioenergy and bioproducts industry.

Reimer, J. J., & Zheng, X. (2016). Economic analysis of an aviation bioenergy supply chain. *Renewable and Sustainable Energy Reviews*. *77*, 945-954.

Reimer, J. J., & Crandall, M. S. (2018). Awaiting Takeoff: New Aviation Fuels from Farms and Forests. *Choices*, Quarter 1. Retrieved from http://www.choicesmagazine.org/choices-magazine/submitted-articles/awaiting-takeoff-new-aviation-fuels-from-farms-and-forests

Renewable Fuels Association (RFA). (2017). *Renewable Fuel Standard Program: Standards for 2018 and Biomass-Based Diesel Volume for 2019*. Retrieved from http://www.ethanolrfa.org/wp-content/uploads/2017/08/RFA-Comments_2018-RVO-Proposed-Rule_Final.pdf

Rosenthal, E. (2008). *GAMS-A user's guide.* Paper presented at the GAMS Development Corporation.

Schimel, D. S., Ojima, D. S., Hartman, M. D., Parton, W. J., Brenner, J., Mosier, A. R., & Grosso, S. J. D. (2001). Simulated Interaction of Carbon Dynamics and Nitrogen Trace Gas Fluxes Using the DAYCENT Model. In S. Hansen, M. J. Shaffer & L. Ma (Eds.), *Modeling Carbon and Nitrogen Dynamics for Soil Management*: CRC Press.

Singh, V., & Sharma, S. K. (2015). Fuel consumption optimization in air transport: a review, classification, critique, simple meta-analysis, and future research implications. *European Transport Research Review*, *7*(2), 12. doi: 10.1007/s12544-015-0160-x

Staples, M. D., Malina, R., Olcay, H., Pearlson, M. N., Hileman, J. I., Boies, A., & Barrett, S. R. (2014). Lifecycle greenhouse gas footprint and minimum selling price of renewable

diesel and jet fuel from fermentation and advanced fermentation production technologies. *Energy & Environmental Science, 7*(5), 1545-1554.

Tao, L., Markham, J. N., Haq, Z., & Biddy, M. J. (2017). Techno-economic analysis for upgrading the biomass-derived ethanol-to-jet blendstocks. *Green Chemistry, 19*(4), 1082-1101.

Ugarte, D. G. D. L. T., & Ray, D. E. (2000). Biomass and bioenergy applications of the POLYSYS modeling framework. *Biomass and Bioenergy, 18*(4), 291-308.

University of Tennessee. (2015). *Field crop budgets.* Retrieved from http://economics.ag.utk.edu/budgets.html

U.S. Department of Agriculture ERS. (2015). *Commodity costs and returns*. Retrieved from https://www.ers.usda.gov/data-products/commodity-costs-and-returns/

U.S. Department of Agriculture NASS. (2011). *CropScape-cropland data layer.* Retrieved from http://nassgeodata.gmu.edu/CropScape

U.S. Department of Agriculture NASS. (2013-15). *Crop values annual summary*. Retrieved from http://usda.mannlib.cornell.edu/MannUsda/viewDocumentInfo.do?documentID=1050

U.S. Department of Agriculture NASS. (2013-15). *Cash rents by county.* Retrieved from https://www.nass.usda.gov/Surveys/Guide_to_NASS_Surveys/Cash_Rents_by_County/

U.S. Department of Agriculture NRCS. (2012). *SSURGO structural metadata*. Retrieved from https://www.nrcs.usda.gov/wps/portal/nrcs/detail/soils/survey/geo/?cid=nrcs142p2_053631

U.S. Energy Information Administration (EIA). (2016). *Jet fuel consumption, price, and expenditure estimates*. Retrieved from https://www.eia.gov/state/seds/data.php?incfile=/state/seds/sep_fuel/html/fuel_jf.html

U.S. Environmental Protection Agency (EPA). (2012). *Development of emission rates for heavy-duty vehicles in the motor vehicle emissions simulator MOVES2010*. Retrieved from https://nepis.epa.gov/Exe/ZyPDF.cgi?Dockey=P100F80L.pdf

U.S. Federal Aviation Administration (FAA). (2017). *History of alternative jet fuel use*. Retrieved from https://www.faa.gov/nextgen/where_we_are_now/nextgen_update/images/pp_ee_sb1_body1.png

Wang, M., Han, J., Dunn, J. B., Cai, H., & Elgowainy, A. (2012). Well-to-wheels energy use and greenhouse gas emissions of ethanol from corn, sugarcane and cellulosic biomass for US use. *Environmental research letters, 7*(4). doi: 10.1088/1748-9326/7/4/045905

Wang, M., Huo, H., & Arora, S. (2011). Methods of dealing with co-products of biofuels in life-cycle analysis and consequent results within the US context. *Energy Policy, 39*(10), 5726-5736.

Wang, W.-C., Tao, L., Markham, J., Zhang, Y., Tan, E., Batan, L., . . . Biddy, M. (2016). Review of Biojet Fuel Conversion Technologies: NREL (National Renewable Energy Laboratory (NREL), Golden, CO (United States)).

Wang, X., Ouyang, Y., Yang, H., & Bai, Y. (2013). Optimal biofuel supply chain design under consumption mandates with renewable identification numbers. *Transportation Research Part B: Methodological, 57*, 158-171.

Winchester, N., Malina, R., Staples, M. D., & Barrett, S. R. (2015). The impact of advanced biofuels on aviation emissions and operations in the US. *Energy Economics, 49*, 482-491.

Winchester, N., McConnachie, D., Wollersheim, C., & Waitz, I. A. (2013). Economic and emissions impacts of renewable fuel goals for aviation in the US. *Transportation Research Part A: Policy and Practice, 58*, 116-128.

Wyman, O. (2017). *Aviation 2.0: Why The Next Airplane You Fly On May Be Using Bio Fuels*. Retrieved from https://www.forbes.com/sites/oliverwyman/2017/03/31/aviation-needs-to-embrace-biofuels-to-keep-up-with-ghg-deals/#224936db7a27

Yao, G., Staples, M. D., Malina, R., & Tyner, W. E. (2017). Stochastic techno-economic analysis of alcohol-to-jet fuel production. *Biotechnology for Biofuels, 10*(1), 18. doi: 10.1186/s13068-017-0702-7

Yu, T. E., English, B. C., He, L., Larson, J. A., Calcagno, J., Fu, J. S., & Wilson, B. (2016). Analyzing Economic and Environmental Performance of Switchgrass Biofuel Supply Chains. *BioEnergy Research, 9*(2), 566-577.

Yue, D., & You, F. (2014). Game-theoretic modeling and optimization of multi-echelon supply chain design and operation under Stackelberg game and market equilibrium. *Computers & Chemical Engineering, 71*, 347-361.

Yue, D., & You, F. (2017). Stackelberg-game-based modeling and optimization for supply chain design and operations: A mixed integer bilevel programming framework. *Computers & Chemical Engineering, 102*, 81-95.

Zhao, X., Brown, T. R., & Tyner, W. E. (2015). Stochastic techno-economic evaluation of cellulosic biofuel pathways. *Bioresource technology, 198*, 755-763.

Appendices

Table 3-A 1: Definitions of identifiers, parameters and variables

Category	Unit	Definition
Identifiers		
$i \epsilon I$		spatial unit for switchgrass production (farmer)
$j \epsilon J$		spatial location for facility establishment
$k \epsilon K$		spatial location of RJF delivery (airport)
$g \epsilon G$		annual capacity of processing facility
$m \epsilon M$		season of the year
$M_{on} \epsilon M$		on-harvest season of the year
$M_{off} \epsilon M$		off-harvest season of the year
$h \epsilon H$		crop (pasture/hay, corn, soybean, wheat, sorghum, cotton)
x		switchgrass
Parameters		
P_j	\$/ton	feedstock price offered at the facility
P_{ih}	\$/ton	crop price
Y_{ih}	ton/acre	crop yield
C_{ih}	\$/acre	production cost of crop
Y_{ix}	ton/acre	yield of switchgrass in each spatial unit
R_{ih}	\$/acre	land rent of crop
α	\$/acre	amortized establishment cost of switchgrass field
β_{ih}	\$/acre	opportunity cost of switchgrass cultivation
AM	\$/acre	annual maintenance cost of switchgrass field
μ_g	\$/plant	amortized investment cost of facility
ω	\$/acre	annual harvest cost for switchgrass
γ	\$/ton	cost per unit of storing switchgrass
θ	\$/ton	cost per unit of transporting switchgrass
ρ	\$/gallon	facility operation cost
δ	\$/gallon	RJF transportation cost
DT	%	dry matter loss during transportation

Table 3- A1 Continued

Category	Unit	Definition
A_{ih}	acre	cropland available in each spatial unit for each crop
DS	%	dry matter loss during storage
σ	gallon/ton	switchgrass-RJF conversion rate (ATJ pathway)
Δ_{mjg}	gallon/season	seasonal RJF production capacity of facility
$Load_{FS}$	ton/truck	amount of switchgrass delivered per truck
$Load_{RJF}$	gallon/truck	amount of RJF delivered per truck
ΔE_{hCO2}	$kgCO_2e$/acre	CO_2 emission from land conversion of crop to switchgrass
ΔE_{hN2O}	$kgCO_2e$/acre	N_2O emission from land conversion of crop to switchgrass
ΔE_{hCH4}	$kgCO_2e$/acre	CH_4 emission from land conversion of crop to switchgrass
$ProE$	$kgCO_2e$/acre	GHG emissions factor from energy use during production
$HarE$	$kgCO_2e$/acre	GHG emissions factor from energy use during harvest
$StorE$	$kgCO_2e$/ton	GHG emissions factor from energy use during storage
$TransE$	$kgCO_2e$ /truck/route	GHG emissions from energy use during transportation
$OperE$	kgCO2e /gallon	GHG emissions from processing facility operations
Variables		
z_{jg}		binary variable: 1 for facility selection, 0 otherwise
X_{ih}	acre	switchgrass acreage harvested during harvest season
XNS_{ij}	ton	switchgrass not stored at the harvest site after harvest
XS_{ij}	ton	switchgrass stored at the harvest site after harvest
XQ_{mij}	ton	switchgrass transported to the facility each season
XO_{mj}	gallon	RJF transported from facility to airport each season

Table 3-A 2: Data source for feedstock-based ethanol production costs

Category	**Source**
Land conversion to switchgrass	Opportunity cost
	Land rents: USDA NASS (U.S. Department of Agriculture, 2013-2015)
	Crop yields: USDA, SSURGO (U.S. Department of Agriculture Nature Resources Conservation Service, 2012)
	Crop price and acreage: USDA NASS (U.S. Department of Agriculture, 2013-2015)
	Crop production cost: USDA ERS (U.S. Department of Agriculture, 2015), POLYSIS (Ugarte & Ray, 2000)
	Switchgrass plantation
	Switchgrass yield: Boyer et al. (2013), Boyer et al. (2012), Jager et al. (2010)
	Production and harvest cost: Larson et al. (2010), University of Tennessee (2015)
Production	Establishment: American Agricultural Economics Association (2000)
	Annual maintenance: American Society of Agricultural and Biological Engineers (2006)
Harvest	Fuels and labors: University of Tennessee (2015)
Storage	Covers and pallets: University of Tennessee (2015)
Transport	Trailer, fuel and labor: University of Tennessee (2015)

Table 3-A 3: Data source for feedstock-based ethanol production emissions

Category	**Source**
Land conversion to switchgrass	Land use change: DayCent (Schimel et al., 2001)
	Weather data: DayMET
	Soil texture: USDA SSURGO (U.S. Department of Agriculture Nature Resources Conservation Service, 2012)
	Management practice for food crops: UT extension budget (University of Tennessee, 2015)
	Management practice for pasture/hay: Bowling, McKinley, and Rawls (2006), Fribourg and Loveland (1978)
	Management practice for switchgrass: Muir et al. (2001)
Production	Fuel usage: GREET (Argone National Laboratory, 2013)
Harvest	Fuel usage: GREET (Argone National Laboratory, 2013)
Storage	Fuel usage: GREET (Argone National Laboratory, 2013)
Transport	Fuel usage: MOVES (U.S. EPA, 2012)

Table 3-A 4: Data source for ethanol-to-RJF conversion

Category	**Source**
Conversion efficiency	Han et al. (2017), Yao et al. (2017)[11]
Conversion costs	Tao et al. (2017), Yao et al. (2017)
GHG emission factors	Elgowainy et al. (2012), Han et al. (2017), Wang et al. (2016)
Co-products yields	Han et al. (2017), Yao et al. (2017)

[11] The conversion efficiency from Yao et al. (2017) refers to feedstock-to-ethanol conversion for switchgrass which was consistently used in estimating feedstock-to-RJF conversion costs and GHG emissions.

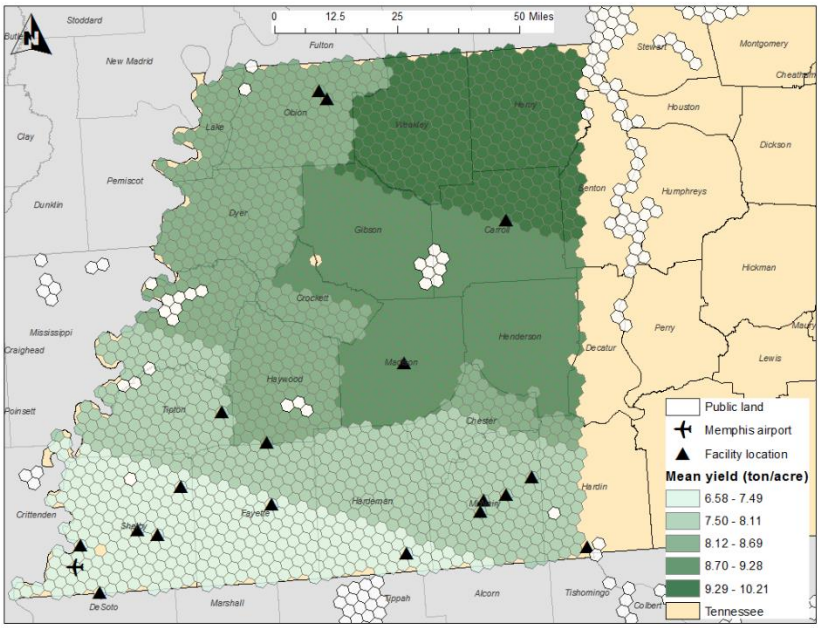

Figure 3-A 1: Potential facility locations and feedstock supply area

Table 3-A 5: Parametric assumptions for cellulosic ATJ conversion[12] pathway

ATJ product	**Conversion yield**	**Unit**	**Source**
RJF	26.72	gallon/ton	Han et al. (2017), Yao et al. (2017)
Cellulosic-gasoline	5.65	gallon/ton	Han et al. (2017), Yao et al. (2017)
Cellulosic-diesel	2.93	gallon/ton	Han et al. (2017), Yao et al. (2017)
ATJ product	**Conversion cost***	**Unit**	**Source**
RJF	1.89	$/gallon	Tao et al. (2017), Yao et al. (2017), Yu et al. (2016)
ATJ product	**Conversion GHG**	**Unit**	**Source**
RJF	2.80	$kgCO_2e$/gallon	Argonne National Laboratory (2017), Yao et al. (2017), Yu et al. (2016)

* All the monetary terms are in 2015 U.S. dollar values.

[12] The parameters for ATJ pathway originally available in energy (mega joule-MJ) units, were converted into volumetric (gallon) units based on energy-equivalence.

Table 3-A 6: Parameters on energy-equivalent substitutes to ATJ products

Fossil fuel	Emission	Unit	Source
CJF	11.2893	$kgCO_2e$/gallon	Wang et al. (2016)
Gasoline	12.2578	$kgCO_2e$/gallon	Elgowainy et al. (2012)
Diesel	12.4956	$kgCO_2e$/gallon	Elgowainy et al. (2012)
Fossil fuel	**Price***	**Unit**	**Source**
CJF	2.4077	$/gallon	BTS (2016b)
Gasoline	2.6688	$/gallon	AFDC (2017)
Diesel	1.7598	$/gallon	AFDC (2017)

* All the monetary terms are in 2015 U.S. dollar values.

Table 3-A 7: RIN credits[13] and parameters for CC scenarios

RIN price*	Unit	Level	Source
2016-A	$/RIN	1.85	RFA (2017)
2017-A	$/RIN	2.69	RFA (2017)
Carbon credit*	**Unit**	**Level**	**Source**
CalCaT-L	$/ton$CO_2e$	11.58	California Carbon Dashboard (2018)
CalCaT-H	$/ton$CO_2e$	22.85	California Carbon Dashboard (2018)
EUETS-H	$/ton$CO_2e$	42.56	Luo and Miller (2013)

* All the monetary terms are in 2015 U.S. dollar values.
Note: 2016-A and 2017-A denote RIN credits for cellulosic biofuel based on average price for 2016 and 2017, respectively. CalCaT-L, CalCaT-H and EUETS-H denote lowest carbon price in the California Cap-and-Trade program, highest carbon price in the California Cap-and-Trade program and highest carbon price in the European Union Emission Trading System, respectively.

[13] Advanced biofuels such as biomass-based biodiesel (BBD) counts as 1.5 or 1.7 RINS (depending on fuel type) to reflect its higher energy content compared to ethanol (Congressional Research Service, 2013). The available RIN prices on cellulosic ethanol were multiplied by a factor of 1.7 for generating cellulosic RJF-based RIN credits.

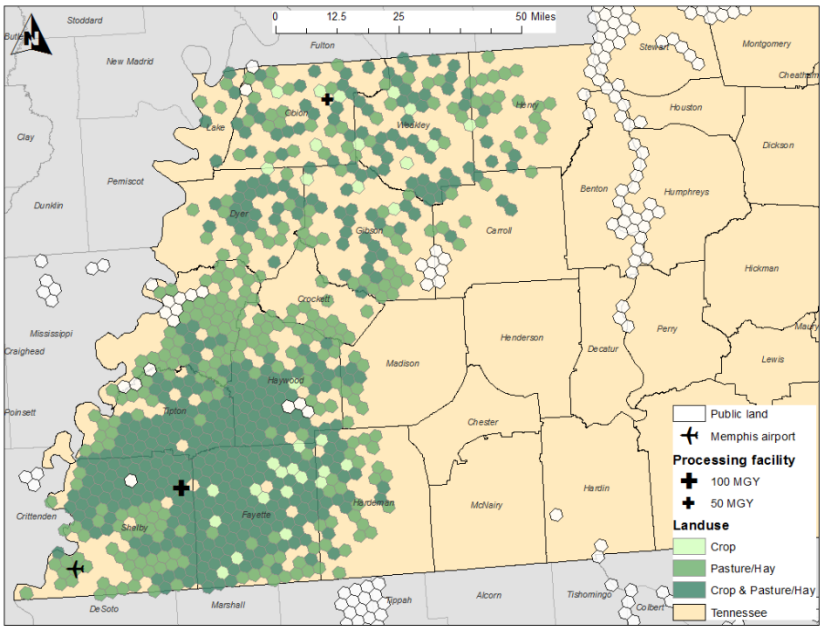

Figure 3-A 2: Optimal land use and facility locations

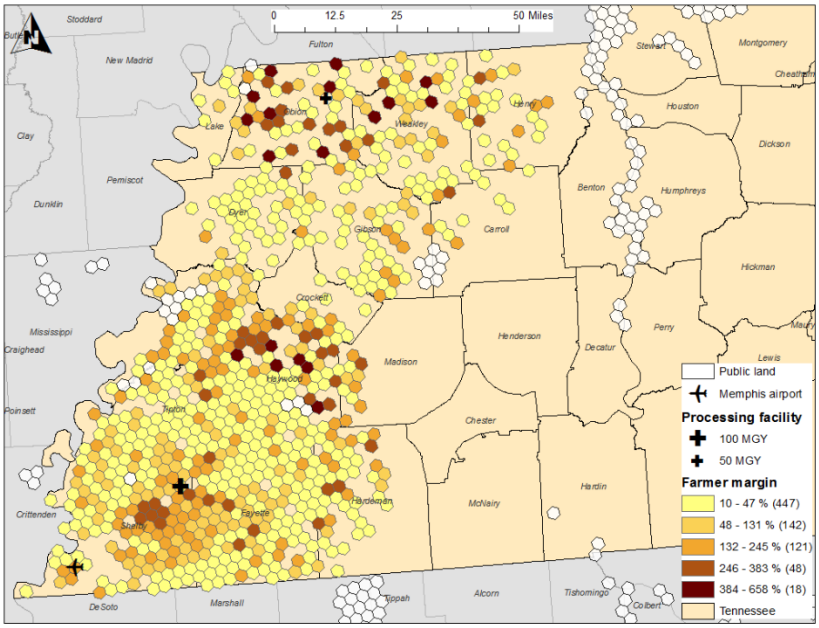

Figure 3-A 3: Margins of individual feedstock suppliers
Note: Number in the parenthesis refers the amount of feedstock suppliers

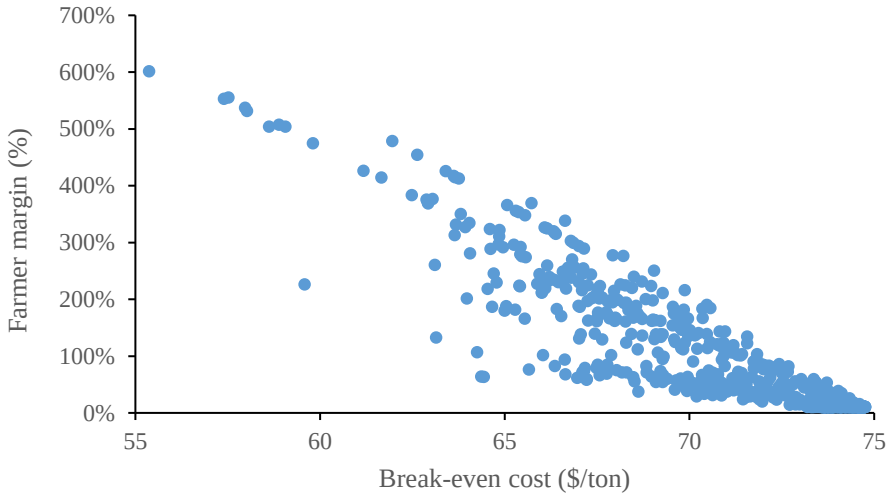

Figure 3-A 4: Feedstock suppliers' break-even costs and margins

Table 3-A 8: Annualized variables for the baseline

Annualized bi-level cost	**Unit**	**Level**
RJF facility investment cost	Million dollars	175.32
Feedstock establishment cost	Million dollars	46.26
Land use opportunity cost	Million dollars	39.88
Feedstock maintenance cost	Million dollars	34.35
Feedstock harvest cost	Million dollars	113.65
Feedstock storage cost	Million dollars	23.97
Feedstock grinding cost	Million dollars	73.75
Feedstock transportation cost	Million dollars	106.73
Feedstock procurement cost	Million dollars	381.72
RJF transportation cost	Million dollars	9.60
RJF conversion cost	Million dollars	514.95
Annualized GHG emission	**Unit**	**Level**
Land use emission	tonCO_2e	(57,299)
Feedstock harvest emission	tonCO_2e	265,319
Feedstock storage emission	tonCO_2e	5,086
Feedstock establishment emission	tonCO_2e	17,773
Feedstock transportation emission	tonCO_2e	26,466
RJF transportation emission	tonCO_2e	3,374
RJF conversion emission	tonCO_2e	380,297
Feedstock grinding emission	tonCO_2e	136,298

Table 3-A 9: Welfare for the baseline

Concept	**Unit**	**Level**
PS-FS	Million dollars	16. 88
PS-RJF	Million dollars	13. 60
Social cost	Million dollars	26.20
Net welfare	Million dollars	4.29

Note: PS-FS and PS-RJF denote surplus for feedstock and RJF producer, respectively.

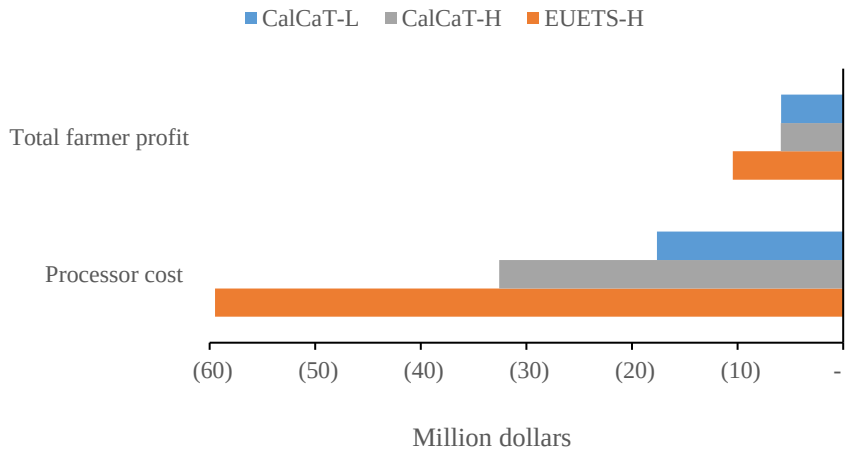

Figure 3-A 5: Reduction in objectives solutions between carbon credit scenarios and the Baseline
Note: CalCaT-L, CalCaT-H and EUETS-H denote lowest carbon price in the California Cap-and-Trade program, highest carbon price in the California Cap-and-Trade program and highest carbon price in the European Union Emission Trading System, respectively.

Table 3-A 10: Difference in annualized variables for carbon credit scenarios compared to Baseline

Annualized bi-level cost	**Unit**	**CalCaT-L**	**CalCaT-H**	**EUETS-H**
Feedstock establishment cost	Million $	0.90	0.90	0.57
Land use opportunity cost	Million $	5.64	5.65	12.20
Feedstock maintenance cost	Million $	0.67	0.67	0.42
Feedstock harvest cost	Million $	0.39	0.39	0.24
Feedstock transportation cost	Million $	(1.72)	(1.70)	(2.98)
RJF transportation cost	Million $	(2.31)	(2.31)	(2.34)
Annualized GHG emission	**Unit**	**CalCaT-L**	**CalCaT-H**	**EUETS-H**
Land use change emission	tonCO_2e	(31,145)	(31,158)	(47,400)
Feedstock harvest emission	tonCO_2e	5,145	5,145	3,242
Feedstock establishment emission	tonCO_2e	345	345	217
Feedstock transportation emission	tonCO_2e	(879)	(865)	(1,369)
RJF transportation emission	tonCO_2e	(1,200)	(1,200)	(1,292)

Note: CalCaT-L, CalCaT-H and EUETS-H denote lowest carbon price in the California Cap-and-Trade program, highest carbon price in the California Cap-and-Trade program and highest carbon price in the European Union Emission Trading System, respectively.

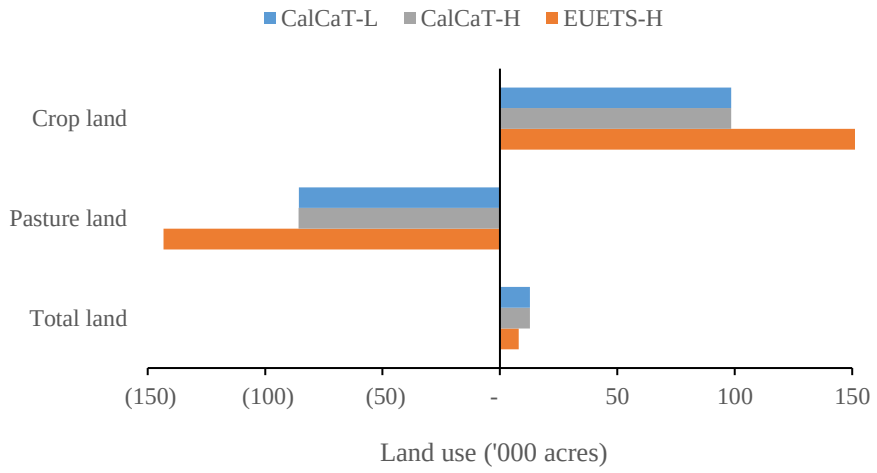

Figure 3-A 6: Difference in land use for carbon credit scenarios compared to Baseline
Note: CalCaT-L, CalCaT-H and EUETS-H denote lowest carbon price in the California Cap-and-Trade program, highest carbon price in the California Cap-and-Trade program and highest carbon price in the European Union Emission Trading System, respectively.

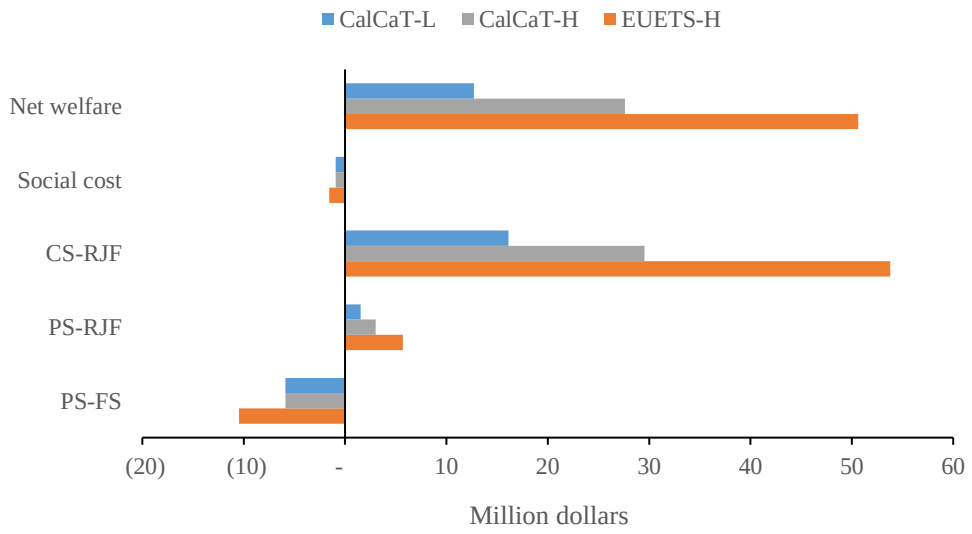

Figure 3-A 7: Difference in net welfare for carbon credit scenarios compared to Baseline
Note: PS-FS, PS-RJF and CS-RJF denote surplus for feedstock producer, surplus for RJF producer and surplus for RJF consumer, respectively. CalCaT-L, CalCaT-H and EUETS-H denote lowest carbon price in the California Cap-and-Trade program, highest carbon price in the California Cap-and-Trade program and highest carbon price in the European Union Emission Trading System, respectively.

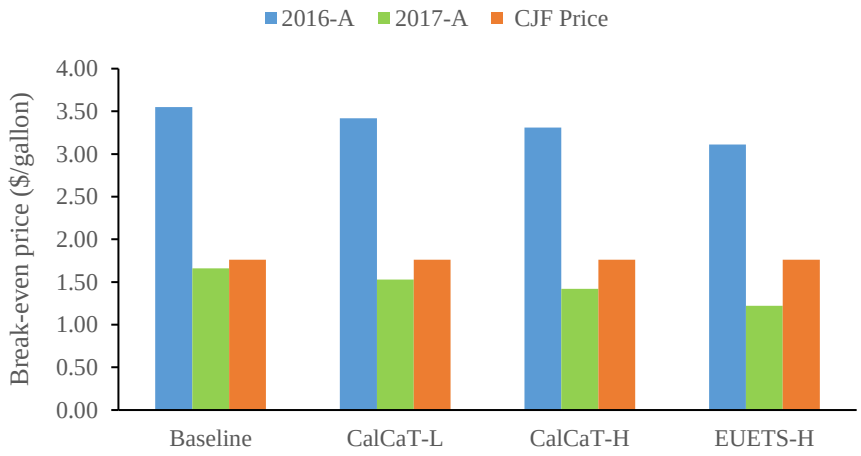

Figure 3-A 8: RJF break-even prices with RIN credits and revenues of co-products
Note: 2016-A and 2017-A denote RIN credits for cellulosic biofuel based on average price for 2016 and 2017, respectively. CalCaT-L, CalCaT-H and EUETS-H denote lowest carbon price in the California Cap-and-Trade program, highest carbon price in the California Cap-and-Trade program and highest carbon price in the European Union Emission Trading System, respectively.

Table 3-A 11: GHG emission abatement costs with 2016-A RIN credit

Variable	Unit	Baseline	CalCaT-L	CalCaT-H	EUETS-H
RJF price	$/gallon	3.6478	3.5293	3.4306	3.2523
Implicit subsidy	$/gallon	1.8880	1.7695	1.6708	1.4925
Abatement cost	$/ton$CO_2$e	198.05	181.73	171.59	151.13

Note: 2016-A denote RIN credit for cellulosic biofuel based on average price for 2016. CalCaT-L, CalCaT-H and EUETS-H denote lowest carbon price in the California Cap-and-Trade program, highest carbon price in the California Cap-and-Trade program and highest carbon price in the European Union Emission Trading System, respectively.

Chapter IV. Designing Cost-effective Payments for Forest-based Carbon Sequestration: An Auction-based Modeling Approach

Abstract

Conservation auctions can reveal information about the opportunity costs of afforestation, which can be combined with the carbon sequestration benefits of land-use changes to design cost-effective payment systems. Furthermore, the impact of integrating cost-benefit information to ensure efficiency gains or to ensure minimal efficiency losses in multi-round conservation auctions, where landowners learn to extract information rents, depends on the level of correlation between costs and benefits. Incorporating discriminatory-price auction theory, and an agent-based model, simulated data is used to examine the cost-efficiency of cost-ranked and cost-benefit-ranked auction-based payment designs for forest-based carbon storage for varying levels of correlation between afforestation opportunity costs and carbon sequestration capacities in static as well as dynamic settings. Results show that the cost-benefit-ranked design is more cost-efficient than the cost-ranked design in a static setting even though the relative spatial heterogeneities of costs and benefits are identical. More importantly, the cost-efficiency of the cost-benefit-ranked design is generally robust to deterioration, when bidders learn over repeated auction rounds, compared with the cost-ranked design, and more resistant to deterioration for some levels of correlation.

Keywords Carbon sequestration, conservation auction, correlation, cost-efficiency, opportunity costs

4.1. Introduction

Payment for ecosystem services (PES), which compensates landowners for the opportunity cost of conservation, is gaining popularity as a policy instrument for environmental conservation because it is more cost-efficient than other indirect approaches (Ferraro & Kiss, 2002; Ferraro & Simpson, 2002; Jack et al., 2008). In general, PES is defined as a voluntary transaction between ecosystem service (ES) users and providers, where the service providers are compensated for an agreed upon bid amount by the users, typically represented by governments or conservation agencies (Wunder, 2005, 2015). The bid amount converges to equilibrium, where the bid equals landowners' opportunity costs of providing ES by overcoming asymmetric information between landowners and conservation agencies seeking to purchase ES (Latacz-Lohmann & Van der Hamsvoort, 1997; Schilizzi & Latacz-Lohmann, 2007; Stoneham et al., 2003). A fixed-rate payment, the most popular form of PES (Zandersen et al., 2009), does not accommodate asymmetric information. Failing to at least partially resolve this asymmetry results in some landowners receiving payments far in excess of their opportunity costs (Ferraro, 2008; Persson & Alpízar, 2013) and large reductions in social welfare arising from the inefficient allocation of payments.

Information asymmetry provides an opportunity to design a PES approach that achieves optimal provision of ES with spatially dependent costs and benefits through a competitive bidding mechanism (Polasky et al., 2014). Conservation agencies around the world are increasingly turning to auctions (hereafter referred to as "conservation auctions") to overcome information asymmetry (Brown et al., 2011; Connor et al., 2008; Stoneham et al., 2003). Standard auction theory primarily uses the independent private values model, where bidders compete for a single indivisible object in a simultaneous non-cooperative game (Milgrom &

Weber, 1982) based on a set of benchmark assumptions: (i) bidders are risk neutral; (ii) bidders have independent private values; (iii) symmetry exists among bidders; (iv) the payment is a function of the bid alone; and (v) the absence of transaction costs (McAfee & McMillan, 1987; Milgrom & Weber, 1982). Although these assumptions are essential in the theoretical design of auctions, they provide little guidance for implementing and analyzing conservation auctions in which multiple landowners with heterogeneous opportunity costs bid for one conservation agency's order in multiple rounds (synonymously referred as "conservation procurement auctions") (Rothkopf & Harstad, 1994; Schilizzi & Latacz-Lohmann, 2007).

Because of the deficit in standard auction theory, few researchers have tried to link standard auction theory to conservation procurement auctions using economic experiments (Cason & Gangadharan, 2004; Cason et al., 2003; Schilizzi & Latacz-Lohmann, 2007) or hypothetical field experiments (Latacz-Lohmann & Van der Hamsvoort, 1997). Nevertheless, the agent-based model, which incorporates the agent's bid-learning behavior, has been applied in multiple-round conservation procurement auctions (Hailu & Schilizzi, 2004; Hailu & Thoyer, 2007; Lennox & Armsworth, 2013). These studies found that conservation auctions are more cost-effective than fixed-rate payment approaches with limited conservation budgets given bidders with heterogeneous opportunity costs. However, the advantage of conservation auctions erodes quickly when bidders learn in successive auction rounds. In general, conservation procurement auctions are substantially more cost-effective than fixed-rate payment approaches, given multiple landowners with heterogeneous opportunity costs of providing ES (Latacz-Lohmann & Schilizzi, 2005).

The cost-efficiency of conservation programs can be enhanced by integrating cost and benefit information into program design. The efficiency gain from integration depends on the

spatial variability of the opportunity costs relative to the environmental benefits. Furthermore, the correlation between the opportunity costs and environmental benefits, along with the landowners' capacities to provide ES, determine the relative gains from incorporating cost-benefit information into an optimal payment system. Although opportunity costs are the most important consideration in devising an optimal conservation payment system, failure to incorporate information about environmental benefits may undermine the cost-efficiency of a conservation program. Even though the costs and benefits of ES have been explored in designing conservation procurement auctions to improve cost-efficiency over fixed-rate systems (Duke et al., 2014; Fooks et al., 2015), limited knowledge is available about how the distributional parameters of costs and benefits impact the cost-efficiency of those auctions. Independent to conservation procurement auction studies, correlation between and variability in the costs and benefits of ES have been analyzed to determine their optimal integration for ensuring a cost-efficient conservation program (Babcock et al., 1997; Ferraro, 2003). Conclusions from these studies, when integrated with insights from auction-based economic experiments, prove useful to conservation agencies in designing a single-round conservation auction (static setting). However, the impact of integrating cost-benefit information to ensure efficiency gains or to ensure minimal efficiency losses in a multi-round conservation auction (dynamic setting), where landowners learn to extract information rents, has not been explored. In addition, knowledge about the impacts of alternative levels of correlation between costs and benefits can help to guide policymakers in choosing an optimal information strategy that ensures the cost-efficiency of a conservation program in a dynamic setting. This study enhances the literature on auction-based economic experiments by estimating the impacts on the cost-efficiency of varying the level of

correlation between opportunity costs and environmental services in multi-round cost-ranked[14] (considers opportunity costs only) and cost-benefit-ranked[15] (considers opportunity costs as well as environmental benefits) conservation auctions.

Ecosystem services received in the form of carbon sequestration from afforestation projects is one way to mitigate the anthropogenic consequences of climate change. Landowners' willingness to accept payment for offering land into an afforestation program and information about the increase in carbon storage from that land are pivotal in designing an optimal payment program for forest-based carbon storage. Conservation auctions can reveal information about the opportunity costs of land-use changes, which can be combined with the carbon sequestration benefits to design a cost-effective payment system. The overall objective of this research is to examine the cost-efficiency of cost-ranked and cost-benefit-ranked auction-based payment designs for forest-based carbon storage for varying levels of correlation between afforestation opportunity costs and carbon sequestration capacities in static as well as dynamic settings. The overarching objective is achieved by simultaneously answering two questions: (1) What are the cost-efficiency gains of cost- and cost-benefit-ranked auction-based payment systems compared to fixed-rate payments under single- and multi-round auctions, and (2) What are the cost-efficiency differences between target-constrained[16] (the conservation or government agency has a fixed conservation target to be achieved) and budget-constrained (the conservation or the government agency has a limited conservation fund to be allocated) models of cost- and cost-benefit-ranked auction-based payment systems under single and multi-round auctions.

---

[14] Equivalent term in the literature is cost-targeting.
[15] Equivalent term in the literature is cost-benefit targeting.
[16] Target refers to hectares of land acquired for afforestation and metric tons of carbon stored in cost-ranked and cost-benefit-ranked designs, respectively.

The study starts with a conceptual framework showing the relationship between conservation payments and correlation between costs and benefits of ES, which in turn determines the efficiency gains/losses under cost-ranked or cost-benefit-ranked auction-based designs. The overbidding inherent in the discriminatory-price auction, which essentially guides the bid simulation for a multi-unit conservation auction, is depicted through theoretically derived Nash-equilibrium bids. The overbidding mechanism, where landowners extract information rents from the conservation agency, determines the gains in efficiency from the auction-based payment designs compared with fixed-rate payments. Using the correlation-driven relationship and discriminatory-price auction theory, an empirical procedure is described that determines the magnitudes of the efficiency gains/losses under alternate payment designs.

To answer the single-round portion of questions (1) and (2), a discriminatory-price auction with a budget constraint is implemented. A discriminatory-price auction is theoretically the multi-unit analogy of the first-price auction (Hailu et al., 2005), where every potential seller in the auction offers a sealed-bid to the buyer and the buyer pays each winning seller an amount equal to the submitted bid. A fixed-rate payment is then selected using the same budget as the auction budget. Equivalently, the land acquired for afforestation using a budget-constrained auction is used as the target in selecting a target-constrained fixed-rate payment. The land acquired for afforestation, or the carbon stored, using the budget-constrained auction is set as the target to be achieved in the target-constrained auction. With opportunity costs arranged in ascending order, the last opportunity cost that exhausts the budget or achieves the target is selected as the fixed-rate payment (Schilizzi & Latacz-Lohmann, 2007).

In answering the multi-round portions of questions (1) and (2), two types of bid-learning algorithms are utilized. These algorithms assume risk-neutrality of the landowners and allow

them to adjust bids in successive rounds based on either the success/failure of their bids alone (referred as L1 type hereafter), or the success/failure of their bids and closest neighbors' bids in the immediately preceding round (referred as L2 type hereafter). Inferences from Nash equilibria optimal bids obtained from the theoretical models are captured in simulating the optimal bids, i.e. submitted bids are an additive combination of land-use opportunity costs and a random stochastic term that captures the overbid amount.

Estimating the impact of varying levels of correlation between costs and benefits is expected to guide policymakers in choosing an optimal information strategy for ensuring the cost-efficiency of a conservation program in a static setting and for ensuring a minimal loss in efficiency under a dynamic setting, regardless of whether the conservation program is budget or target constrained.

4.2. Literature Review

Empirical assessment of real-world conservation contracts provides valuable insights in designing and implementing effective auctions. In the literature on the effective design and implementation of multi-unit, multi-round conservation procurement auctions, few studies have linked existing conservation auction theory with auction-based economic experiments, which include controlled laboratory experiments, hypothetical field experiments, and agent-based models. Auction-based payment systems evaluated in the literature outperform fixed-rate systems in achieving cost-efficiency (Cason & Gangadharan, 2004; Hailu & Schilizzi, 2004; Schilizzi & Latacz-Lohmann, 2007; Stoneham et al., 2003). Similarly, the budget-constrained model is more cost-effective than the target-constrained model when bidders learn to extract information rents from the conservation agency in multiple auction rounds (Schilizzi & Latacz-Lohmann, 2007). Additionally, improved cost-efficiency has been found in payment systems that

integrate information on conservation costs and environmental benefits (Babcock et al., 1997; Duke et al., 2014; Ferraro, 2003; Fooks et al., 2015). Few studies have shown the impact of correlation between conservation costs and benefits, and their relative spatial variability in ensuring efficiency gains in information-optimal payment systems (Babcock et al., 1997; Ferraro, 2003).

Related to question (1), the literature shows auction-based payments are more cost-efficient than fixed-rate payments, but the advantage erodes quickly under repetition of the conservation auction (Cason & Gangadharan, 2004; Hailu & Schilizzi, 2004; Schilizzi & Latacz-Lohmann, 2007; Stoneham et al., 2003). The efficiency reduction in succeeding rounds stems from bid-learning behavior as participants adjusted bids to extract higher information rents from the conservation agency. The Conservation Reserve Program (CRP), implemented by the U.S. Department of Agriculture (USDA), is the world's largest practical application of a multi-round conservation auction (Hellerstein et al., 2015). The cost-efficiency of the CRP gradually decreased with the beneficiaries learning to extract information rents from the government with multiple rounds of contracting (Reichelderfer & Boggess, 1988). Latacz-Lohmann and Van der Hamsvoort (1997) are the first to use auction theory to derive an optimal bidding strategy for a budget-constrained procurement auction and apply it to a hypothetical conservation auction. They showed auctions are generally superior to a fixed-rate payment system because they introduce an element of competition between landowners. Stoneham et al. (2003)'s empirical analysis of a discriminatory-price auction for procuring ES (Victoria's Bush Tender Australia) suggested that, when landholders have heterogeneous non-standard environmental benefits, the auction reduces costs by as much as seven times compared to fixed-price systems to achieve the same conservation benefits. Hailu and Schilizzi (2004) presented an agent-based model to obtain

optimal bids using a discriminatory sealed-bid auction in which submitted bids are ranked by benefit-cost ratios. They showed that the relative advantage of the discriminatory auction over a fixed-payment system deteriorates when bidders learn in a dynamic setting. They also demonstrated that the advantage of the auction over fixed-rate payments is larger for higher fixed-payment levels.

Related to question (2), the literature shows that, though there is no difference in cost-efficiency for an auction constrained by a conservation fund or a target in a single-round, the cost-efficiency of the target-constrained model degrades more quickly than the cost-efficiency of the budget-constrained model under multiple rounds (Schilizzi & Latacz-Lohmann, 2007). This result is attributed to the design of the target-constrained auction itself, because the target must be achieved regardless of budgetary requirement. Schilizzi and Latacz-Lohmann (2007) used controlled laboratory experiments to investigate the budgetary performance of procurement auctions against an equivalent fixed-rate payment. They showed that both the target- and budget-constrained models achieve greater cost-efficiency than the fixed-rate payment program, but that their advantages deteriorate quickly under auction repetition as bidders learn. They also found that the target-constrained auction is more vulnerable to repetition than the budget-constrained auction because the conservation target is unyielding.

Regarding the general question of whether the cost-ranked or cost-benefit-ranked designs perform better in ensuring cost-efficiency gains from competitive bidding, the literature suggests that payment designs based solely on conservation costs or environmental benefits suffer from efficiency losses compared to designs based on cost-benefit ratios (Babcock et al., 1997; Duke et al., 2014; Ferraro, 2003; Fooks et al., 2015). Connor et al. (2008) provided an empirical assessment of the cost-effectiveness of the discriminatory auction (Catchment Care

Auction Australia), and found that the advantage of the discriminatory auction over the uniform payment system depends primarily on cost-benefit prioritization rather than the opportunity cost-revealing mechanism inherent in the auction design. They showed that the transaction and administration costs of auction implementation further reduce the auction's advantage over uniform payments. Glebe (2013) derived theoretical conditions under which concealing or revealing information about site-specific environmental benefits improves auction performance; however, a hypothetical conservation auction provided no guidance for optimal information policy. Duke et al. (2014) provided empirical evidence for the superiority of binary optimization and benefit-cost targeting over sole benefit- or cost-targeting strategies for defining payments under a constrained conservation fund. Fooks et al. (2015) used experimental techniques to explore how endogenous entry in dynamic setting affects auction performance for participants competing solely on costs or cost-benefit ratios for contracting farmland into the CRP. They found cost-efficiency gains for the cost-benefit-ranked auction over the cost-ranked auction from 5% to 15%.

Efficiency gains for cost-benefit-ranked designs over cost-ranked designs are primarily determined by the correlation between conservation costs and benefits and their relative variability (Babcock et al., 1997; Ferraro, 2003). Babcock et al. (1997) found that efficiency losses resulting from targeting low opportunity cost lands or high environmental benefit lands compared to benefit-cost targeting depend on the joint spatial distribution of costs and benefits, i.e. relative variability and the level of correlation between them. Ferraro (2003) described the policy-level implications of integrating cost and benefit information in designing conservation payments considering different levels of relative spatial variability and correlation across conservation costs and benefits. These studies are based on rankings of the conservation costs

and/or benefits with no information on cost-revealing mechanisms, and are primarily focused on a static environment with conservation costs remaining stationary. This study augments the literature by introducing a conservation auction that reveals the opportunity costs of conservation before ranking them, and then conceptualizes the bid-learning behavior of participants in a multi-round conservation auction through an agent-based model. Thus, main objective of this study is to estimate the impacts of integrating cost and benefit information into payment designs to ensure efficiency gains, or minimal efficiency losses, in a multi-round conservation auction where landowners learn to extract information rents. This study improves upon the existing literature by estimating the impacts on the cost-efficiency of single and multi-round cost-ranked and cost-benefit-ranked conservation auctions. The impacts of varying the level of correlation between conservation costs and environmental benefits on the cost-efficiency of procurement auctions in a dynamic setting are yet to be explored. This study contributes to the literature of auction-based economic experiments by estimating the impacts of different levels of correlation between opportunity costs and environmental services on the cost-efficiencies of the cost-ranked and cost-benefit-ranked, multi-round conservation auctions. The resulting impacts will help guide policymakers in choosing optimal information strategies to ensure the cost-efficiency of conservation programs in static and dynamic settings.

4.3. Conceptual Framework

The most commonly used reverse auction in conservation programs, i.e. the discriminatory-price auction is defined, and then the overbidding inherent in the auction through theoretically derived Nash-equilibrium bids is explored (see Proposition 1 below). The overbidding mechanism used by landowners to extract information rent from the conservation agency largely determines the gains in efficiency of auction-based payments compared with uniform payments. The answers to

questions (1) and (2) depend on Proposition 1 (see below), which guides the bid simulation for multi-unit conservation auctions. Polasky et al. (2014) demonstrated that landowners will bid truthfully, assuming the conservation agency has an ex-ante commitment to conservation payments based on the ES social benefits rather than the submitted bids. As such, the payment for each unit of ES will be uniform for all landowners, ruling out price discrimination. Nevertheless, this study uses a discriminatory-price auction to design payments based either explicitly or implicitly on opportunity costs (with inherent overbids), and the associated ES benefits.

Then, the relationship between conservation payments and correlation is described, which determines cost-efficiency[17] gains or losses under cost-ranked or cost-benefit-ranked price discrimination auction-based designs (see Proposition 2 below). The overall objective of estimating cost-efficiencies across different levels of correlation under cost-ranked and cost-benefit-ranked designs is influenced by Proposition 2 (see below). Following discriminatory-price auction theory and the correlation between costs and benefits, this study provides an empirical procedure that determines the efficiency gains or losses under alternate payment designs with respect to answering questions (1) and (2). In answering these questions relevant to multi-round auctions, two bid-learning algorithms are utilized. These algorithms assume landowners are risk-neutral and allow landowners to adjust bids in successive rounds based on the success/failure of their bids alone or the combined knowledge of their bids and nearest neighbors' bids in the immediately preceding round.

[17] Unless otherwise stated cost-efficiency refers to dollar value corresponding to one additional metric ton of carbon sequestered in this study.

4.3.1. Discriminatory-price Auction

When there are multiple sellers and a single buyer of a good, a reverse auction is implemented. Under a first-price reverse auction, each potential seller offers a private bid (sealed-bid) to the buyer. The buyer selects the seller with the lowest bid and pays their bid for the good. However, a first-price reverse auction is designed to sell/buy a single unit of a good. In the case of multiple units of a good or service being sold, as in the case of allocating multiple land parcels owned by numerous landowners for carbon sequestration through afforestation, discriminatory-price or uniform-price reverse auctions are used (Hellerstein et al., 2015; Latacz-Lohmann & Schilizzi, 2005).

The discriminatory-price auction is theoretically analogous to the multi-unit, first-price auction. In the discriminatory-price auction, multiple sellers can be winners based on the bids they offer, subject to the quantity desired or the budgetary constraint of the buyer. Every potential seller in the auction offers a sealed-bid to the buyer. The buyer sorts bids from lowest to highest and pays the bid amounts to the lowest bidders until the desired quantity has been purchased or the allocated budget has been spent. Since the discriminatory-price auction allows bidders to determine their payment bids, their bids and conjectures about the highest bid acceptable to the seller determine their probabilities of winning. Consequently, bidders can extract information rent by bidding higher than their actual opportunity costs. That being said, overbidding is higher for lower-cost bidders and lower for higher-cost bidders (Latacz-Lohmann & Schilizzi, 2005; Latacz-Lohmann & Van der Hamsvoort, 1997; Schilizzi & Latacz-Lohmann, 2007; Schilizzi & Latacz-Lohmann, 2013).

An approximate cap can be imposed to manage overbidding. Setting a reserve price or bid cap becomes more essential for multi-round auctions as bidders learn optimal bidding

strategies in succeeding rounds (Latacz-Lohmann & Schilizzi, 2005; Stoneham et al., 2003). However, providing a bid cap is not as important in discriminatory auctions involving a limited budget since the budget constraint itself serves as an implicit bid cap (Latacz-Lohmann & Schilizzi, 2005; Schilizzi & Latacz-Lohmann, 2013; Stoneham et al., 2003). This study starts with the Nash-equilibrium bidding strategy in a reverse-auction setting for a single good (see section 4-B1 of Appendix 4-B) and then moves to optimal bids in a more complex multi-unit conservation auction constrained by a conservation budget or a target ES amount. The impact on bidding behavior under an implicit bid cap in a budget-constrained model and a bid-cap free target-constrained model is explored in sections 4-B2 and 4-B3 of Appendix 4-B, respectively.

Proposition 1. Overbidding is the dominant strategy in the discriminatory-price auction, and overbidding is higher for bidders with lower opportunity costs than for bidders with higher opportunity costs regardless of whether the conservation auction is constrained by a budget or a target. (See Appendix 4-B for the proof)

4.3.2. Correlation and Payment Design

In this section, an expression for the efficiency response from integrating cost and benefit information into the design of conservation payments is derived, which is central to the overall objective of estimating cost-efficiencies across different levels of correlation under cost-ranked and cost-benefit-ranked designs. The expression relates cost-efficiency to the correlation coefficient between costs and benefits, assuming all other distributional parameters involving opportunity costs and conservation benefits are constant. This relationship guides the efficiency impacts of various levels of correlation between conservation costs and environmental benefits for cost-ranked and cost-benefit-ranked auctions that determine payments for forest-based carbon

storage. The expression that follows depends only on the linear relationship between two variables irrespective of their distributions.

Assuming timber harvesting and going back to the original land use are restricted, a landowner facing the decision to change parcel *i* of non-forestland category *g* (e.g., grassland, pastureland, cropland) to forestland *f* has an opportunity cost[18] of afforestation c_{igf}, expressed as:

$$c_{igf} = nr_{ig} + fc_f + vc_f, \qquad (4-1)$$

where nr_{ig} is the expected net return from *g* for parcel *i*, fc_f is the annuity value of the investment cost in dollars per hectare associated with changing the parcel from its current land use to forest, and vc_f is the management cost of established forest in dollars per hectare.

Following Proposition 1, the Nash-equilibrium bid ($/hectare) for a discriminatory-price auction is:

$$b_{igf} = c_{igf} + \varepsilon_{igf}, \qquad (4-2)$$

where ε_{igf} is the overbid amount ($/hectare) inherent in the discriminatory-price auction. Let ρ_{ce} be the correlation between the opportunity costs and environmental benefits:

$$\rho_{ce} = \frac{Cov(ce)}{\sqrt{Var(c)}\sqrt{Var(e)}} = \frac{\sum_{i\in I} c_{igf}e_{igf} - n\mu_c\mu_e}{\sigma_c\sigma_e}, \qquad (4-3)$$

$$\rho_{ce}\sigma_c\sigma_e = c_{igf}e_{igf} + \sum\nolimits_{-i\in I} c_{-igf}e_{-igf} - n\mu_c\mu_e, \qquad (4-4)$$

[18] Opportunity cost is assumed an aggregate of costs related to participation and complying with the afforestation program conditions i.e. foregone expected net returns from the current land use, annualized forest investment costs, and forest maintenance costs; of which later two are assumed independent of landowner and current land use.

$$c_{igf} = \frac{\rho_{ce}\sigma_c\sigma_e + n\mu_c\mu_e - \sum_{-i\in I} c_{-igf}e_{-igf}}{e_{igf}}, \qquad (4-5)$$

where σ_c and σ_e are standard deviations of the opportunity cost and environmental benefit distributions, respectively, with μ_c and μ_e denoting the means of the corresponding distributions. Equation (4-5) relates the opportunity cost of land use change to the correlation between the opportunity costs and environmental benefits of afforestation.

Proposition 2. The level of correlation between opportunity costs and environmental benefits determines the cost-efficiency of auction-based conservation payments. Additionally, the marginal impact of correlation on cost-efficiency depends not only on the ES-supplying capacity of the selected parcels but also on the spatial distributions, or the spatial heterogeneities, of the opportunity costs and environmental benefits. (See sections 4.3.2.1, and 4.3.2.2 below for the proof)

4.3.2.1. Correlation and Cost-ranked Design

Assuming the winners are selected based on the cost rankings of the submitted bids b_{igf} (obviously these bids are greater than the opportunity costs), the conservation agency maximizes land acquisition for afforestation irrespective of the carbon sequestering benefits e_{igf}. As such, the correlation has no impact on land acquisition since the environmental benefits are not considered in selecting parcels, resulting in no change in the efficiency of the land selected i.e. procurement-efficiency in $/hectare. Nevertheless, total benefits in terms of carbon stored depend on the carbon storage capacities of the land corresponding to cost-ranked bids. Thus, correlation has implicit cost-efficiency consequences.

Let s_{igf} be the hectares of *g* selected for conversion to *f* with *CE* denoting the cost-efficiency of the conservation auction. Dividing total conservation costs by the total amount of

carbon sequestered, provides the cost-efficiency of the payment in dollar per metric ton of carbon stored:

$$CE = \frac{\sum_{i \in I} b_{igf}\, s_{igf}}{\sum_{i \in I} s_{igf} e_{igf}}, \qquad (4-6)$$

$$CE = \frac{\sum_{i \in I} (c_{igf} + \varepsilon_{igf})\, s_{igf}}{\sum_{i \in I} s_{igf}\, e_{igf}}, \qquad (4-7)$$

$$CE = \frac{\sum_{i \in I} \left(\frac{\rho_{ce}\sigma_c\sigma_e + n\mu_c\mu_e - \sum_{-i \in I} c_{-igf} e_{-igf}}{e_{igf}} + \varepsilon_{igf}\right) s_{igf}}{\sum_{i \in I} s_{igf}\, e_{igf}}, \qquad (4-8)$$

where all terms are defined earlier.

Equation (4-8) shows that, even though the environmental benefits are irrelevant in the selection of winning bids, correlation has implicit consequences with respect to the cost-efficiency of the cost-ranked design through the environmental benefits associated with the selected parcels.

Equation (4-9) demonstrates how the implicitly determined cost-efficiency of the cost-ranked conservation auction responds to change in correlation:

$$\frac{\partial CE}{\partial \rho_{ce}} = \frac{\sum_{i \in I} \left(\frac{\sigma_c\sigma_e}{e_{igf}}\right) s_{igf}}{\sum_{i \in I} s_{igf}\, e_{igf}}, \qquad (4-9)$$

where $\frac{\partial CE}{\partial \rho_{ce}}$ is the marginal impact on cost-efficiency for a given change in correlation.

4.3.2.2. Correlation and Cost-benefit-ranked Design

In this section, the relationship between cost-efficiency and correlation is developed when bids are selected based on cost-benefit rankings. Assuming the winners are decided by the cost-benefit rankings obtained by dividing the submitted bids b_{igf}, defined in equation (4-2), by the

respective gains in carbon storage e'_{igf} from changing a non-forest land category g to forestland f, the optimal bids for the conservation agency are:

$$d_{igf} = \frac{b_{igf}}{e'_{igf}} = \frac{c_{igf} + \varepsilon_{igf}}{e'_{igf}}, \qquad (4-10)$$

where d_{igf} is the optimal bid in \$/ton of carbon sequestered.

Equation (4-10) shows that, when the conservation agency maximizes the amount of carbon sequestered, correlation has an indirect impact on parcel selection since selection is based on the rankings of both opportunity costs and environmental benefits, resulting in changes in procurement-efficiency.

Since parcels are selected based on both the opportunity costs and carbon storage capacities of the parcels, correlation directly influences the cost-efficiency of the cost-benefit-ranked design. Let s_{igf} be the hectares of g selected for conversion to f with CE' denoting the cost efficiency of the cost-benefit-ranked conservation auction. The cost-efficiency of the payment in \$/ton of carbon stored is obtained by dividing total conservation cost by total tons of carbon sequestered:

$$CE' = \frac{\sum_{i \in I} d_{igf}\, s_{igf} e'_{igf}}{\sum_{i \in I} s_{igf} e'_{igf}}, \qquad (4-11)$$

$$CE' = \frac{\sum_{i \in I} \left(\frac{c_{igf} + \varepsilon_{igf}}{e'_{igf}}\right) s_{igf} e'_{igf}}{\sum_{i \in I} s_{igf} e'_{igf}}, \qquad (4-12)$$

$$CE' = \frac{\sum_{i \in I} \left(\frac{\rho_{ce}\sigma_c\sigma_e + n\mu_c\mu_e - \sum_{-i \in I} c_{-igf} e_{-igf}}{e_{igf}} + \varepsilon_{igf}\right) s_{igf} e'_{igf}}{\sum_{i \in I} s_{igf} e'_{igf}}. \qquad (4-13)$$

Thus, correlation determines cost-efficiency, which is a direct consequence of the carbon storage capacities corresponding to the parcels selected based on cost-benefit-ranked bids. The

cost-efficiency of the cost-benefit-ranked conservation auction responds to changes in correlation:

$$\frac{\partial CE'}{\partial \rho_{ce}} = \frac{\sum_{i \in I} (\frac{\sigma_c \sigma_e}{e_{igf}})\, s_{igf}}{\sum_{i \in I} s_{igf} e'_{igf}}. \qquad (4-14)$$

From equations (4-8) and (4-13), we see that correlation has implicit or explicit impacts on cost-efficiency through the environmental benefits of the selected parcels. Additionally, variability in the cost and benefit distributions directly impacts the cost-efficiency of payment designs.

From equations (4-9) and (4-14), we see that the marginal impact of correlation on cost-efficiency depends not only on the ES-supplying capacity of the selected parcels but also on the spatial distributions, or the spatial heterogeneities, of the opportunity costs and environmental benefits.

The influence of correlation alone in determining the cost-efficiencies of auction-based payment designs can be estimated by holding the variability in opportunity costs and environmental benefits constant.

Assuming $e'_{igf} > e_{igf}$, the relationship between equations (4-8) and (4-13) is:

$$CE' \leq CE. \qquad (4-15)$$

Similarly, the relationship between equations (4-9) and (4-14) is:

$$\frac{\partial CE'}{\partial \rho_{ce}} \leq \frac{\partial CE}{\partial \rho_{ce}}. \qquad (4-16)$$

If the conservation agency selected parcels with equal opportunity costs and areas, the cost-efficiency of the conservation program for a given degree of correlation and the change in cost-efficiency with respect to a change in correlation would depend on the carbon storage benefits associated with the selected parcels. Since the parcels selected by the cost-benefit-

ranked design are generally expected to have greater environmental benefits than those selected by the cost-ranked design, the cost-benefit-ranked design is expected to be more cost-effective than the cost-ranked design for a given level of correlation (equation (4-15)), and the reduction in cost-efficiency is expected to be lower for the cost-benefit-ranked design than for the cost-ranked design for a given increase in correlation (equation (4-16)).

The conceptual framework described above explores the Nash-equilibrium bids for a multi-unit conservation auction, i.e. a discriminatory-price auction, given a limited budget or a minimal conservation target, revealing the overbidding mechanism that allows landowners to extract information rents from the conservation agency in the form of overbids (Proposition 1). Furthermore, it shows that landowners with lower opportunity costs overbid more than landowners with higher opportunity costs. Similarly, it explains the relationship between conservation payments and correlation, which in turn determines cost-efficiency gains/losses under cost-ranked or cost-benefit-ranked auction-based designs (Proposition 2).

4.4. Empirical Methods

Empirical analysis, for a given level of correlation, estimates the efficiency of the conservation auction where Proposition 1 guides the simulation of the overbids inherent in the discriminatory-price auction, whereas the magnitudes of the efficiency gains/losses under alternate payment designs is determined by Proposition 2. To reveal the opportunity costs of conservation, a discriminatory-price auction is implemented. The submitted bids are either cost ranked or cost-benefit ranked to determine the winners. Based on whether the payment program is constrained by a limited conservation fund or a specified conservation target, either budget-constrained (BC) or target-constrained (TC) models are used. The cost-efficiency outcomes from the models are compared against the fixed-rate payment system. Subsequently, the efficiency losses, when

bidders learn in a dynamic setting, are compared across the models. The efficiencies of the cost-ranked and cost-benefit-ranked designs are compared across five levels of correlation between opportunity costs and conservation benefits.

With respect to evaluating the effect of correlation on efficiency, bids are formed using a stochastic term for overbidding, mimicking a discriminatory-price auction. In the dynamic setting, a simple repetitive bid-learning algorithm is utilized (see section 4.4.1 below for details). The winning bids are then chosen using binary linear optimization under budget and target constraints (see section 4.4.2 below for details). Cost-efficiencies of the payments selected using discriminatory-price auctions with budget and target constraints are compared with an equivalent fixed-rate payment system.

4.4.1. Bid Simulation and Learning

Bids are simulated for the initial auction round using a random term that denotes the amount of overbidding (see equation (4-2)). The overbid ε_{igf} is managed following Proposition 1, such that the overbid is highest for the lowest opportunity-cost landowner and decreased as the opportunity cost increased. To model the bid-learning behavior in multiple auction rounds, a simplistic version of the agent-based model is implemented, which simulates bids as information unfolds in subsequent rounds.

4.4.1.1. Type L1 Bidders

This bid-learning algorithm uses the immediately preceding outcome of the individual bidder. If the landowner's bid is accepted in any round *n*, the bidder either maintains the bid or increases it by 10% in the next round (Lennox & Armsworth, 2013). If the landowner's bid is rejected in any round *n*, the bidder either decreases the bid by 10% or maintains the bid in the next round

(Lennox & Armsworth, 2013). A bid below the opportunity cost is avoided by either decreasing the bid by 10% or decreasing it to the opportunity cost, whichever is higher.

Assuming the bidder is risk neutral, equal probability is assigned to choosing each option for each outcome, and the bid in the $(n+1)^{th}$ round is:

$$b_{igf}^{(n+1)} = \begin{cases} \dfrac{\left[b_{igf}^{n} + 1.1\left(b_{igf}^{n}\right)\right]}{2} & if\ q_{igf}^{n} = 1 \\ \dfrac{\left[Max\left\{0.9\left(b_{igf}^{n}\right), c_{igf}\right\} + b_{igf}^{n}\right]}{2} & if\ q_{igf}^{n} = 0 \end{cases}, \qquad (4-17)$$

where q_{igf} is a binary variable equal to 1 if parcel *i* in land-use *g* is selected for change to forest *f*, 0 otherwise.

4.4.1.2. Type L2 Bidders

This bid-learning algorithm uses the immediately preceding outcomes of the individual bidder and the nearest-neighborhood bidder. If the landowner's and the neighbor's bids are accepted in any round *n*, conditional on the latter's bid being higher than the former's bid, the former would submit a bid in the next round equal to the mean of what each of them would have submitted independently if they had won. If the landowner's bid is accepted and the neighbor's bid is rejected in any round *n*, conditional on the latter's bid being higher than the former's bid, the former would submit a bid in the next round equal to the mean of their bids.

If the landowner's bid is accepted and the neighbor's bid is rejected in any round *n*, conditional on the latter's bid being lower than the former's bid, the former would submit a bid in the next round exactly equal to what the former would have submitted independently if the former had won. If the landowner's bid is rejected in any round *n*, irrespective of the neighbor's bid, the former would submit a bid in the next round exactly equal to what the former would

have submitted independently if the former had lost. For each combination, the bid in the $(n+1)^{th}$ round is:

$$b_{igf}^{(n+1)} = \begin{cases} \dfrac{\left[1.05\left(b_{igf}^{n}\right) + 1.05\left(\bar{b}_{igf}^{n}\right)\right]}{2} & if\ \ q_{igf}^{n} = \bar{q}_{igf}^{n} = 1, and\ \ \bar{b}_{igf}^{n} > b_{igf}^{n} \\ \dfrac{\left[b_{igf}^{n} + \bar{b}_{igf}^{n}\right]}{2} & if\ q_{igf}^{n} = 1, \bar{q}_{igf}^{n} = 0, and\ \ \bar{b}_{igf}^{n} > b_{igf}^{n} \\ \dfrac{\left[b_{igf}^{n} + 1.1\left(b_{igf}^{n}\right)\right]}{2} & if\ \ q_{igf}^{n} = 1, \bar{q}_{igf}^{n} = 0, and\ \ \bar{b}_{igf}^{n} < b_{igf}^{n} \\ \dfrac{\left[Max\left\{0.9\left(b_{igf}^{n}\right), c_{igf}\right\} + b_{igf}^{n}\right]}{2} & if\ \ q_{igf}^{n} = 0 \end{cases},$$

$$(4-18)$$

where $\bar{b}_{igf}$ and $\bar{q}_{igf}$ are the submitted bid and a binary variable for parcel selection, respectively, for the nearest neighbor.

The simulations are extended for 10 bidding rounds for each type of bidder. The winning bids are selected at each auction round using binary linear optimization.

4.4.2. Binary Linear Optimization

4.4.2.1. Cost-ranked Design

The conservation agency ranks the submitted bids b_{igf} in ascending order and selects bids from the lowest toward the highest until the budget is exhausted (BC model). To ensure maximum land acquisition, the binary linear optimization model is:

$$Maximize: \pi = \sum_{i \in I} \sum_{g \in G} q_{igf} \times s_{igf}\ . \qquad (4-19)$$

Subject to

$$\sum_{i \in I} \sum_{g \in G} b_{igf} \times q_{igf} \times s_{igf} \leq \theta. \qquad (4-20)$$

The maximum land π that could be changed to forest is obtained by solving the above binary linear optimization, where θ denotes the conservation agency's budget constraint. The model implicitly determines the amount of carbon sequestered when land-use g is changed to forest.

Suppose the conservation agency sets a conservation target equal to the maximum land achieved in the BC model and achieves that target at minimal cost (TC model). This assumption is made so the BC and TC models could be compared on a level playing field, especially in the multi-round auction. The binary linear optimization model is:

$$Minimize: \theta = \sum_{i \in I} \sum_{g \in G} b_{igf} \times q_{igf} \times s_{igf} \ . \qquad (4-21)$$

Subject to

$$\sum_{i \in I} \sum_{g \in G} q_{igf} \times s_{igf} \ \geq \pi. \qquad (4-22)$$

The minimum budget θ required to change a targeted amount of land to forest is obtained by solving the above binary linear optimization, where π denotes the targeted amount of land-use g changed to forest.

4.4.2.2. Cost-benefit-ranked Design

The conservation agency ranks the bids d_{igf} in ascending order and selects from the lowest toward the highest until the budget is exhausted (BC model). To ensure maximum carbon storage, the binary linear optimization model is:

$$Maximize: \pi = \sum_{i \in I} \sum_{g \in G} q_{igf} \times s_{igf} \times e_{igf}. \qquad (4-23)$$

Subject to

$$\sum_{i \in I} \sum_{g \in G} d_{igf} \times q_{igf} \times s_{igf} \times e_{igf} \leq \theta. \qquad (4-24)$$

The maximum carbon that could be sequestered π by changing eligible land into forest is obtained by solving the above binary linear optimization, where θ denotes the budget constraint of the conservation agency. The model determines the amount of land-use g for change to forest.

Suppose the conservation agency sets the conservation target equal to the maximum carbon sequestered in the BC model and minimizes the cost of achieving that target (TC model). Again, this assumption allowed comparison of the BC and TC models on a common footing, especially in multi-round auction. The binary linear optimization model is:

$$Minimize: \theta = \sum_{i \in I} \sum_{g \in G} d_{igf} \times q_{igf} \times s_{igf} \times e_{igf}. \qquad (4-25)$$

Subject to

$$\sum_{i \in I} \sum_{g \in G} q_{igf} \times s_{igf} \times e_{igf} \geq \pi. \qquad (4-26)$$

The optimization model estimates the minimum budget θ required to sequester the targeted amount of carbon, where π denotes the targeted amount of carbon sequestered.

4.5. Data

Simulated data representing 100 bidders/landowners/parcels is used to compare the cost-efficiencies of cost-ranked and cost-benefit-ranked auction designs against fixed-rate payments, in the presence of variation in correlation between opportunity costs and environmental benefits.

Because the spatial heterogeneities in opportunity costs and benefits influence the cost-efficiencies of the conservation auction designs, this study focuses on varying the level of correlation between costs and benefits, assuming constant and approximately equal relative

spatial variability (coefficient of variation, i.e. CV) of the cost and benefit distributions. Landowner-specific opportunity cost of afforestation i.e. net return from a parcel's current land use (primarily) in $/hectare, area under the current land use in hectares, net gain in carbon sequestration from afforestation of the parcel in ton/hectare, and error term capturing the overbid in $/hectare are all simulated in R using the following random uniform distributions:

$$100 \leq c_{igf} \leq 1000, 50 \leq s_{igf} \leq 500, 5 \leq e_{igf} \leq 45, 5 \leq \varepsilon_{igf} \leq 15.$$

After fixing the opportunity cost and the area under the current land use for each parcel, the net gain in carbon sequestration is assigned to each parcel so that the correlation between the opportunity costs and the carbon net gains varied to produce datasets with five different correlations between the opportunity costs and the environmental benefits:

$$\rho_{ce} \in \{-1, -0.5, 0, 0.5, 1\}.$$

A hypothetical budget outlay of $5 million is used in the BC model. The CVs of simulated cost and benefit distributions are approximately equal to 0.45. Though not necessarily a requirement for this study, the simulated opportunity cost of afforestation i.e. net return from a parcel's current land use (primarily), and the net gains in carbon sequestration from afforestation are within the range used in existing literature (Nielsen et al., 2014; Smith et al., 2006; Stavins & Richards, 2005). The amounts of overbidding, however, are simulated to closely mimic the Nash-equilibria bids for the corresponding opportunity costs.

4.6. Results and Discussions

4.6.1. Fixed-rate Payment and Discriminatory-price Auction in a Static Setting

This section shows the advantages in cost-efficiency of cost-ranked and cost-benefit-ranked discriminatory-price auctions compared with an equivalent fixed-rate payment under budget and

target constraints in a static setting with varying levels of correlation between opportunity costs and carbon storage benefits.

Figures 4-A1 and 4-A2 show the cost-efficiencies of the fixed-rate payments and the cost-ranked and cost-benefit-ranked auction payments for the budget- and target-constrained models respectively. The cost-efficiency of the fixed-rate payment changed across the correlations as well as between the BC and TC models. The cost-efficiencies of the auction-based payments changed across the correlations but are identical for the BC and TC models. The auctions have gains in cost-efficiency compared with fixed-rate payments, which are more prominent for the TC model. Across all payment designs, the most cost-efficient scenario occurred with perfect negative correlation between costs and benefits, whereas the least cost-efficiency occurred with perfect positive correlation between costs and benefits.

4.6.2. BC and TC Discriminatory-price Auctions in a Dynamic Setting

In this section, cost-efficiencies of the two discriminatory-price auction designs is compared under the assumption that bidders learn with repeated rounds to extract information rents from the conservation agency. The efficiency deterioration for the BC and TC models is evaluated.

4.6.2.1. Type L1 Bidders

Figures 4-A3 and 4-A4 show the cost-efficiency losses when the BC cost-ranked and cost-benefit-ranked designs continue for 10 successive rounds. The efficiency losses for the cost-ranked design are 21% ($\rho_{ce} = -1$), 20% ($\rho_{ce} = -0.5$), 26% ($\rho_{ce} = 0$), 46% ($\rho_{ce} = 0.5$), and 34% ($\rho_{ce} = 1$) (Figure 4-A3), whereas the efficiency losses for the cost-benefit-ranked design remained 22% ($\rho_{ce} = -1$), 25% ($\rho_{ce} = -0.5$), 24% ($\rho_{ce} = 0$), 29% ($\rho_{ce} = 0.5$), and 5% ($\rho_{ce} = 1$) (Figure 4-A4).

Figures 4-A5 and 4-A6 show the cost-efficiency losses when the TC cost-ranked and cost-benefit-ranked auction designs continue for 10 consecutive rounds. The efficiency losses for the cost-ranked design are 44% ($\rho_{ce} = -1$), 39% ($\rho_{ce} = -0.5$), 44% ($\rho_{ce} = 0$), 50% ($\rho_{ce} = 0.5$), and 32% ($\rho_{ce} = 1$) (Figure 4-A5), whereas the efficiency losses for the cost-benefit-ranked design remained 47% ($\rho_{ce} = -1$) 46% ($\rho_{ce} = -0.5$), 42% ($\rho_{ce} = 0$), 38% ($\rho_{ce} = 0.5$), and 6% ($\rho_{ce} = 1$) (Figure 4-A6).

For a given level of correlation between the opportunity costs and carbon storage capacities, the BC model suffered a lower loss in cost-efficiency than the TC model. However, the efficiency differences between the BC and TC models are larger for the cost-ranked design compared to the cost-benefit-ranked design.

4.6.2.2. Type L2 Bidders

Figures 4-A7 and 4-A8 show the cost-efficiency losses when the BC cost-ranked and cost-benefit-ranked designs continue for 10 successive rounds. The efficiency losses for the cost-ranked design are 26% ($\rho_{ce} = -1$), 31% ($\rho_{ce} = -0.5$), 39% ($\rho_{ce} = 0$), 39% ($\rho_{ce} = 0.5$), and 44% ($\rho_{ce} = 1$) (Figure 4-A7), whereas those of cost-benefit-ranked design remained 30% ($\rho_{ce} = -1$), 29% ($\rho_{ce} = -0.5$), 27% ($\rho_{ce} = 0$), 28% ($\rho_{ce} = 0.5$), and 5% ($\rho_{ce} = 1$) (Figure 4-A8).

Figures 4-A9 and 4-A10 show the cost-efficiency losses when the TC cost-ranked and cost-benefit-ranked auction designs continue for 10 successive rounds. The efficiency losses for the cost-ranked design are 52% ($\rho_{ce} = -1$), 49% ($\rho_{ce} = -0.5$), 41% ($\rho_{ce} = 0$), 57% ($\rho_{ce} = 0.5$), and 38% ($\rho_{ce} = 1$) (Figure 4-A9), whereas those for the cost-benefit-ranked design remained 60% ($\rho_{ce} = -1$), 48% ($\rho_{ce} = -0.5$), 41% ($\rho_{ce} = 0$), 35% ($\rho_{ce} = 0.5$), and 1% ($\rho_{ce} = 1$) (Figure 4-A10).

Contrary to L1 bidders, no obvious cost-efficiency differences existed between BC and TC models for the cost-ranked design for L2 bidders compared to the cost-benefit-ranked design for a given level of correlation, but the losses in cost-efficiency are higher for L2 bidders for cost-ranked designs compared to L1 bidders.

For perfectly positive correlation between opportunity costs and environmental benefits, the cost-benefit-ranked design suffered lower cost-efficiency losses under repeated rounds than the cost-ranked design whether for L1 or L2 type bidders. Although the cost-efficiency gains from repeated auction rounds are highest for both the cost- and cost-benefit-ranked designs with perfectly negative correlation in a static setting, their efficiency losses are highest in the dynamic setting for both designs if the conservation program has a strict conservation target. In general, the efficiency losses are higher for cost-ranked designs for L2 compared to L1 bidders, whereas the losses remained almost similar for cost-benefit-ranked designs across L1 and L2 bidders.

4.6.3. Fixed-rate Payment and Discriminatory-price Auction in a Dynamic Setting

To see whether the inclusion of spatial information on both costs and benefits, i.e. the cost-benefit-ranked design, improved the cost-efficiency of forest-based carbon sequestration payments compared with the fixed-payment design in a static setting, and whether this information helped in minimizing the efficiency losses when bidders learn to extract information rents in a dynamic setting, the losses or gains in efficiency is compared under the assumption of a strictly limited conservation fund of $5 million.

The differences in cost-efficiency between designs at each level of correlation are influenced by the relative spatial variabilities in the opportunity costs and carbon storage capacities (environmental benefits). The simulated data on opportunity costs (net returns, primarily) and carbon storage capacities have almost identical relative spatial variabilities. Had

there been a greater CV for benefits compared with costs, the cost-benefit-ranked design might have been more cost-efficient than the cost-ranked design. This analysis, however, focused on estimating the efficiency losses or gains of these two designs by controlling for the distribution parameters of costs and benefits and allowing for different levels of correlations between costs and benefits.

Compared with the auction-equivalent, fixed-rate payment under a budget constraint in a static setting, the cost-efficiency gains for the cost-ranked design are 16% ($\rho_{ce} = -1$), 16% ($\rho_{ce} = -0.5$), 26% ($\rho_{ce} = 0$), 31% ($\rho_{ce} = 0.5$), and 36% ($\rho_{ce} = 1$) (Figure 4-A11), whereas the efficiency gains for the cost-benefit-ranked design are 17% ($\rho_{ce} = -1$), 25% ($\rho_{ce} = -0.5$), 35% ($\rho_{ce} = 0$), 39% ($\rho_{ce} = 0.5$), and 40% ($\rho_{ce} = 1$) (Figure 4-A12).

In the case of L1 bidders, after 10 auction rounds, the cost-efficiency gains for the cost-ranked design are -1% ($\rho_{ce} = -1$), 0% ($\rho_{ce} = -0.5$), 7% ($\rho_{ce} = 0$), -1% ($\rho_{ce} = 0.5$), and 14% ($\rho_{ce} = 1$) (Figure 4-A11), whereas for the cost-benefit-ranked design they are -1% ($\rho_{ce} = -1$), 7% ($\rho_{ce} = -0.5$), 19% ($\rho_{ce} = 0$), 21% ($\rho_{ce} = 0.5$), and 37% ($\rho_{ce} = 1$) (Figure 4-A12). However, in the case of L2 bidders, the cost-efficiency gains for the cost-ranked design are -6% ($\rho_{ce} = -1$), -10% ($\rho_{ce} = -0.5$), -3% ($\rho_{ce} = 0$), 4% ($\rho_{ce} = 0.5$), and 8% ($\rho_{ce} = 1$) (Figure 4-A11), whereas for the cost-benefit-ranked design they are -8% ($\rho_{ce} = -1$), 3% ($\rho_{ce} = -0.5$), 17% ($\rho_{ce} = 0$), 22% ($\rho_{ce} = 0.5$), and 37% ($\rho_{ce} = 1$) (Figure 4-A12).

Thus, the gain in cost-efficiency deteriorated more noticeably for the cost-ranked design in a dynamic context than for the cost-benefit-ranked design at each level of correlation whether the bidders were of L1 or L2 type. Furthermore, the difference in efficiency losses between L1 and L2 type bidders is higher for the cost-ranked design, with L2 bidders suffering greater

deterioration in cost-efficiency. However, the efficiency loss is almost stable across L1 and L2 type bidders in the case of the cost-benefit-ranked design.

Even though the relative spatial heterogeneities of costs and benefits are almost identical, the advantages of cost-benefit-ranked, auction-based payment designs over cost-ranked designs are evident in a dynamic setting, especially for strong positive correlation between costs and benefits. Conversely, when costs and benefits has strong negative correlation, cost-benefit ranked designs lose their advantage over fixed-rate payment designs rather quickly when bidders learn, because the low opportunity cost bidders extract maximum information rent by bidding higher while still being selected because of higher environmental benefits.

To summarize, the cost-benefit-ranked design is more cost-efficient than the cost-ranked design in a static setting even though the relative spatial heterogeneities are almost identical. More importantly, the cost-efficiency of the cost-benefit-ranked design is generally more robust to deterioration when bidders learn in different ways over repeated auction rounds and more resistant to erosion for certain levels of correlation compared to the cost-ranked design.

4.7. Conclusions

The existing literature on auction-based economic experiments has contributed to answering questions related to the cost-efficiency of different designs and types of conservation auctions. This study expands the literature by estimating the impact of correlation between conservation costs and environmental benefits on the cost-efficiency of conservation auctions in a dynamic setting. Specifically, the impact on cost-efficiency of cost-ranked and cost-benefit-ranked multi-round conservation auctions is estimated. The impact of correlation is estimated while controlling for the relative spatial variability between costs and benefits in a dynamic setting when bidders learn to extract information rents.

Using simulated data, this study showed that the auctions have efficiency gains compared to a fixed-rate payment design, and the efficiency gains are more prominent for the TC model compared to the BC model. The cost-efficiency of fixed-rate payment changed across correlations as well as the BC and TC models, which however, differed with the auction designs. The cost-efficiencies of the auction-based payment designs changed as the correlation between costs and benefits changed, but remained identical between the BC and TC models. Across both the fixed-rate and auction-based payment designs, cost-efficiency is highest for perfect negative correlation between costs and benefits, whereas it is lowest when correlation approaches perfectly positive. Another important feature common to both the cost- and cost-benefit-ranked designs is that the BC and TC models yield the same cost-efficiency in a static setting even though they differ across spatial correlations.

In a dynamic setting where bidders extract information rents through learning, holding correlation between costs and benefits constant, the BC model suffered less deterioration in efficiency, compared to the corresponding TC model. In addition, the efficiency difference between BC and TC models increased in subsequent rounds when correlation between costs and benefits became more negative. However, the efficiency losses are greater for cost-ranked design compared to the cost-benefit-ranked design, especially when bidders learned through their own and their neighbor's experience. For perfect positive correlation between environmental benefits and opportunity costs, the cost-benefit-ranked design suffered the smallest efficiency losses under repeated auction rounds. Although efficiency gains are highest for both the cost- and cost-benefit-ranked designs with perfect negative correlation between costs and benefits in a static setting, efficiency losses are highest for both designs in a dynamic setting when the conservation program had a fixed target to achieve.

Considering the potential impacts of correlation in determining an optimal information strategy for designing a cost-efficient payment for forest-based carbon sequestration under multi-round conservation auctions, this study examined the cost-efficiency of cost-ranked and cost-benefit-ranked auction-based payment designs for forest-based carbon storage for varying levels of correlation between afforestation opportunity costs and carbon sequestration capacities in static as well as dynamic settings. One limitation of this study is that the costs of administering the auction-based conservation programs are not addressed which might impact the cost-efficiency of the auction-based payments. Furthermore, opportunity costs are uniformly distributed guaranteeing high spatial correlation. However, a random distribution of opportunity costs in a landscape with low spatial correlation might influence bid-learning behavior differently, and thus influence cost-efficiency differently. Future research can focus on designing laboratory experiments taking current framework as a benchmark, to estimate the cost-efficiency of multi-round auction-based payments while taking into account administrative costs of program implementation, and spatial dependence among landowner opportunity costs.

References

Babcock, B. A., Lakshminarayan, P., Wu, J., & Zilberman, D. (1997). Targeting tools for the purchase of environmental amenities. *Land Economics*, 325-339.

Brown, L. K., Troutt, E., Edwards, C., Gray, B., & Hu, W. (2011). A uniform price auction for conservation easements in the Canadian prairies. *Environmental and Resource Economics, 50*(1), 49-60.

Cason, T. N., & Gangadharan, L. (2004). Auction design for voluntary conservation programs. *American Journal of Agricultural Economics, 86*(5), 1211-1217.

Cason, T. N., Gangadharan, L., & Duke, C. (2003). A laboratory study of auctions for reducing non-point source pollution. *Journal of environmental economics and management, 46*(3), 446-471.

Connor, J. D., Ward, J. R., & Bryan, B. (2008). Exploring the cost effectiveness of land conservation auctions and payment policies. *Australian journal of agricultural and resource economics, 52*(3), 303-319.

Duke, J. M., Dundas, S. J., Johnston, R. J., & Messer, K. D. (2014). Prioritizing payment for environmental services: Using nonmarket benefits and costs for optimal selection. *Ecological economics, 105*, 319-329.

Ferraro, P. J. (2003). Assigning priority to environmental policy interventions in a heterogeneous world. *Journal of Policy Analysis and Management, 22*(1), 27-43.

Ferraro, P. J. (2008). Asymmetric information and contract design for payments for environmental services. *Ecological economics, 65*(4), 810-821.

Ferraro, P. J., & Kiss, A. (2002). Direct payments to conserve biodiversity. *Science, 298*(5599), 1718-1719.

Ferraro, P. J., & Simpson, R. D. (2002). The cost-effectiveness of conservation payments. *Land Economics, 78*(3), 339-353.

Fooks, J. R., Messer, K. D., & Duke, J. M. (2015). Dynamic entry, reverse auctions, and the purchase of environmental services. *Land Economics, 91*(1), 57-75.

Glebe, T. W. (2013). Conservation auctions: should information about environmental benefits be made public? *American Journal of Agricultural Economics, 95*(3), 590-605.

Hailu, A., & Schilizzi, S. (2004). Are auctions more efficient than fixed price schemes when bidders learn? *Australian Journal of Management, 29*(2), 147-168.

Hailu, A., Schilizzi, S., & Thoyer, S. (2005). *Assessing the performance of auctions for the allocation of conservation contracts: Theoretical and computational approaches.* Paper presented at the Paper selected for the American Agricultural Economics Association Annual Meeting, Providence, Rhode Island.

Hailu, A., & Thoyer, S. (2007). Designing Multi-unit Multiple Bid Auctions: An Agent-based Computational Model of Uniform, Discriminatory and Generalised Vickrey Auctions. *Economic Record, 83*(s1), S57-S72.

Harris, M., & Raviv, A. (1981). Allocation mechanisms and the design of auctions. *Econometrica: Journal of the Econometric Society*, 1477-1499.

Hellerstein, D., Higgins, N., & Roberts, M. J. (2015). *Options for Improving Conservation Programs: Insights From Auction Theory and Economic Experiments*. Economic Research Report, U.S. Department of Agriculture, Economic Research Service. Retrieved from https://papers.ssrn.com/sol3/papers.cfm?abstract_id=2737112

Jack, B. K., Kousky, C., & Sims, K. R. (2008). Designing payments for ecosystem services: Lessons from previous experience with incentive-based mechanisms. *Proceedings of the National Academy of Sciences, 105*(28), 9465-9470.

Latacz-Lohmann, U., & Schilizzi, S. (2005). Auctions for conservation contracts: a review of the theoretical and empirical literature. *Report to the Scottish Executive Environment and Rural Affairs Department, 15*.

Latacz-Lohmann, U., & Van der Hamsvoort, C. (1997). Auctioning conservation contracts: a theoretical analysis and an application. *American Journal of Agricultural Economics, 79*(2), 407-418.

Lennox, G. D., & Armsworth, P. R. (2013). The ability of landowners and their cooperatives to leverage payments greater than opportunity costs from conservation contracts. *Conservation Biology, 27*(3), 625-634.

McAfee, R. P., & McMillan, J. (1987). Auctions and bidding. *Journal of economic literature, 25*(2), 699-738.

Milgrom, P. R., & Weber, R. J. (1982). A theory of auctions and competitive bidding. *Econometrica: Journal of the Econometric Society*, 1089-1122.

Nielsen, A. S. E., Plantinga, A. J., & Alig, R. J. (2014). *New cost estimates for carbon sequestration through afforestation in the United States*. General Technical Report, U.S. Department of Agriculture, Pacific Northwest Research Station. Retrieved from http://citeseerx.ist.psu.edu/viewdoc/download?doi=10.1.1.643.3064&rep=rep1&type=pdf

Persson, U. M., & Alpízar, F. (2013). Conditional cash transfers and payments for environmental services—a conceptual framework for explaining and judging differences in outcomes. *World Development, 43*, 124-137.

Polasky, S., Lewis, D. J., Plantinga, A. J., & Nelson, E. (2014). Implementing the optimal provision of ecosystem services. *Proceedings of the National Academy of Sciences, 111*(17), 6248-6253.

Reichelderfer, K., & Boggess, W. G. (1988). Government decision making and program performance: the case of the conservation reserve program. *American Journal of Agricultural Economics, 70*(1), 1-11.

Riley, J. G., & Samuelson, W. F. (1981). Optimal auctions. *The American Economic Review, 71*(3), 381-392.

Rothkopf, M. H., & Harstad, R. M. (1994). Modeling competitive bidding: A critical essay. *Management science, 40*(3), 364-384.

Schilizzi, S., & Latacz-Lohmann, U. (2007). Assessing the performance of conservation auctions: an experimental study. *Land Economics, 83*(4), 497-515.

Schilizzi, S., & Latacz-Lohmann, U. (2013). Conservation tenders: linking theory and experiments for policy assessment. *Australian journal of agricultural and resource economics, 57*(1), 15-37.

Smith, J. E., Heath, L. S., Skog, K. E., & Birdsey, R. A. (2006). *Methods for calculating forest ecosystem and harvested carbon with standard estimates for forest types of the United States*. General Technical Report, U.S. Department of Agriculture Forest Service, Northeastern Research Station. Retrieved from http://www.actrees.org/files/Research/ne_gtr343.pdf

Stavins, R. N., & Richards, K. R. (2005). *The cost of U. S. forest-based carbon sequestration*. Pew Economics Report, Pew Center on Global Climate Change. Retrieved from

https://www.c2es.org/site/assets/uploads/2005/01/cost-us-forest-based-carbon-sequestration.pdf

Stoneham, G., Chaudhri, V., Ha, A., & Strappazzon, L. (2003). Auctions for conservation contracts: an empirical examination of Victoria's BushTender trial. *Australian journal of agricultural and resource economics, 47*(4), 477-500.

Wunder, S. (2005). *Payments for environmental services: some nuts and bolts.* CIFOR Occasional Paper, Center for International Forestry Research, Bogor, Indonesia. Retrieved from https://vtechworks.lib.vt.edu/bitstream/handle/10919/66932/2437_009_Infobrief.pdf?sequence=1&isAllowed=y

Wunder, S. (2015). Revisiting the concept of payments for environmental services. *Ecological economics, 117*, 234-243.

Zandersen, M., Bråten, K. G., & Lindhjem, H. (2009). *Payment for and management of ecosystem services*: Nordic Council of Ministers.

Appendices

Appendix 4-A. Tables and Figures

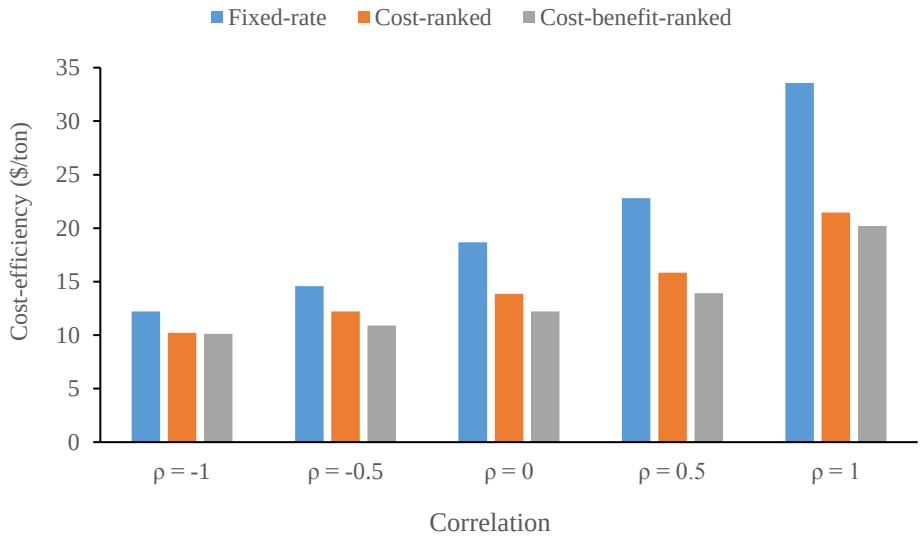

Figure 4-A 1: Cost-efficiencies of the payment designs for the BC model

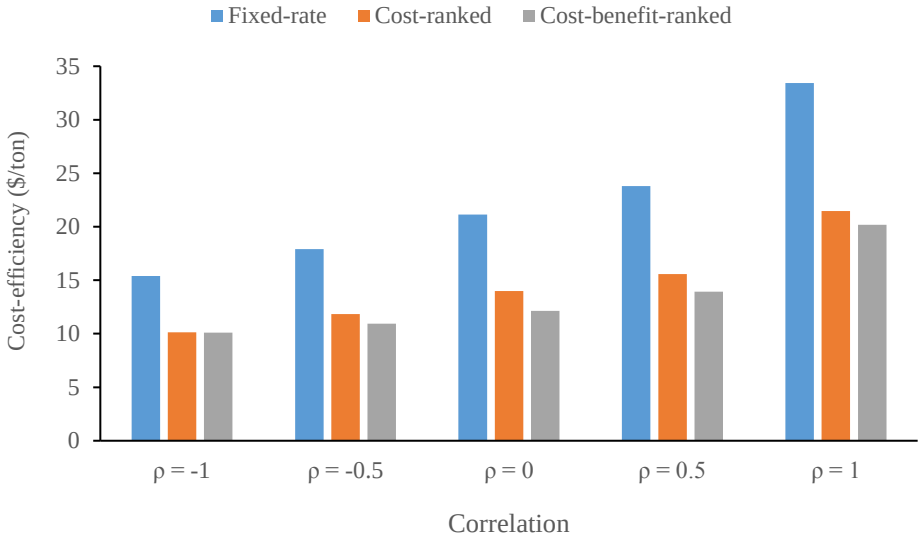

Figure 4-A 2: Cost-efficiencies of the payment designs for the TC model

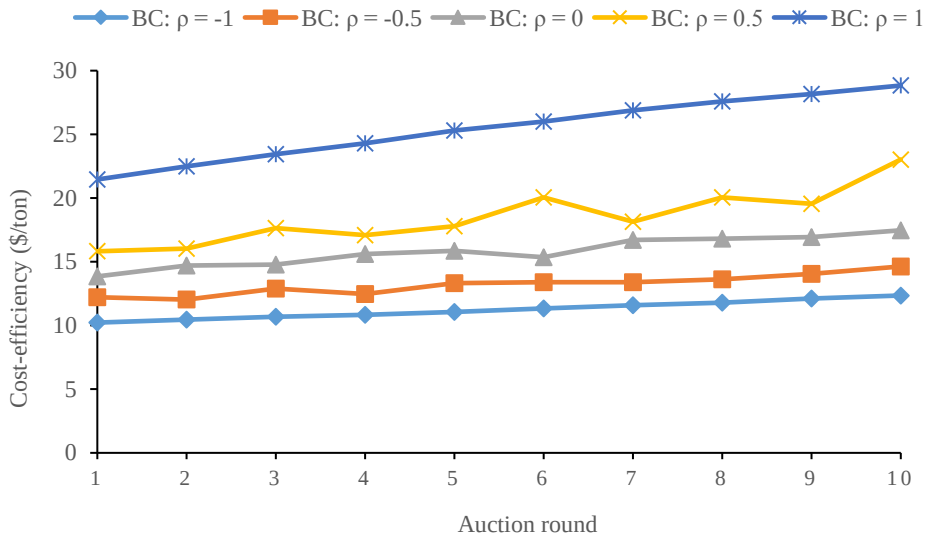

Figure 4-A 3: Cost-efficiencies of the cost-ranked BC auction under multiple rounds (L1)
Note: BC refers to budget-constrained auction with given correlation.

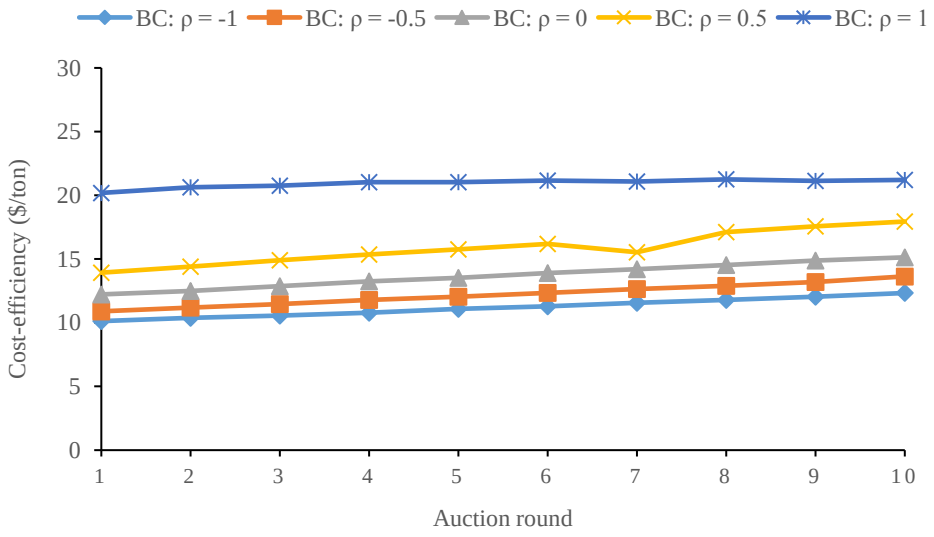

Figure 4-A 4: Cost-efficiencies of the cost-benefit-ranked BC auction under multiple rounds (L1)
Note: BC refers to budget-constrained auction with given correlation.

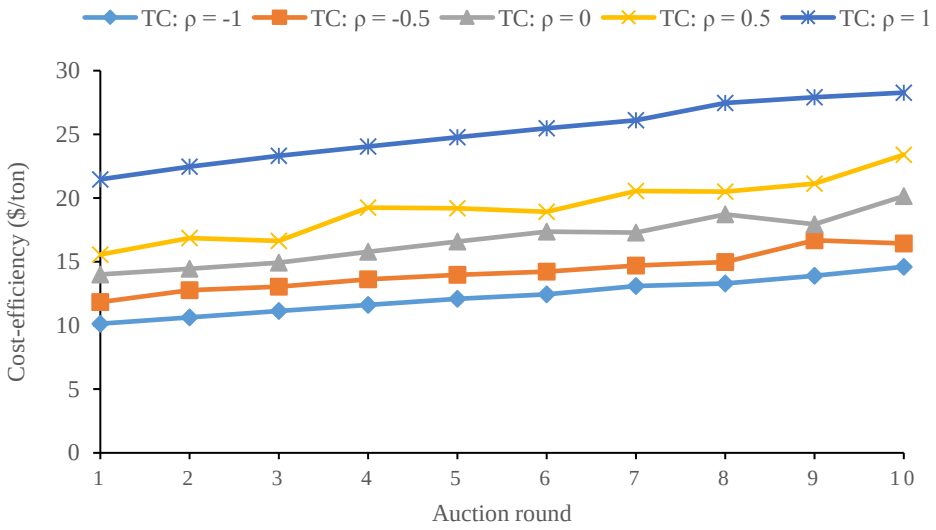

Figure 4-A 5: Cost-efficiencies of the cost-ranked TC auction under multiple rounds (L1)
Note: TC refers to target-constrained auction with given correlation.

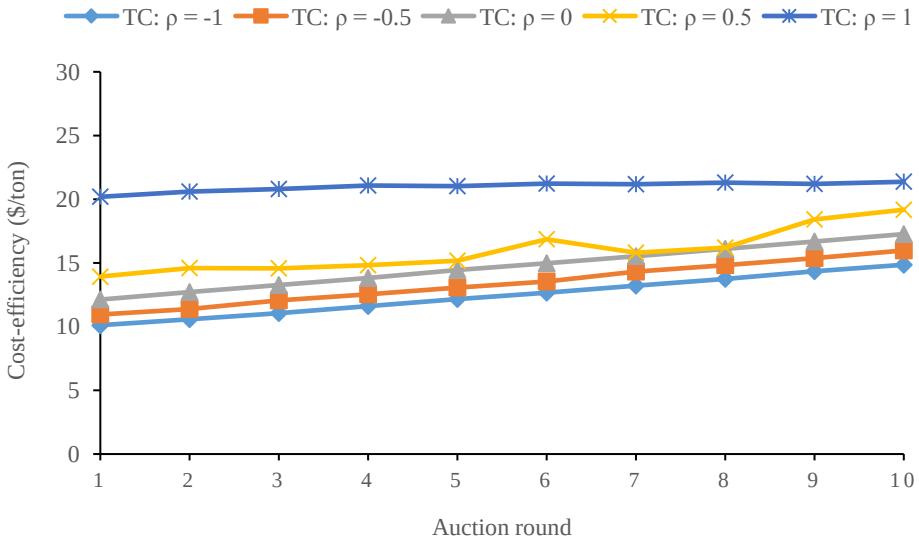

Figure 4-A 6: Cost-efficiencies of the cost-benefit-ranked TC auction under multiple rounds (L1)
Note: TC refers to target-constrained auction with given correlation.

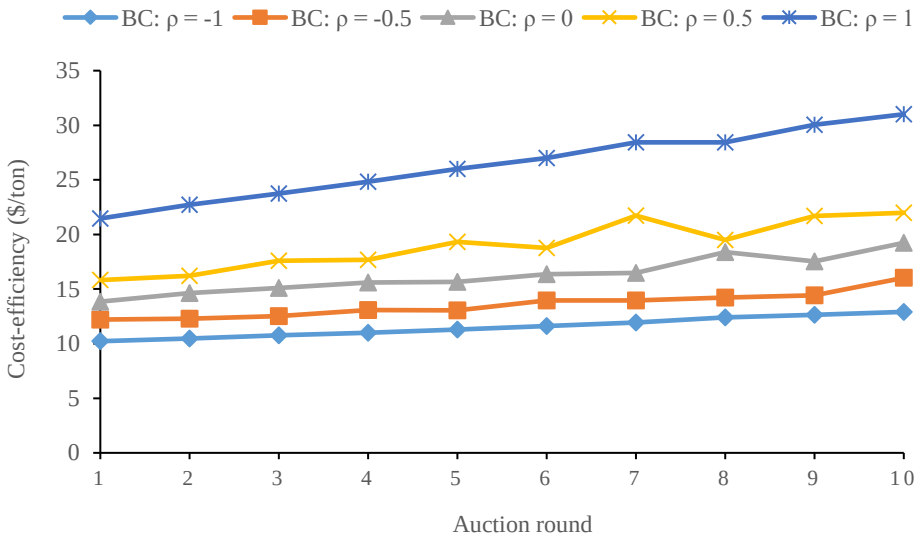

Figure 4-A 7: Cost-efficiencies of cost-ranked BC auction under multiple rounds (L2)
Note: BC refers to budget-constrained auction with given correlation.

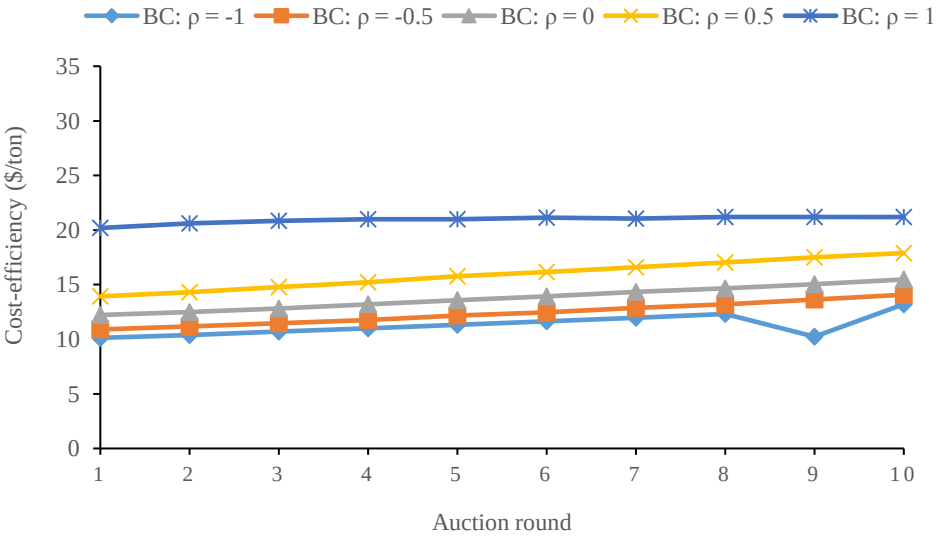

Figure 4-A 8: Cost-efficiencies of cost-benefit-ranked BC auction under multiple rounds (L2)
Note: BC refers to budget-constrained auction with given correlation.

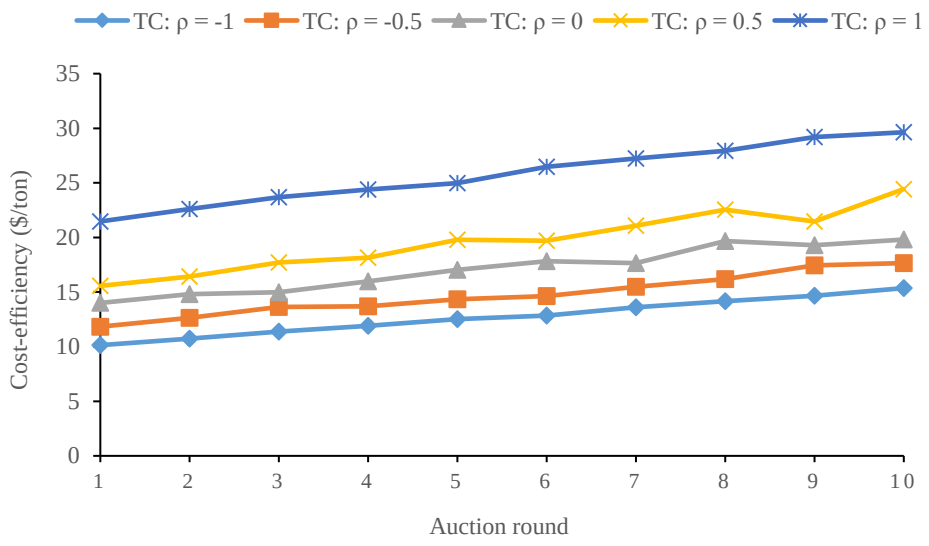

Figure 4-A 9: Cost-efficiencies of cost-ranked TC auction under multiple rounds (L2)
Note: TC refers to target-constrained auction with given correlation.

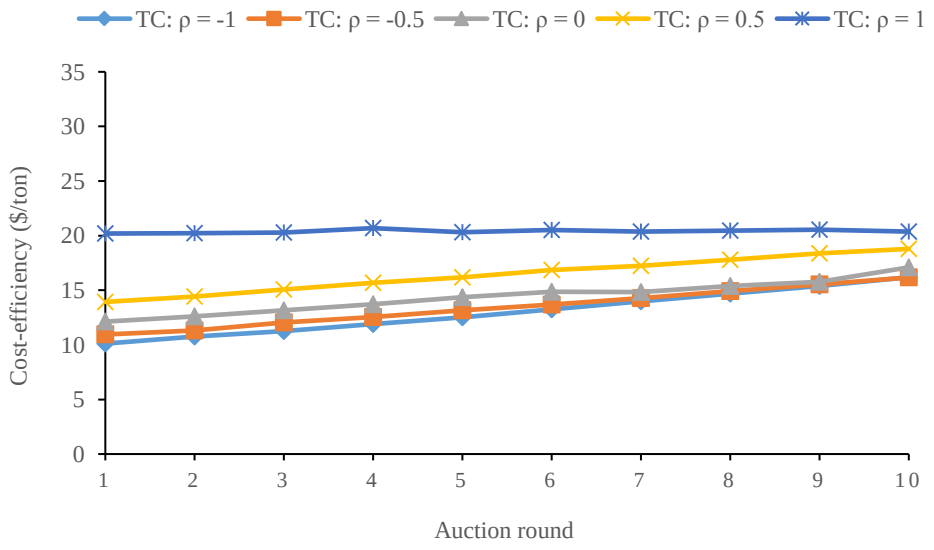

Figure 4-A 10: Cost-efficiencies of cost-benefit-ranked TC auction under multiple rounds (L2)
Note: TC refers to target-constrained auction with given correlation.

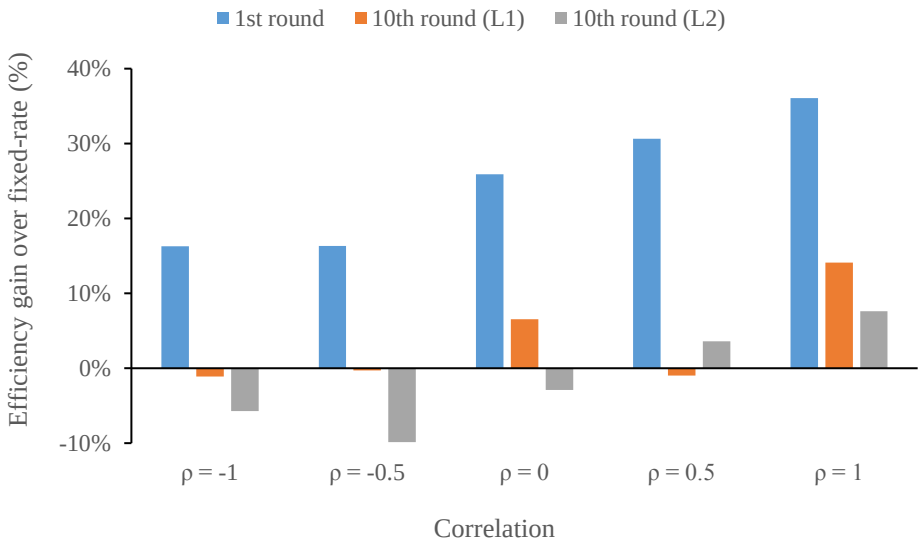

Figure 4-A 11: Cost-efficiency gains of cost-ranked BC auctions with L1 and L2 bidders
Note: L1 and L2 refer to types of bid learning behaviors.

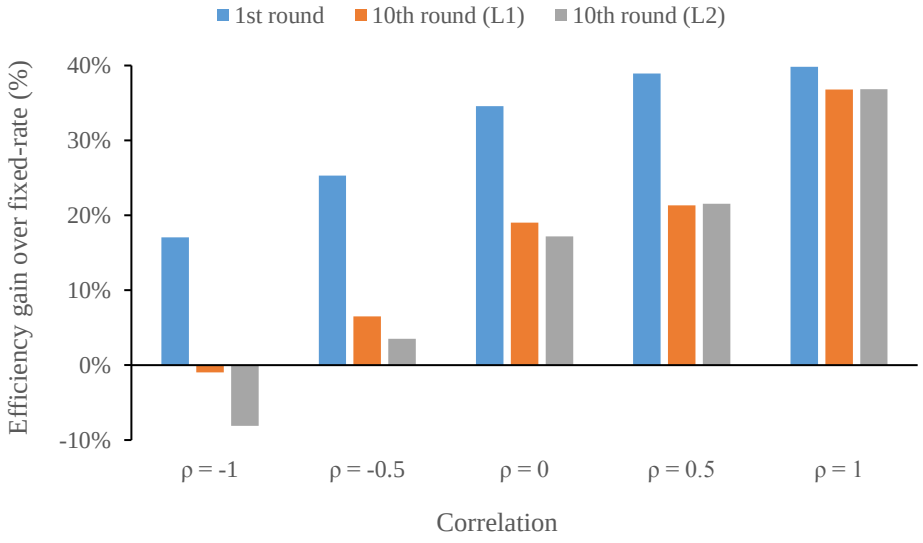

Figure 4-A 12: Cost-efficiency gains of cost-benefit-ranked BC auctions with L1 and L2 bidders
Note: L1 and L2 refer to types of bid learning behaviors.

Appendix 4-B. Nash-equilibria Bids in Reverse Auctions

This proof is a re-derivation and confirmation of the theoretical results of Harris and Raviv (1981), Latacz-Lohmann and Van der Hamsvoort (1997), and Hailu et al. (2005) with minor extensions.

4-B1. Nash-equilibrium Bid in a Single-unit First-price Reverse Auction

The independent private-values model for selling a single indivisible good has been well evaluated in the auction literature (McAfee & McMillan, 1987; Milgrom & Weber, 1982; Riley & Samuelson, 1981). The Nash equilibrium bidding strategy corresponding to the first-price sealed-bid auction provides an analogous framework for a single-unit reverse/procurement auction (Hailu et al., 2005).

Let the opportunity cost of a land-use change for bidder/landowner *i* be c_i, the bidding function for bidder *i* be $b_i(c_i)$, and *F* be the distribution function for the opportunity costs of the bidders. Assume potential sellers have private opportunity costs drawn from the same distribution, and further assume that the bidders are risk neutral and maximize expected payoffs. Bidder *i* will win if all other bidders have a higher opportunity cost than *i*, the probability of which is:

$$Pr(c_i < c_j) = [1 - F\ (c_i)]^{n-1}\ \forall\, j \neq i. \qquad (4-B1)$$

The Nash-equilibrium bidding strategy is:

$$B(c) = b \rightarrow c = B^{-1}(b). \qquad (4-B2)$$

Each bidder tries to maximize the expected payoff:

$$Max{:}\,\pi(b,c) = \ (b-c)[1 - F\ (B^{-1}(b))]^{n-1}. \qquad (4-B3)$$

The first-order condition for maximization, with respect to $b^*(c)$ is:

$$(n-1)(b^*(c)-c)[1-F(B^{-1}(b^*(c)))]^{n-2}f(B^{-1}(b^*(c)))\frac{1}{B'(B^{-1}(b^*(c)))}+[1-$$

$$F(B^{-1}(b^*(c)))]^{n-1}=0, \qquad (4-B4)$$

where *f(c)* and *F(c)* denote the density and distribution functions of the opportunity costs respectively.

At symmetric equilibrium:

$$B(c)=b^*(c), \qquad (4-B5)$$

$$(n-1)(B(c)-c)[1-F(c)]^{n-2}f(c)+[1-F(c)]^{n-1}B'(c)=0. \qquad (4-B6)$$

Integrating both sides of equation (4-B6) with respect to *c*, and rearranging we have:

$$b^*(c)=c+\frac{\int_c^z[1-F(u)]^{(n-1)}\,du}{[1-F(c)]^{(n-1)}}. \qquad (4-B7)$$

Suppose the opportunity costs of the bidders are independently and identically distributed and distributed uniformly within the range of *x* and *z*. The optimal bid becomes:

$$b^*(c)=c+\frac{1}{n}(z-c). \qquad (4-B8)$$

We see that overbidding is the dominant strategy in the first-price sealed-bid reverse auction, and the amount of the overbid ε_i is:

$$\varepsilon_i=b_i^*-c_i=\frac{1}{n}(z-c_i). \qquad (4-B9)$$

Let b_1 and b_2 be the optimal bids for bidders with opportunity costs c_1 and c_2 respectively with ε_1 and ε_2 being deviations from the opportunity costs:

$$\varepsilon_1=b_1-c_1=\frac{1}{n}(z-c_1), \qquad (4-B10)$$

$$\varepsilon_2=b_2-c_2=\frac{1}{n}(z-c_2). \qquad (4-B11)$$

Since $c_2 > c_1$, $\varepsilon_1 > \varepsilon_2$, which shows that overbidding is higher for bidders with lower opportunity costs compared to bidders with higher opportunity costs.

4-B2. Nash-equilibrium Bid in a Multi-unit Budget-constrained Auction

When the conservation agency reveals to the bidders a limited budget for procuring environmental services, bidders form expectations for the implicit bid cap and try to maximize expected payoffs (Latacz-Lohmann & Van der Hamsvoort, 1997). Let b_{igf} denote the bid submitted for changing land-use g to forest f in dollar per hectare. The probability that the bid b_{igf} is accepted depends upon the implicit bid cap h:

$$Pr\left(b_{igf} < h\right) = \int_b^{\beta} g\left(b_{igf}\right)db = \left[1 - G\left(b_{igf}\right)\right], \qquad (4-B12)$$

where the density function $g(b_{igf})$ and the distribution function $G(b_{igf})$ characterize the bidder's expectations for the bid cap h.

Assuming risk neutral behavior of the bidder, each bidder tries to maximize expected profit:

$$Max\ E(\pi(b_{igf})) = (\pi_f + b_{igf})\,\mathrm{Pr}(b_{igf} < h) + \pi_{ig}[1 - Pr(b_{igf} < h)], \qquad (4-B13)$$

where π_{ig} denotes profit under the current land use and π_f denotes profit from forest under a conservation contract had there been no conservation payment.

The first-order condition, with respect to b^*_{igf} is:

$$(\pi_f + b^*_{igf})\left[-g\left(b^*_{igf}\right)\right] + \left[1 - G\left(b^*_{igf}\right)\right] + \pi_{ig}g\left(b^*_{igf}\right) = 0, \qquad (4-B14)$$

giving:

$$b^* = (\pi_{ig} - \pi_f) + \frac{\left[1 - G\left(b^*_{igf}\right)\right]}{g\left(b^*_{igf}\right)}. \qquad (4-B15)$$

The term $(\pi_{ig} - \pi_f)$ is essentially the opportunity cost of participating in the conservation program. With $\pi_{ig} = nr_{ig}$ and $\pi_f = -(fc_f + vc_f)$, the optimal bid is:

$$b^*_{igf} = nr_{ig} + fc_f + vc_f + \frac{\left[1 - G\left(b^*_{igf}\right)\right]}{g(b^*_{igf})}, \qquad (4 - B16)$$

$$b^*_{igf} = c_{igf} + \frac{\left[1 - G\left(b^*_{igf}\right)\right]}{g(b^*_{igf})}. \qquad (4 - B17)$$

Assuming the bidder's expectation of the bid cap is uniformly distributed between α and β such that the probability of the bid being accepted is unity for expectations below or equal to α and zero for bid expectations equal or above β, the optimal bid is:

$$b^*_{igf} = c_{igf} + \frac{\beta - c_{igf}}{2}. \qquad (4 - B18)$$

We can see that overbidding is the dominant strategy in the budget-constrained discriminatory-price auction, and the amount of the overbid ε_{igf} is:

$$\varepsilon_{igf} = b^*_{igf} - c_{igf} = \frac{\beta - c_{igf}}{2}. \qquad (4 - B19)$$

Let b^1_{igf} and b^2_{igf} be the optimal bids for bidders with opportunity costs $c^1_{igf}$and c^2_{igf} respectively with ε^1_{igf} and ε^2_{igf} being the overbids:

$$\varepsilon^1_{igf} = b^1_{igf} - c^1_{igf} = \frac{\beta - c^1_{igf}}{2}, \qquad (4 - B20)$$

$$\varepsilon^2_{igf} = b^2_{igf} - c^2_{igf} = \frac{\beta - c^2_{igf}}{2}. \qquad (4 - B21)$$

Since $c_{igf}^2 > c_{igf}^1,\ \varepsilon_{igf}^1 > \varepsilon_{igf}^2$, which shows that overbidding is higher for bidders with lower opportunity costs than for bidders with higher opportunity costs.

4-B3. Nash-equilibrium Bid in a Multi-unit Target-constrained Auction

Assume *n* bidders trying to sell at most one unit of the good, where the conservation agency has an overall demand for *m* units of that good. Bidder *i* wins if at least (*n-m*) bidders have higher opportunity costs than *i*. The probability that the bid b_i is accepted is equivalent to the probability that c_i is lower than the mth order statistic among the (*n-1*) rival opportunity costs (Harris & Raviv, 1981):

$$G(c) = \frac{(n-1)!}{[(n-m-1)!\,(m-1)!]}\int_c^z [F(u)]^{(m-1)}[1-F(u)]^{(n-m-1)} f(u)\,du, \qquad (4-B22)$$

where *f(c)* and *F(c)* denote the density and distribution functions of the opportunity costs, respectively, with *z* being the upper limit of the distribution.

The Nash-equilibrium bidding strategy is:

$$B(c) = b \rightarrow c = B^{-1}(b). \qquad (4-B23)$$

And, each bidder tries to maximize the expected payoff:

$$Max{:}\,\pi(b,c) = \ (b-c)G(B^{-1}(b)). \qquad (4-B24)$$

The first-order condition, with respect to $b^*(c)$ is:

$$G(B^{-1}(b^*(c))) + (b^*(c)-c)G'(B^{-1}(b^*(c)))\frac{d(B^{-1}(b^*(c)))}{d\big(b^*(c)\big)} = 0. \qquad (4-B25)$$

Recalling the property:

$$\frac{d(B^{-1}(b^*(c)))}{d(b^*(c))} = \frac{1}{B'(B^{-1}(b^*(c)))}, \qquad (4-B26)$$

equation (4-B25) simplifies to:

$$G(B^{-1}(b^*(c))) + (b^*(c) - c)G'(B^{-1}(b^*(c)))\frac{1}{B'(B^{-1}(b^*(c)))} = 0. \qquad (4-B27)$$

At symmetric equilibrium, we have:

$$B(c) = b^*(c), \qquad (4-B28)$$

$$G(c) + (B(c) - c)\frac{G'(c)}{B'(c)} = 0, \qquad (4-B29)$$

$$G(c)B'(c) + B(c)G'(c) = cG'(c). \qquad (4-B30)$$

Integrating both sides of equation (4-B30) with respect to *c*, we get:

$$G(c)B(c) = \int_c^z cG'(u)du, \qquad (4-B31)$$

$$b^*(c) = \frac{\int_c^z cG'(u)du}{\int_c^z G(u)du}. \qquad (4-B32)$$

From equation (4-B22), for a uniform distribution between 0 and 1, we have:

$$G(c) = \frac{(n-1)!}{[(n-m-1)!\,(m-1)!]}\int_c^1 u^{(m-1)}[1-u]^{(n-m-1)}\,du. \qquad (4-A33)$$

Subsequently,

$$G'(c) = \frac{(n-1)!}{[(n-m-1)!\,(m-1)!]}u^{(m-1)}[1-u]^{(n-m-1)}. \qquad (4-A34)$$

Substituting into equation (4-B32), the optimal bid becomes:

$$b^*(c) = \frac{\int_c^1 u^m[1-u]^{(n-m-1)}\,du}{\int_c^1 u^{(m-1)}[1-u]^{(n-m-1)}\,du}. \qquad (4-B35)$$

Plugging in some values for *n*, *m*, and *c*, it is not hard to see that overbidding is the dominant strategy in the target-constrained discriminatory-price auction, and overbidding is higher for bidders with lower opportunity costs than for bidders with higher opportunity costs.

Chapter V. Conclusions

Terrestrial carbon sequestration is one of the ways to mitigate future adverse consequences of climate change. Reduced rate of release of greenhouse gas (GHG) emissions using feedstock-based renewable fuels, and atmospheric carbon captured from ecosystem restoration practices such as afforestation are long-term solutions to mitigating GHG emissions. This dissertation assessed the effects of policy supports and voluntary incentive programs on renewable fuel production and forest-based carbon sequestration.

Large scale production of biofuels from non-edible feedstocks with substantially less GHG emissions compared to fossil fuels, and socio-economic development of the rural community has been the focus of stakeholders involved in the research and development of biofuels. However, higher costs of feedstock production and biofuel processing, along with investment risks hinder large-scale deployment of biofuels at present.

In the first essay, an integrated approach to switchgrass-based bioethanol production is employed to evaluate the impacts of policy supports on supply chain decisions driven primarily by yield uncertainty and the associated investment risk. Specifically, impacts of federally subsidized Biomass Crop Assistance Program (BCAP) on optimal land use and biorefinery location decisions are evaluated in presence of feedstock yield uncertainty while addressing risk preferences of the biofuel sector in terms of supply-chain cost. A two-stage stochastic mixed integer linear programming (MILP) is employed to design an optimal supply-chain while minimizing the expected system cost under feedstock yield uncertainty. Furthermore, the expected cost minimization model, which assumes risk-neutrality in the biofuel production is later extended to Conditional Value-at-Risk (CVaR) minimization model considering the risk-averse nature of the biofuel sector under uncertainty of high costs. Applicability of the stochastic model is illustrated through a case study in west Tennessee.

Results indicated that BCAP subsidies are more encouraging to the risk-averse biofuel industry compared to the risk-neutral biofuel sector. CVaR minimization model in general selected more land for switchgrass cultivation compared to the expected cost minimization model in an effort to reduce the high costs of low yield scenarios. More land for feedstock cultivation in CVaR minimization model meant larger subsidies in terms of both the establishment and land rent (annual) payments under BCAP. With subsidies, crop land selection increased with corresponding decrease in pasture land use irrespective of the risk attitude of the biofuel industry. Biofuel shortage associated with high costs in risk management model is reduced by favoring land selection with higher spatial yields with BCAP subsidies. Furthermore, higher spatial yields mostly correspond to lands with higher opportunity costs which are effectively reduced after BCAP land rent payments. Consequently, both the expected cost and risk are reduced by a higher percent for a risk-averse biofuel sector compared to a risk-neutral one with the BCAP subsidies.

Major contribution of this study is the impact assessment of federally subsidized biomass programs on the investment decisions (including land allocation) of a risk-sensitive biofuel industry under feedstock supply uncertainty. From methodological perspective, risk-optimal designs emerged from integrated supply-chain optimization can serve as guidelines in decision-making process for large-scale biofuel production under strategic uncertainties.

Considered as a potential approach to mitigate GHG emissions from the aviation sector, renewable jet fuel (RJF) production remains negligible, mainly because of the novelty of the feedstock-based conversion technologies and the associated costs. The second essay presented economic and environmental analysis of commercial-scale RJF production using switchgrass-based alcohol-to-jet (ATJ) technology using a game-theoretic model that accounts for potential

economic interaction between feedstock producers and the RJF processor. Specifically, impacts of RJF production from switchgrass on farmland allocation, processing facility configuration, and GHG emissions are estimated in response to fulfilling the RJF demand at the Memphis International Airport in west Tennessee. A potential carbon market is used to explore the impact of hypothetical carbon credits on the optimal decisions of the participants leading to changes in the GHG emissions, economic surpluses, and net supply-chain welfare.

The results indicated that feedstock suppliers' aggregate economic surplus is about $16.88 million without the provision of tradable carbon credits (Baseline) while majority of them received a margin up to 47 % over their opportunity costs of land conversion. Given the Stackelberg nature of the game, the processor (leader) influenced the land use decisions of the competing farmers (followers) through its facility location decisions under carbon credits. The processor's cost decreased by $17.65 to 59.50 million simultaneously resulting in a surplus decline of $5.88 to 10.45 million for the feedstock suppliers, compared to the Baseline, given the availability of carbon credits. As the RJF price decreased with higher carbon credits, the net supply-chain welfare increased by $12.71 to 50.62 million corresponding to the $16.12 to 53.79 million increments in the airlines' surpluses, compared to the Baseline. The ATJ products achieved a 62.5 to 65% life-cycle analysis (LCA)-based GHG emission reduction through displacement of the fossil fuels. Availability of renewable identification number (RIN) credits in addition to the revenues from co-products, largely determined the processor break-even prices and the subsequent RJF prices. Satisfying the assumed profit margins of the processor needed an implicit subsidy from the airlines, of $1.49 to $1.89/gallon if the cellulosic RIN credits remained at 2016 average, which are equivalent to GHG emission abatement costs of $151 to 198/ton$CO_2$e for the airlines.

Considering the attention paid by the U.S. aviation sector with respect to GHG emissions, this study provided useful insights into economic and environmental impacts of large-scale RJF production. Specifically, the importance of market-based instrument in the form of tradable carbon credits along with RIN credits to achieve the desired economic viability and emission abatement goals is made explicit through a Stackelberg interaction between the supply-chain participants.

Conservation programs such as afforestation which can sequester a large amount of atmospheric CO_2, are adopting competitive bidding in the form of conservation auction to overcome information asymmetry in securing cost-efficiency. But, the efficiency gains of auction-based payments remain doubtful as landowners learn to extract higher information rents from the conservation agency under multiple rounds of procurement. The cost-efficiency of multi-round auction-based payments can be enhanced by integrating cost and benefit information into program design, which further depends on the correlation between the opportunity costs and environmental benefits of conservation.

In the third essay, the cost-efficiency of cost-ranked and cost-benefit-ranked auction-based payment designs is examined for forest-based carbon storage with varying degree of correlation between opportunity costs of afforestation and carbon sequestration capacities in a static as well as dynamic setting. Bids (opportunity costs of afforestation inclusive of overbids) are simulated following discriminatory-price auction, and the bid learning behavior of the landowners in multiple rounds is conceptualized through an agent-based model. The outcomes from the models are analyzed for cost-efficiency gains against an equivalent fixed-rate payment, while estimating magnitude of efficiency losses when bidders learn in subsequent rounds.

Simulation results indicated that auctions have efficiency gains compared to a fixed-rate payment design, which are larger for the target-constrained model compared to the budget-constrained model. Although efficiency gains are highest for both the cost- and cost-benefit-ranked designs with perfect negative correlation between costs and benefits in a static setting, efficiency losses are highest for both designs in a dynamic setting when the conservation program has a fixed target to achieve. The decrease in efficiency gains are greater for cost-ranked design compared to the cost-benefit-ranked design, especially when bidders learned through their own and their neighbor's experience. For perfect positive correlation between environmental benefits and opportunity costs, the cost-benefit-ranked design suffered the smallest efficiency losses under repeated auction rounds. More importantly, the cost-efficiency of the cost-benefit-ranked design is generally more robust to deterioration when bidders learn in different ways over repeated auction rounds and more resistant to erosion for certain levels of correlation compared to the cost-ranked design.

Given the empirical limitation of real world conservation auctions, this study provided insights on information optimal strategies for designing conservation payments through auction-based simulation experiment simultaneously capturing bid learning behavior of the landowners in multi-round procurement auctions through an agent-based model. With primary focus on estimating potential impacts of correlation in deciding an optimal information strategy for achieving cost-efficiency of conservation payments, outcomes from this study are expected to guide decision makers in choosing an optimal payment design that ensures efficiency gains for auction-based payments compared to fixed-rate payments, and more importantly ensures minimal loss in cost-efficiency in a dynamic setting.

Vita

Bijay P. Sharma was born on 5th of July 1985 in Nepal. He received Bachelor of Agricultural Sciences and Masters of Science in Agricultural Economics from Tribhuvan University, Nepal in the year 2009 and 2012, respectively. He is expected to fulfill his degree requirements for PhD in Natural Resource Economics in July 2018. The author is an applied economist willing to experiment with new approaches and ideas in the field of resource management for optimal functioning of the society.